# Gated First-Passage Processes

A thesis submitted in partial fulfillment of the requirements of the degree of **Doctor of Philosophy**

विद्या वाचस्पति की
उपाधि की अपेक्षाओं की आंशिक पूर्ति में प्रस्तुत शोध प्रबंध

द्वारा / By
आंजनेय कुमार / **Aanjaneya Kumar**

पंजीकरण सं. / Registration No.
20193700

शोध प्रबंध पर्यवेक्षक / Thesis Supervisor
एम. एस. संथानम / **M. S. Santhanam**


INDIAN INSTITUTE OF SCIENCE EDUCATION AND RESEARCH PUNE
भारतीय विज्ञान शिक्षा एवं अनुसंधान संस्थान पुणे

2024

# Certificate

Certified that the work incorporated in the thesis entitled **"Gated First-Passage Processes"** submitted by **Aanjaneya Kumar** was carried out by the candidate, under my supervision. The work presented here or any part of it has not been included in any other thesis submitted previously for the award of any degree or diploma from any other university or institution.

Date: June 12, 2024

Prof. M.S. Santhanam

(Supervisor)

# Declaration

**Name of Student:** Aanjaneya Kumar

**Reg. No.:** 20193700

**Thesis Supervisor:** Prof. M. S. Santhanam

**Department:** Physics

**Date of joining program:** August 1, 2019

**Date of Pre-Synopsis Seminar:** March 14, 2024

**Title of Thesis:** Gated First-Passage Processes

I declare that this written submission represents my idea in my own words and where others' ideas have been included; I have adequately cited and referenced the original sources. I declare that I have acknowledged collaborative work and discussions wherever such work has been included. I also declare that I have adhered to all principles of academic honesty and integrity and have not misrepresented or fabricated or falsified any idea/data/fact/source in my submission. I understand that violation of the above will be cause for disciplinary action by the Institute and can also evoke penal action from the sources which have thus not been properly cited or from whom proper permission has not been taken when needed.

The work reported in this thesis is the original work done by me under the guidance of Professor M. S. Santhanam.

Date: June 13, 2024

Aanjaneya Kumar

(20193700)

# Acknowledgments

This thesis marks the end of a whole decade that I've spent at IISER Pune. To put it in perspective, this duration amounts to

- more than $\frac{1}{3}$ of my human existence
- more than $\frac{1}{2}$ of the existence of IISER Pune
- 100% of my adult life.

For 9 out of these 10 years, I have had the great pleasure of working with Prof. M. S. Santhanam. After having just finished a course on *Waves and Oscillations* taught by Prof. Santhanam at the end of my first year of undergrad studies, I approached him for ideas regarding how I could productively spend the upcoming summer vacation in 2015. He suggested I look at the book *Nonlinear Dynamics and Chaos* by Steven Strogatz. Towards the end of the summer vacation, in an email titled *Nonlinear dynamics and possible opportunities*, I wrote to him about my progress with the book and a number of different directions in which I got sidetracked. Most importantly, I told him about how I came across the fascinating world of Complex Systems — a field that was mentioned on his web page as well — and asked if I could further explore this field with him. Despite being abroad at that time, Prof. Santhanam very generously replied and agreed to discuss further with me after his travels. This was the start of a series of discussions and brainstorming sessions where Prof. Santhanam's patience, gentle guidance, and encouragement to explore ideas on my own, allowed me to find directions that interested me and develop my own research program. I sincerely hope that the series of discussions that we started 9 years ago never ends.

I would also like to take this opportunity to thank Prof. Deepak Dhar, who has been a mentor to me for the past 7 years, including being my Master's thesis supervisor. I first met Deepak on the day he joined IISER Pune and right from that day, I have looked up to his ability to extract insight about complex issues by asking (and answering) seemingly simple but incisive and fundamental questions. His guiding philosophy of *learning to walk before you run* is something that I strive

to adhere to in most of my research endeavors, with the added caveat that I'm still struggling to crawl.

During the past decade, I have been privileged to have had the unofficial mentorship of several other faculty members throughout my academic journey – both inside IISER Pune and outside. I gratefully acknowledge *Profs. Bijay Agarwalla, Amit Apte, Bhas Bapat, Arijit Bhattachayay, Sourabh Dube, Peter Eckersley, Dave Feldman, Anil Gangal, Denis Grebenkov, Anirban Hazra, M. S. Madhusudhan, Nishad Matange, Arnab Pal, Sudha Rajamani, Kabir Ramola, Shlomi Reuveni, Sanjib Sabhapandit, Tridib Sadhu, Anders Sandberg, Seema Sharma*, and *Steven Spallone* for their support in various forms at different stages of my stay at IISER Pune. One of the things that makes IISER Pune stand out from all other institutes is its amazing administrative staff. Their approachability and efficiency provide the researchers with a space where they can truly focus on their research. I, along with all students, research fellows, and faculty members of IISER Pune, will forever be grateful to them.

At this point, I would like to invoke the old African proverb *"If you want to go fast, go alone; if you want to go far, go together"* and thank a number of people who metaphorically slowed down their speeds to walk with me (while simultaneously complaining about my abnormally fast literal walking speed). So, *Aakriti, Aayush, Aayushi, Abhishek A, Abhishek S, Aditya K(h), Aditya K(o), Adithya, Aniket, Ankita, Anwesha, Aritra, Basila, Carla, Danish, David, Dhruba, Gaurav, Hanna, Harshini, Jayant, Kavya, Kritika, Kush, Leah, Mayank, Megha, Mitali, Mohan, Nandini, Nida, Nisarg, Nishant, Neeraj, Ofek, Onkar, Ramesh, Rasha, Ritam, Rohit, Rounak, Sambit, Sandeep C, Sandeep J, Sayantika, Shashank, Shivam, Shraddha, Shubham, Siddhant, Sidharth, Sonal, Sravya, Sreeram, Sudheesh, Suman, Sushant, Vaibhav, Vikram, Visakh, Vishnu, Veda, Yashaswika, Yuval, and Zakhiya*, I would just like to say thank you for everything. Given that one of the themes of this thesis is "missing information", it is very likely that I might have missed thanking someone. But I hope that they will feel my gratitude through my everyday actions. After all, another theme of this thesis is "inference from incomplete information."

This acknowledgments section would not be complete without a sincere thanks to my family. I have been extremely lucky to be born into a family that has always recognized the importance of education and has pushed me to become the person that I am today. I will always be grateful to them for their consistent support and belief in me.

And finally, the most difficult part – I would like to express my sincerest gratitude to IISER Pune. I call this the most difficult part because of two reasons. First, it isn't even clear to me what IISER Pune actually is – is it the roads, the campus, the culture, or the people? Most likely, it is a combination of all these things, which adds up to more than the sum of its parts. But second, even if I knew what IISER Pune truly was, there is no way that I can convey to it what it really meant to me. So here's all I will say: Thank you for accepting me and providing me with a space where I could make mistakes, learn from them (if I wanted to), and grow as a human being. Thank you for introducing me to a community where I could form relationships that I now realize would last a lifetime. Thank you for being a place I could call home. I end this note with the hope that this place will continue to inculcate a sense of belonging in academia, and in the world, to young adults for many years to come.

– *Aanjaneya* (aanjaneyak@gmail.com)

*Here's to the ones who dream*

*Foolish as they may seem*

*Here's to the hearts that ache*

*Here's to the mess we make* [1]

[1] *La La Land (2016)*, wrongly announced the Best Picture at the $89^{th}$ Academy Awards, 2017.

# Abstract

The first-passage time of a stochastic time-series, defined to be the time taken by it to cross a predefined threshold for the first time, has a wide range of applications across disciplines. However, if the time-series can only be intermittently observed, then its key features can be missed. In particular, the instance at which we actually observe the time-series to be above the threshold for the first time, called the detection time or the gated first-passage time, can be strikingly different from the true first-passage time. In this thesis, we first put forth a general framework for computing the statistics of the detection time and discuss its connection to a classic problem in chemical kinetics. Our central result is that the first detection time is related to and is obtainable from the first-passage time distribution. The applicability of our framework is demonstrated in several model systems, including the SIS compartmental model of epidemics, logistic models and birth-death processes with resetting. Following this discussion, we address the inverse problem of reconstructing the true first-passage time statistics purely from gated observations. We develop a universal—model free—framework for the inference of first-passage times from the detection time statistics. Moreover, when the underlying model is known, this framework allows us to infer physically meaningful model parameters. The results are then leveraged to infer the gating rates via the hitherto overlooked short-time regime of the measured detection time distributions. Put together, the unified framework of gated first-passage processes opens a novel peephole into a myriad of systems whose direct observation is limited because of their underlying physics or imperfect observation conditions. We conclude the thesis with a discussion of three key applications of the theory – (i) determining the optimal rate of sampling a first-passage process, (ii) understanding the extreme value statistics of a partially observed-stochastic time-series, and (iii) inferring missing statistics in real-world time-series data.

# Synopsis

The first-passage time of a stochastic time-series, defined to be the time taken by it to cross a pre-defined threshold for the first time, has a wide range of applications across disciplines [1]. How long does it take for a chemical reaction to be triggered? Or what is the time taken for an order to be executed in the stock market? These disparate examples fall under the purview of first-passage processes. However, in several realistic scenarios, the time-series of interest can only be intermittently observed. In such cases, key features of the time-series can be missed. In particular, the instance at which we actually observe the time-series to be above the threshold for the first time, called the *first detection time* or the *gated first-passage time*, can be strikingly different from the true first-passage time. Despite its ubiquity and practical relevance, a discussion of the statistics of the first detection time, or more generally, the impact of partial observability in first-passage processes is missing. This thesis is an attempt towards bridging this gap.

**Chapter 1 – Introduction**

Chapter 1 contains an introduction and motivation to the study of first-passage processes. After a brief survey of the literature and some of its key applications, we highlight a number of scenarios where the underlying stochastic process of interest can only be partially observed and thus the notion of first-passage times must be generalized. We discuss one such generalization, called the gated first-passage time or the first detection time, which explicitly takes into account the partial observability of the underlying process. We conclude this chapter by outlining the general modeling framework that will form the backbone of the rest of the thesis and discuss its connection to a classic problem in chemical kinetics.

**Chapter 2 – First Detection of Threshold Crossing Events under Intermittent Sensing**

In Chapter 2, we derive general formulas for computing the statistics of the gated first-passage times. Using these results, we establish that the first detection time is related to and is obtainable from the first-passage time distribution. We show that these results hold for Markov processes in

continuous and discrete space, and also a class of non-Markov process called the renewal process. The applicability of our results is then demonstrated in several model systems, including the SIS compartmental model of epidemics, logistic models and birth-death processes with resetting. Finally, we leverage the framework to extract further insight into the statistics of gated first-passage times. This chapter details the work which has been published in Refs. [2] and [3].

**Chapter 3 – Inference from Gated First-Passage Times**

While the central result established in the previous chapter dictates that the statistics of the first detection time is obtainable from the knowledge of the first-passage time distribution, in most practically relevant scenarios, only the detection time is measurable and the aim is to uncover the properties of the underlying process from purely measurable quantities. To address this challenge, in Chapter 3, we introduce a model-free formalism for the inference of first-passage times from the detection times of gated first-passage processes. Furthermore, we show that when some information about the underlying process is known, this framework also provides a way to infer physically meaningful parameters, e.g., diffusion coefficients. Finally, we show how to infer the gating rates themselves via the hitherto overlooked *short-time regime* of the measured detection times. The robustness of the approach and its insensitivity to underlying details are illustrated in several settings of physical relevance. The results presented in this chapter have been published in Ref. [4].

**Chapter 4 – Applications**

Chapter 4 contains an illustration of three distinct applications of the framework developed in this thesis. The first application deals with the challenge of optimally sampling a first-passage process when there are costs associated with making measurements of the process of interest. Next, we show how the framework of gated first-passage processes can be used to obtain insight into the statistics of extremes of partially observed time-series. Finally, we show how our results on stochastic bridges apply to the practically relevant case of working with real data generated by a single realization of a sparsely sampled stochastic process.

**Chapter 5 – Summary and Outlook**

We conclude this thesis in Chapter 5 by providing a summary of the key results presented in this thesis. We then outline a number of possible directions in which the modeling framework can be extended to be able to cater to different scenarios of potential interest. The broadly applicable and vastly unexplored field of partially observed stochastic processes has a number of interesting research avenues beyond first-passage phenomena. We conclude by highlighting a few interesting open directions that an interested reader could potentially think about exploring.

**References**

1. Sidney Redner. A guide to first-passage processes. Cambridge university press (2001).

2. Aanjaneya Kumar, Aniket Zodage, M. S. Santhanam. *First detection of threshold crossing events under intermittent sensing,* Physical Review E, **104**, L052103 (2021).

3. Yuval Scher, Aanjaneya Kumar, M. S. Santhanam, Shlomi Reuveni. *Continuous gated first-passage processes, arXiv*:2211.09164 (2022)

4. Aanjaneya Kumar, Yuval Scher, Shlomi Reuveni, M. S. Santhanam. *Inference from gated first-passage times,* Physical Review Research **5**, L032043 (2023).

# List of Publications

The contents of the thesis are based on the following papers.

1. **Aanjaneya Kumar**, Aniket Zodage, M. S. Santhanam. *First detection of threshold crossing events under intermittent sensing,* Physical Review E, 104(5), L052103 (2021)

2. **Aanjaneya Kumar**, Yuval Scher, Shlomi Reuveni, M. S. Santhanam. *Inference from gated first-passage times,* Physical Review Research 5(3), L032043 (2023)

3. Yuval Scher, **Aanjaneya Kumar**, M. S. Santhanam, Shlomi Reuveni. *Continuous gated first-passage processes,* ArXiv Preprint *arXiv*:2211.09164. *Under review in Reports of Progress in Physics* (2024)

4. **Aanjaneya Kumar**, Shlomi Reuveni, M. S. Santhanam. *Extreme value statistics of partially-observed time-series (In preparation)*

5. **Aanjaneya Kumar**, Yuval Scher, Shlomi Reuveni, M. S. Santhanam. *Optimal detection of gated first-passage processes (In preparation)*

Articles from other projects published during my PhD which are not included in this thesis:

1. **Aanjaneya Kumar**, Deepak Dhar. *TASEP speed process: an effective medium approach,* Journal of Statistical Mechanics: Theory and Experiment, 2020, 013211. (2020)

2. **Aanjaneya Kumar**, Deepak Dhar. *Improved upper bounds on the asymptotic growth velocity of Eden clusters,* Journal of Statistical Physics, 180, 710-720. (2020)

3. **Aanjaneya Kumar**, Suman Kulkarni, M. S. Santhanam. *Extreme events in stochastic transport on networks,* Chaos 30, 043111 (2020)

4. **Aanjaneya Kumar**, Valerio Capraro, Matjaz Perc. *The evolution of trust and trustworthiness,* Journal of the Royal Society Interface 17, 20200491 (2020)

5. **Aanjaneya Kumar**, Sandeep Chowdhary, Valerio Capraro, Matjaz Perc. *Evolution of honesty in higher-order social networks,* Physical Review E 104, 054308 (2021)

6. **Aanjaneya Kumar**, Peter Grassberger, Deepak Dhar. *Chase-Escape percolation on the 2D square lattice,* Physica A 577, 126072 (2021)

7. Sandeep Chowdhary, **Aanjaneya Kumar**, Giulia Cencetti, Iacopo Iacopini, Federico Battiston. *Simplicial contagion in temporal higher-order networks,* Journal of Physics: Complexity 2, 035019 (2021)

8. Denis Grebenkov, **Aanjaneya Kumar**. *Reversible target-binding kinetics of multiple impatient particles,* The Journal of Chemical Physics 156, 084107 (2022)

9. Denis Grebenkov, **Aanjaneya Kumar**. *First-passage times of multiple diffusing particles with reversible target-binding kinetics,* Journal of Physics A: Mathematical and Theoretical 55, 325002 (2022)

10. **Aanjaneya Kumar**, Arnab Pal. *Universal framework for record ages under restart,* Physical Review Letters 130, 157101 (2023)

11. Ritam Pal, **Aanjaneya Kumar**, M. S. Santhanam. *Depolarization of opinions on social networks through random nudges,* Physical Review E 108, 034307 (2023)

12. Deepak Dhar, R. Rajesh, **Aanjaneya Kumar**. *Phase transitions in systems of particles with only hard-core interactions,* Europhysics Letters 143, 61001 (2023)

13. Ritam Pal, **Aanjaneya Kumar**, M. S. Santhanam. *Universal statistics of competition in democratic elections,* ArXiv preprint arXiv:2401.05065 (2024)s

# Contents

# CHAPTER 1

# Introduction

How long does it take for a chemical reaction to be triggered? What is the time taken for an order to be executed in the stock market? When will the temperature in a given city cross its all-time-high value? The answer to these disparate questions falls under the purview of *first-passage processes* – a theme that lies at the heart of this thesis. The aim of this chapter is two-fold. First, we give a brief overview of first-passage processes and their applications. Next, we highlight an important but overlooked class of problems that motivated this thesis and introduce the reader to the theory of *gated first-passage processes*.

## 1.1 What is a First-Passage Process?

In many practically relevant situations, the time taken for an observable of interest to reach a pre-determined threshold for the first time is of immense interest and carries practical value. We call this time the first-passage time, and the process in which such a first-passage time is of interest is termed as a first-passage process. Figure 1.1 is a schematic representation of the first-passage time of a time-series. The importance of first-passage processes is recognized universally across scientific disciplines, owing to its ubiquity and wide-ranging applications [1–7]. The study of first-passage processes has a long history [1–3], and has a large number of applications in areas of physical sciences [1, 4, 8, 9], engineering [2, 10–12], finance [5, 13, 14] and biology [6, 7, 15].

### 1.1.1 Applications of First-Passage Processes

The following contains a few interdisciplinary examples of first-passage processes.

**Finance**

In financial markets, consider the scenario of a stock price reaching a certain threshold level, triggering a trading decision. The time it takes for the stock price to first cross this threshold can be modeled using first-passage processes. This concept is particularly relevant in high-frequency trading, where algorithms are designed to execute trades based on rapid changes in stock prices,

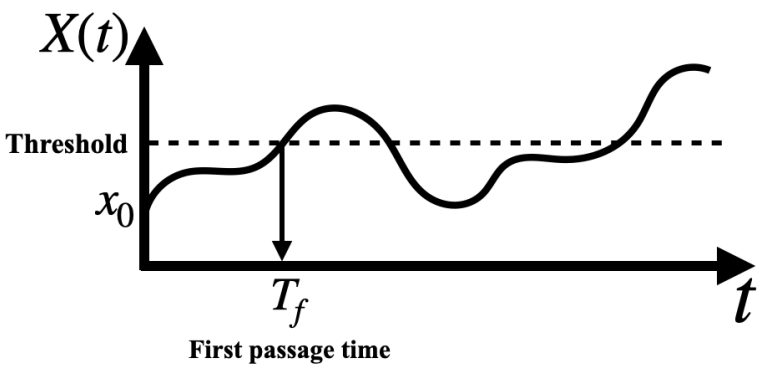


Figure 1.1: Schematic depiction of a stochastic process $X(t)$, starting from $x_0$, evolving in time. The instance at which $X(t)$ crosses the pre-defined threshold (marked as dashed line) is termed the first-passage time ($T_f$).

and understanding first-passage time statistics can inform the design of efficient trading strategies.

**Biology**

Imagine a biological cell signaling pathway where a signaling molecule must bind to a receptor for a specific cellular response to occur. The time it takes for the molecule to first bind to the receptor is determined by first-passage time [15]. This phenomenon is crucial in drug development, where researchers aim to design molecules that efficiently bind to receptors within a certain time frame to elicit a desired therapeutic effect. Other examples in biology include neuronal systems, in which a neuron fires only when a fluctuating voltage level first crosses a specified threshold [15, 16].

**Physics**

Random walks in ordered and disordered media are used to model a wide range of physical processes [17]. Studies of first-passage statistics of these random walks allow us to obtain information about the medium – for example, the time taken for a diffusing Brownian particle to cover a fixed distance can be used to infer the diffusion coefficient. Another direct example of the application of first-passage ideas in Physics is the classic Kramers' problem, where we wish to find the rate at which a diffusing particle escapes from a potential well or crosses a potential barrier [18].

**Computer Science**

An imminent example of the application of first-passage times in computer science comes from randomized search algorithms [19]. In simple words, a randomized search algorithm employs

some form of randomness as part of its logic or procedure to perform a search task. In this case, the first-passage time provides an invaluable tool to quantify the time taken for the search task to terminate. Even beyond computer science, search processes are ubiquitous – an animal searching for food or prey, a reactant diffusing around until it finds its target, or simply humans searching for their house keys. All of these examples can be cast as first-passage processes.

## 1.2 Incorporating Imperfect Observations

In the discussion so far, we have put forth the notion of a first-passage process and listed some of its interdisciplinary applications. However, in the examples listed above and in others discussed throughout the vast literature on first-passage processes, there is an implicit assumption of perfect detection conditions – the notional sensor, which monitors the first occurrence of a first-passage event, is active at all times. This is not always realistic.

In several practical applications, there is an energy cost associated with an always-on sensor, and the threshold crossing events in processes of interest can thus be only monitored intermittently. A principal example is the wireless sensor networks widely deployed to monitor rare events at remote locations and operate under tight energy constraints [20, 21]. These sensors are typically not always active in order to optimize power consumption and reduce the need for maintenance [22–24]. Intermittent sensing has been extensively deployed in industrial and military environments [25] to detect events and is even thought to be the future trend for Internet-of-Things and wireless monitoring technologies [26]. In several bio-chemical processes too, the sensors make stochastic transitions between active and inactive states [27]. A relevant example is of the heat shock response in a cell due to environmental stresses [28, 29]. The HSF family of proteins, which upregulate heat shock proteins when the heat stress crosses a threshold, can perform this upregulation if it is present in its trimeric state, while in its monomeric state, it is considered to be inactive.

The precise gap that this thesis wishes to address is the following: the first-passage time statistics carry invaluable information about a stochastic process of interest, but they are often inaccessible to direct measurement. The relevant quantity of interest then is the first detection time, which denotes the first time the time-series is *observed* above the threshold (as schematically outlined in Fig. 1.2). While of utmost practical importance, this quantity has not been discussed

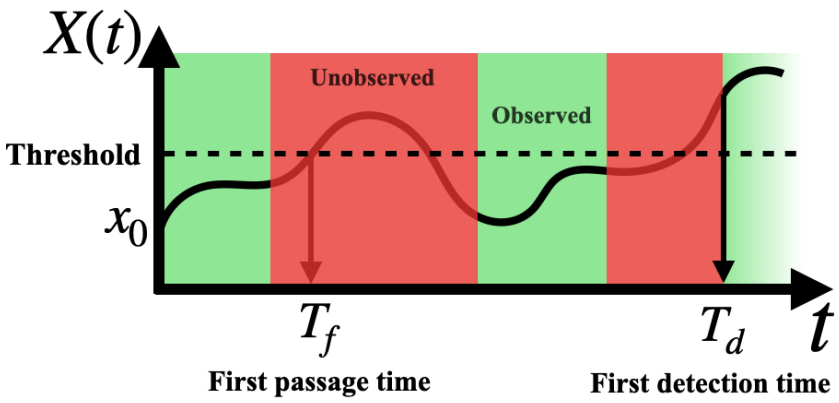


Figure 1.2: A stochastic process $X(t)$ being intermittently observed due to imperfect observations conditions. While imperfect observation conditions are ubiquitous and can arise due to a number of reasons, an important consequence of such conditions is that key quantities, such as the first-passage time, can be missed. Then, the relevant quantity is the first detection time $T_d$, which is the first time when $X(t)$ is observed to be above the threshold. The study of this quantity is a central component of this thesis.

in the literature so far. In this thesis, we wish to uncover the statistics of the first detection time and establish exact results through which the statistics of this observable can be computed in a wide range of stochastic processes of interest. To do so, we build a framework to study the first detection time, allowing us to make three significant advances.

1. We relate the statistics of the first detection time to the first-passage time statistics and leverage it to uncover universal properties about the detection times and their connection with the classic first-passage problems. These results lie at the heart of Chapter 2 of this thesis and have been presented in Refs. [30] and [31].

2. By building a model-free framework, we demonstrate that the first detection time statistics of a stochastic process can be used to recover its first-passage time statistics and infer other physically meaningful quantities and parameters of that stochastic process. These ideas are discussed in detail in Chapter 3 of this thesis and have been published in Ref. [32].

3. The frameworks developed in Chapters 2 and 3 can be extended to applications beyond the realm of first-passage processes. In particular, we demonstrate in Chapter 4 how these frameworks can be used to (a) compute the optimal sampling rate of a first-passage process, (b) obtain the extreme-value statistics of a partially observed time-series, and (c) compute statistics of missing events from a single realization of a sparsely sampled time-series.

## 1.3 The Modeling Approach: Gated First-Passage Processes

In this section, we introduce the reader to the basic setting and modeling approach that we will work with to address the central question of studying first-passage processes under conditions of imperfect observations. Our modeling approach consists of two independent components.

- First, we consider an "underlying process" $X_{x_0}(t)$, initially at $x_0$, modeled as a continuous-time Markov process in 1-dimension, i.e., in continuous space, we can assume that $X_{x_0}(t)$ is a fluctuating quantity that can possibly take real values, whereas in discrete space, it can take integer values. In both cases, we are interested in the time taken for $X_{x_0}(t)$ to cross a pre-defined threshold $x^*$ for the first time, called the first-passage time. This random variable is denoted by $T_f(x^*|x_0)$ and its probability density is written as $F_t(x^*|x_0)$.

- Second, to model imperfect observation conditions, we assume that the stochastic process of interest is being monitored by a sensor that stochastically switches between on and off states. We model this sensor by a two-state continuous-time Markov process that intermittently switches between an active ($A$) state and an inactive ($I$) state. This sensor switches from state $A$ to $I$ at rate $\alpha$, and from $I$ to $A$ at rate $\beta$. For $\sigma_0, \sigma \in \{A, I\}$, we define $p_t(\sigma|\sigma_0)$ to be the probability that the sensor is in state $\sigma$ at time $t$, given that it was in state $\sigma_0$ initially.

The sensor, as described above, acts like a gate – the process of interest can only be observed when the sensor is on (the gate is "open") and when the sensor is off (the gate is "closed"), the process cannot be observed. We thereby term the study of first-passage processes being monitored by such a sensor as *gated first-passage processes*.

It is possible that when the first-passage event occurs (at time $T_f(x^*|x_0)$), the sensor is off, and thus this event is missed. In such a case, the relevant quantity of interest is the first detection time $T_d(x_0, \sigma_0)$, which denotes the first time the process is *observed* to be above the threshold $x^*$ given that the process was initially at $x_0$ and the initial state of the sensor was $\sigma_0$. More precisely, this refers to the first time when the underlying process is in a state $x > x^*$ while the sensor is in its active state $A$. Understandably, the first detection time $T_d(x_0, \sigma_0)$ is also called the gated first-passage time, and we denote its probability density by $D_t(x_0, \sigma_0)$.

### 1.3.1 Analogy with Imperfect Chemical Reactions

The framework outlined above has a close analogy with a class of imperfect chemical reactions called gated chemical reactions. To illustrate this analogy, we consider a prototypical scenario where a diffusing reactant can potentially react when it collides with a target. However, we additionally require the collision to be 'fertile'. It is known that certain reactants undergo stochastic transitions between reactive and non-reactive internal states. These transitions act like a gate: a reaction can only happen when the gate is open, *i.e.,* the reactant collides with the target when it is in its reactive internal state. This analogy is schematically illustrated in Fig. 1.3.

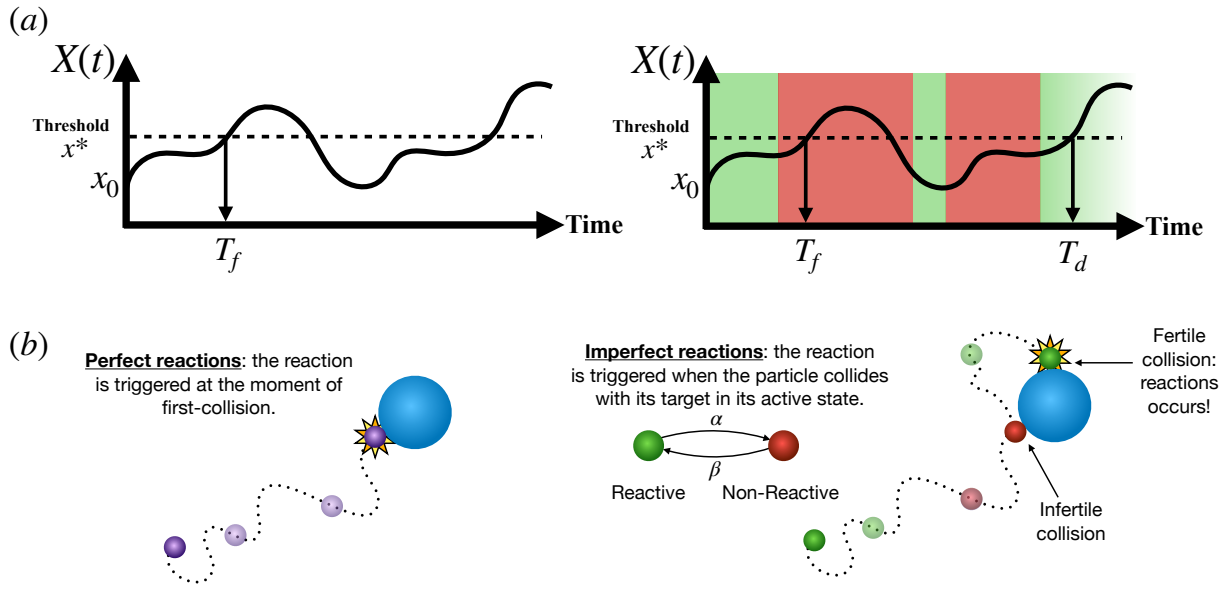


Figure 1.3: The analogy between (a) intermittent sensing of a first-passage process and (b) a gated reaction. In the case of the first detection of the threshold crossing event under intermittent sensing, the detection can only take place when the process is above the threshold *and* the sensor is on. In a similar vein, a gated reaction is triggered when the reactant collides with its target *while* being in its reactive state.

These chemical reactions are termed gated reactions. This term was originally introduced in the work of Perutz and Mathews on ligand binding by methaemoglobin [33]. The macroscopic kinetics of these so-called gated reactions has a history spanning over four decades now [9, 10, 34–44], and more recently, the study of single-particle gated reactions has gained interest [31, 32, 45–49].

An important consequence of this close analogy between the problem of detecting threshold crossing events under intermittent sensing and computing the reaction time statistics of gated

chemical reactions is that both these problems can be studied using the same formalism. Though the central theme of the thesis is studying threshold crossing events in stochastic time-series, we will demonstrate in subsequent chapters how our results can be leveraged to provide solutions to some outstanding puzzles in the literature of gated chemical reactions.

## 1.4 Conclusion

Having established the key motivations and setting up the basics of our problem statement and modeling approach, we are now ready to dive into the more technical aspects of this thesis. To ensure a smooth reading experience, we have tried to keep the presentation of the subsequent chapters self-contained to a large extent. This introductory chapter sets the stage for each of the following chapters to be read independently of each other. Our central objective throughout this thesis is to uncover new insight into the statistics of gated first-passage processes and to better understand the cross-disciplinary implications of our results.

# CHAPTER 2

# First Detection of Threshold Crossing Events under Intermittent Sensing

In the previous chapter, we established the motivation for our work and the preliminary setup of our approach. We now shift our focus towards making those ideas more concrete. In this chapter, we will aim to establish a connection between the statistics of the first-passage time and the first detection time of a stochastic process and then leverage it to derive general formulas for computing the statistics of the first detection times.

## 2.1 Problem Statement

Our primary objective in this chapter is to extend the standard notion of threshold crossing and first-passage times to include the concept of intermittent sensing by an independent sensor that stochastically switches between active and inactive states. The central quantity of interest is the first detection time distribution of the threshold crossing event by the sensor. This can be thought of as first detection of an extreme event [50–52] or a general threshold activated process [53–57] under intermittent sensing.

Concretely, we will assume throughout this chapter that the underlying process $X_{x_0}(t)$, initially in state $x_0$, follows Markovian evolution. The case of discrete state space and continuous state space will be treated separately for reasons explained in Sec. 2.3.2. In the case of discrete states, we will assume that $X_{x_0}(t)$ can take integer values $x \in \mathbb{Z}$ and transitions take places only between nearest integers, i.e., the only allowed transitions from state $x$ are to states $x+1$ or $x-1$. Similarly, while considering continuous state space, we will assume that the stochastic process $X_{x_0}(t)$ can take real values $x \in \mathbb{R}$, and is continuous. A stochastic sensor intermittently monitors whether the process of interest has crossed the pre-defined threshold $x^*$ or not. A threshold crossing event is detected only if $X_{x_0}(t) \geq x^*$ *and* the sensor is active.

### 2.1.1 Dynamics of the Gate: Explicit Formula for $p_t(\sigma|\sigma_0)$

The sensor is modeled as a two-state continuous-time Markov process that intermittently switches between an active ($A$) state and an inactive ($I$) state. This sensor switches from state $A$ to $I$ at rate $\alpha$, and from $I$ to $A$ at $\beta$. For $\sigma_0, \sigma \in \{A, I\}$, we define $p_t(\sigma|\sigma_0)$ to be the probability that the gate is in state $\sigma$ at time $t$, given that it was in state $\sigma_0$ initially, and let $\pi_A = \beta/\lambda$ and $\pi_I = \alpha/\lambda$ denote the equilibrium occupancy probabilities of states $A$ and $I$ respectively, where $\lambda = \alpha + \beta$ is the relaxation rate to equilibrium.

To obtain the sensor dynamics propagator $p_t(\sigma|\sigma_0)$, we note that $p_t(A|A)$ is governed by the following differential equation

$$\frac{dp_t(A|A)}{dt} = -\alpha p_t(A|A) + \beta\left(1 - p_t(A|A)\right), \tag{2.1}$$

and from normalization we have $p_t(I|A) = 1 - p_t(A|A)$. Similarly,

$$\frac{dp_t(A|I)}{dt} = -\alpha p_t(A|I) + \beta\left(1 - p_t(A|I)\right), \tag{2.2}$$

and $p_t(I|I) = 1 - p_t(A|I)$. The solutions for these differential equations are

$$\begin{aligned} p_t(A \mid I) &= \pi_A(1 - e^{-\lambda t}), \\ p_t(I \mid I) &= \pi_I + \pi_A e^{-\lambda t}, \\ p_t(A \mid A) &= \pi_A + \pi_I e^{-\lambda t}, \\ p_t(I \mid A) &= \pi_I(1 - e^{-\lambda t}). \end{aligned} \tag{2.3}$$

It is evident that in the long time limit, these probabilities tend to the corresponding equilibrium occupancy probabilities, *i.e.,* $\lim_{t\to\infty} p_t(A|A) = \lim_{t\to\infty} p_t(A|I) = \pi_A$ and $\lim_{t\to\infty} p_t(I|A) = \lim_{t\to\infty} p_t(I|I) = \pi_I$.

It is important to note that $\sigma_0$ need not only be either $A$ or $I$, but can also be a mixture, where it is initially in state $A$ with some probability $p_A$ and in $I$ with probability $p_I$. One such practically relevant mixture preparation is the equilibrium initial condition $\sigma_0 = E$ where $p_A = \pi_A$ and $p_I = \pi_I$. This initial condition could especially be important in some cases where the sensor initialization is not possible, e.g. gated chemical reactions. Thus, the most natural initial condition is $\sigma_0 = E$, which is asymptotically reached starting from any other initial condition.

## 2.2 Connecting the First-Passage and First Detection Statistics

The first step of our analysis consists of decomposing the first detection time density $D_t(x_0, \sigma_0)$ into two parts as follows

$$D_t(x_0, \sigma_0) = F_t(x^*|x_0)p_t(A|\sigma_0) + \int_0^t F_{t'}(x^*|x_0)p_{t'}(I|\sigma_0) \cdot D_{t-t'}(x^*, I)\, dt'. \tag{2.4}$$

The above equation essentially classifies all possible ways in which a detection event can take place at time $t$ in two parts.

1. The first term on the RHS accounts for all the events when the first-passage occurs at time $t$, and it is immediately detected as the sensor is active.

2. The second term on the RHS represents the weight of all events in which the first-passage occurs at some time $t' < t$, but is missed as the sensor is inactive. But then, starting from the new initial condition where the process is at $x^*$ and the sensor is in state $I$, a detection event occurs in time $t - t'$.

Equation (2.4) forms the backbone of our analysis and holds for both types of processes considered in this thesis – continuous Markov processes or with discrete states and nearest neighbor transitions. By defining the Laplace transform of a probability density $f(t)$ as

$$\mathcal{L}\{f(t)\} = \widetilde{f}(s) = \int_0^\infty e^{-st} f(t)\, dt, \tag{2.5}$$

we note that the Laplace transform of $D_t(x_0, \sigma_0)$ satisfies

$$\widetilde{D}_s(x_0, \sigma_0) = \mathcal{L}\{F_t(x^*|x_0)p_t(A|\sigma_0)\} + \mathcal{L}\{F_t(x^*|x_0)p_t(I|\sigma_0)\} \cdot \widetilde{D}_s(x^*, I). \tag{2.6}$$

Equation (2.6) uses the convolution theorem [17] which can be simply stated as

$$\mathcal{L}\left\{\int_0^t f(t')g(t-t')\, dt'\right\} = \widetilde{f}(s)\widetilde{g}(s). \tag{2.7}$$

To proceed with our analysis, we shift our focus to the term $D_t(x^*, I)$, which denotes the probability density of the first detection of a threshold crossing event occurring at time $t$, given that the underlying process starts from the threshold $x^*$ when the sensor is inactive. The analysis of

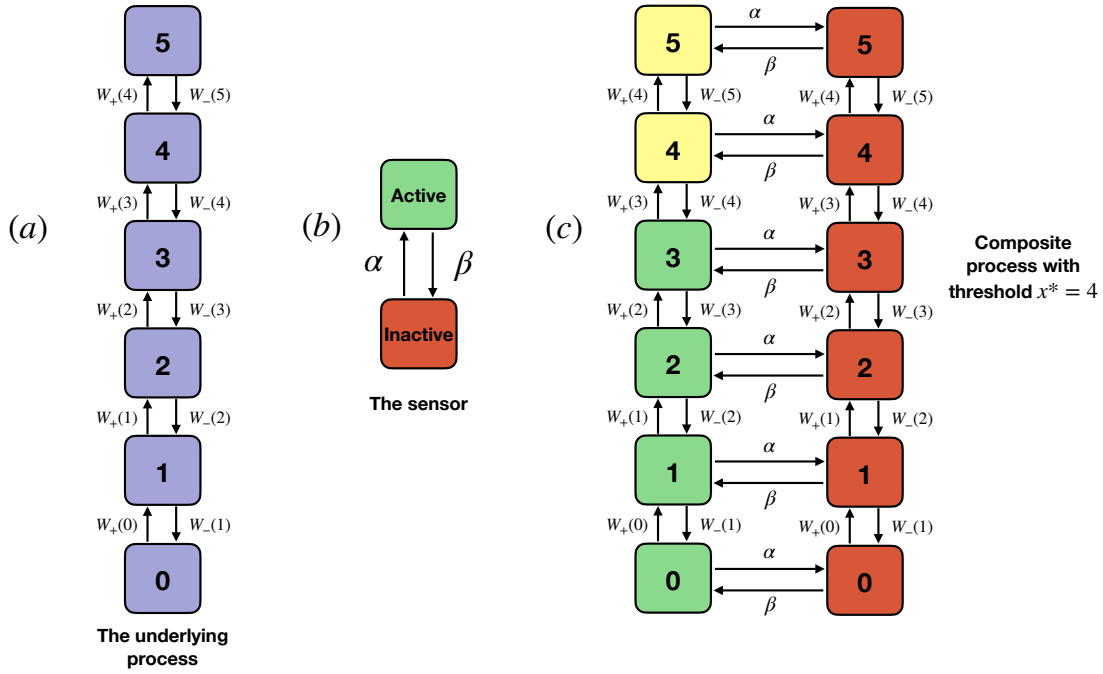


Figure 2.1: (a) An example of a discrete state Markov process – a birth-death process as the underlying process – with 6 states in total, (b) a sensor, modeled as a two-state Markov process, switching between active and inactive states. (c) The composite process with threshold $x^* = 4$. The threshold crossing event can be detected in the states marked in yellow.

this term quite sensitively depends on whether the underlying process of interest is a continuous process or has a discrete state-space.

In the section that follows, we discuss the case of discrete states and illustrate our results. This will be followed by a discussion of why the formalism fails to generalize to continuous processes and how this can be remedied.

## 2.3 Discrete State Markov Processes

To study Markov processes with a discrete state-space, we take the underlying process of interest to be a Markovian continuous-time birth-death process (BDP), which has previously been used to study a variety of processes [58–69]. Though in this section, we consider BDPs with a finite number of states, it is important to note that generalization to discrete state processes with infinite number of states is straightforward.

The state of the BDP can be interpreted as the stress or damage accumulated over time or any other physical quantity where threshold crossing is of prime interest. The BDP is defined

on the state space $\mathcal{S} = \{0, 1, 2, \cdots, N\}$ with its dynamics governed by the rates $W_+(j)$ and $W_-(j)$ for transitioning from state $j$ to states $j+1$ and $j-1$ respectively, where $j \in \mathcal{S}$, with $W_+(N) = W_-(0) = 0$, while $W_\pm(j) > 0$ for $j \notin \{0, N\}$. Figure 2.1(a) is an illustration of a BDP with $N = 5$. The probability of finding the BDP in state $x \in \mathcal{S}$ at time $t$, given that the system started from state $x_0 \in \mathcal{S}$ initially, is given by the propagator $C(x, t|x_0)$, and its Laplace transform is denoted by $\widetilde{C}(x, s|x_0)$. A well studied quantity of the BDP is the first-passage time distribution, denoted by $F_t(x^*|x_0)$, which is the probability density that the BDP reaches state $x^*$ for the first time, at time $t$, given that it started from state $x_0$. Through the renewal formula [1], the Laplace transform of the first-passage time density is given by $\widetilde{F}_s(x^*|x_0) = \frac{\widetilde{C}(x^*,s|x_0)}{\widetilde{C}(x^*,s|x^*)}$, for $x_0 \neq x^*$. This analysis assumes perfect detection, *i.e.*, as soon as the threshold $x^*$ is reached, the event is detected.

As previously outlined, this BDP is being monitored by a stochastic sensor depicted in Fig. 2.1 (b). The Markov diagram of the composite process, *i.e.*, the underlying process and the sensor combined, is shown in Fig. 2.1 (c) for the special case of $N = 5$, and threshold $x^* = 4$. The composite process is another continuous-time Markov process on the state space $\mathbb{S} = \mathcal{S} \times \Omega$. The key object of interest is the statistics of the first detection time of a threshold crossing event, defined as the first time when the composite process is found in any of the states $(x, A)$ such that $x \geq x^*$, where $x^*$ is the pre-defined threshold. The states in which such a detection event can take place, called "absorbing states", are denoted in yellow color in Fig. 2.1 (c). The composite process has a total of $N - x^* + 1$ absorbing states.

In the analysis that follows, the knowledge of $C(x^*, t|x_0)$ for the BDP is assumed. This is known exactly for a variety of examples [60, 70, 71]. Furthermore, the propagator can be obtained, in principle, for any BDP governed by an $N \times N$ tridiagonal Markovian transition matrix $\mathbb{W}$ as $C(x^*, t|x_0) = \langle x^*| e^{\mathbb{W}t} |x_0\rangle$ where $\langle l| = (0\ 0\ 0 \ldots 0\ 1\ 0 \ldots 0)$ denotes a row vector with $1$ as its $l^{\text{th}}$ element, with $0$ elsewhere.

## 2.3.1 Results

### 2.3.1.1 Distribution of the First Detection Time

Equation (2.4) contains the quantity $D_t(x^*, I)$, which is central to our analysis. In fact, the computation of this quantity requires different approaches in discrete and continuous state-space set-

tings. For the case of discrete states, it can be seen that the quantity $D_t(x^*, I)$ satisfies the following decomposition

$$D_t(x^*, I) = \beta e^{-\beta t} \int_t^\infty F_{t'}(x^* - 1|x^*)\, dt' + \int_0^t e^{-\beta t'} F_{t'}(x^* - 1|x^*) \cdot D_{t-t'}(x^* - 1, I)\, dt'. \quad (2.8)$$

In the above equation, we express the density $D_t(x^*, I)$ as a sum of two contributions:

1. The first term of the RHS denotes the weight of events where the sensor turns active at time $t$, and until then, the underlying process, which is initially at $x^*$, has not ventured to states below $x^*$.

2. The second term of the RHS accounts for the possibilities where the underlying BDP goes to state $x^* - 1$ at some time $t' < t$ before the sensor has been able to turn active. Starting from the new initial condition where the BDP is in state $x^* - 1$ and the sensor is in state $I$, we now require a detection event to occur in time $t - t'$.

Compactly, we may express Eqs. (2.4) and (2.8) as

$$D_t(x_0, \sigma_0) = f_1(t) + \int_0^t f_2(t') D_{t-t'}(x^*, I) dt', \quad (2.9)$$

$$D_t(x^*, I) = f_3(t) + \int_0^t e^{-\beta t'} F_{t'}(x^* - 1|x^*) D_{t-t'}(x^* - 1, I) dt' \quad (2.10)$$

where $x_0 < x^*$ and we define the following functions for brevity:

$$f_1(t) = F_t(x^*|x_0) p_t(A|\sigma_0), \quad (2.11)$$

$$f_2(t) = F_t(x^*|x_0) p_t(I|\sigma_0), \quad (2.12)$$

$$f_3(t) = \beta e^{-\beta t} \int_t^\infty F_{t'}(x^* - 1|x^*) dt'. \quad (2.13)$$

We obtain $D_t(x^* - 1, I)$ from Eq. (2.9) in terms of $D_t(x^*, I)$, and taking a Laplace transform of Eqs. (2.9) and (2.10), we can write

$$\widetilde{D}_s(x_0, \sigma_0) = \widetilde{f}_1(s) + \frac{\widetilde{f}_2(s) \left( \widetilde{f}_3(s) + \widetilde{f}_4(s) \widetilde{F}_{s+\beta}(x^* - 1|x^*) \right)}{1 - \widetilde{f}_5(s) \widetilde{F}_{s+\beta}(x^* - 1|x^*)}. \quad (2.14)$$

where we define:

$$f_4(t) = F_t(x^*|x^* - 1)p_t(A|I), \tag{2.15}$$

$$f_5(t) = F_t(x^*|x^* - 1)p_t(I|I). \tag{2.16}$$

Equation 2.14 is a central result of this chapter that asserts that the first detection time statistics can be obtained in terms of the first-passage time distribution. The first term on the RHS, $f_1(t)$, denotes the trajectories where the first-passage time and first detection time coincide, whereas the second term accounts for all trajectories where the first-passage event goes unnoticed, and detection happens at a later time. In the limit of $\alpha \to 0^+$, then $f_2(t) \to 0$, when $\sigma_0 = A$, and it leads to $D_t(x_0, \sigma_0) = F_t(x^*|x_0)$. This is consistent with the expectation that in the $\alpha \to 0^+$ limit, deactivation of the sensor is extremely unlikely and renders the composite process equivalent to a simple BDP.

### Interpreting the First Detection Time Formula

We noted in Eq. 2.14 that in Laplace space, $\widetilde{D}_s(x_0, \sigma_0)$ is expressed as

$$\widetilde{D}_s(x_0, \sigma_0) = \underbrace{\widetilde{f}_1(s)}_{\substack{\text{First detection} \\ \text{at first-passage}}} + \underbrace{\frac{\widetilde{f}_2(s)\left(\widetilde{f}_3(s) + \widetilde{f}_4(s)\widetilde{F}_{s+\beta}(x^* - 1|x^*)\right)}{1 - \widetilde{f}_5(s)\widetilde{F}_{s+\beta}(x^* - 1|x^*)}}_{\substack{\text{First detection happening} \\ \text{strictly after first-passage event}}}.$$

The second term on the RHS can be understood intuitively if expressed as the following

$$\underbrace{\widetilde{f}_2(s)}_{\substack{\text{Factor I:} \\ \text{First-passage} \\ \text{while sensor} \\ \text{is inactive}}} \cdot \underbrace{\frac{1}{1 - \widetilde{f}_5(s)\widetilde{F}_{s+\beta}(x^* - 1|x^*)}}_{\substack{\text{Factor II: Accounts for the} \\ \text{number of undetected threshold} \\ \text{crossings before first detection}}} \cdot \underbrace{\left(\widetilde{f}_3(s) + \widetilde{f}_4(s)\widetilde{F}_{s+\beta}(x^* - 1|x^*)\right)}_{\substack{\text{Factor III: Ensures detection} \\ \text{of threshold crossing event}}}. \tag{2.17}$$

Factor II is the sum of the following geometric series in Laplace space, which accounts for the number of threshold crossings that go undetected before eventual detection:

$$\begin{aligned}\frac{1}{1 - \widetilde{f}_5(s)\widetilde{F}_{s+\beta}(x^* - 1|x^*)} =& 1 + \left(\widetilde{f}_5(s)\widetilde{F}_{s+\beta}(x^* - 1|x^*)\right) \\ &+ \left(\widetilde{f}_5(s)\widetilde{F}_{s+\beta}(x^* - 1|x^*)\right)^2 + \left(\widetilde{f}_5(s)\widetilde{F}_{s+\beta}(x^* - 1|x^*)\right)^3 + \cdots\end{aligned} \tag{2.18}$$

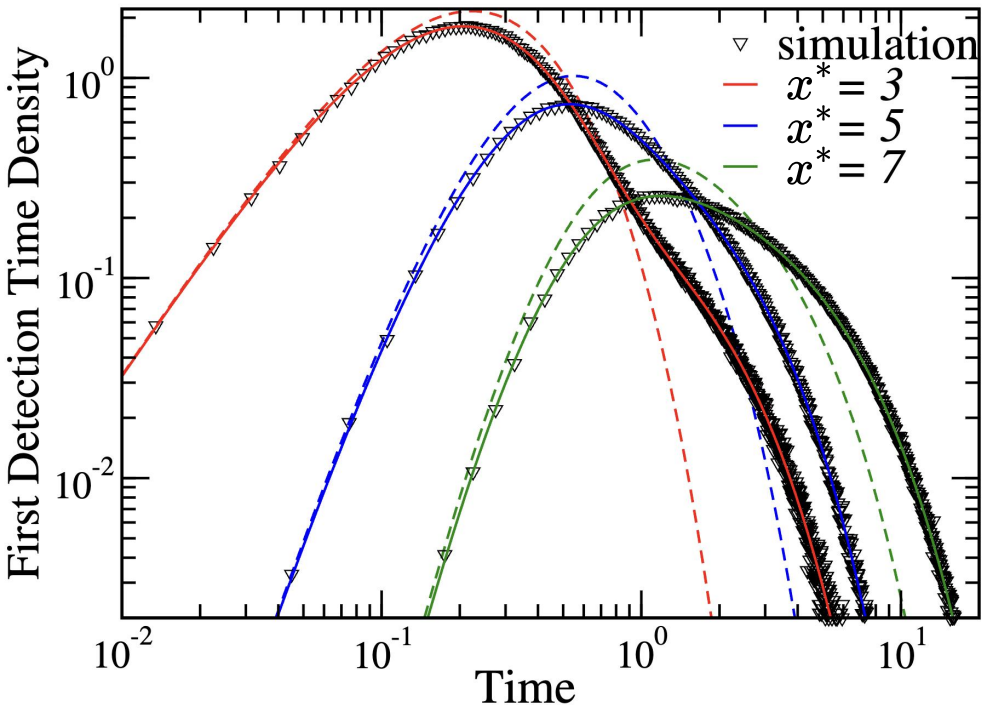


Figure 2.2: The first detection time distribution for the BDP with stochastic switching (solid lines), with $x_0 = 0, N = 20, \gamma = 0.1$ and $k = 1$, shown for threshold values $x^* = 3, 5, 7$ and $\alpha = \beta = 1$. The symbols are from simulations. The dashed lines are first detection time distributions if the sensor is *not* intermittent and is always on.

Factor III consists of two different terms:

1. $\widetilde{f}_3(s)$: since the last undetected threshold crossing, the birth-death process stays above the threshold, and at time $t$, the sensor becomes active, and thus the threshold crossing event is detected.

2. $\widetilde{f}_4(s)\widetilde{F}_{s+\beta}(x^* - 1|x^*)$: since the last undetected threshold crossing, the birth-death process stays above the threshold for some time and remains undetected. It then comes below the threshold, and finally, the birth-death process reaches the threshold at time $t$ when the sensor is active.

Both the terms add up to give two different ways of detecting the threshold crossing event. Overall, our central result computes the sum of probabilities of all trajectories where the first detection of the threshold crossing event occurs at time $t$, and the sum can be expressed completely in terms of the first-passage probabilities without any imperfect sensing.

To illustrate these results, consider a BDP with transition rates $W_+(j) = \gamma(N - j)$ and

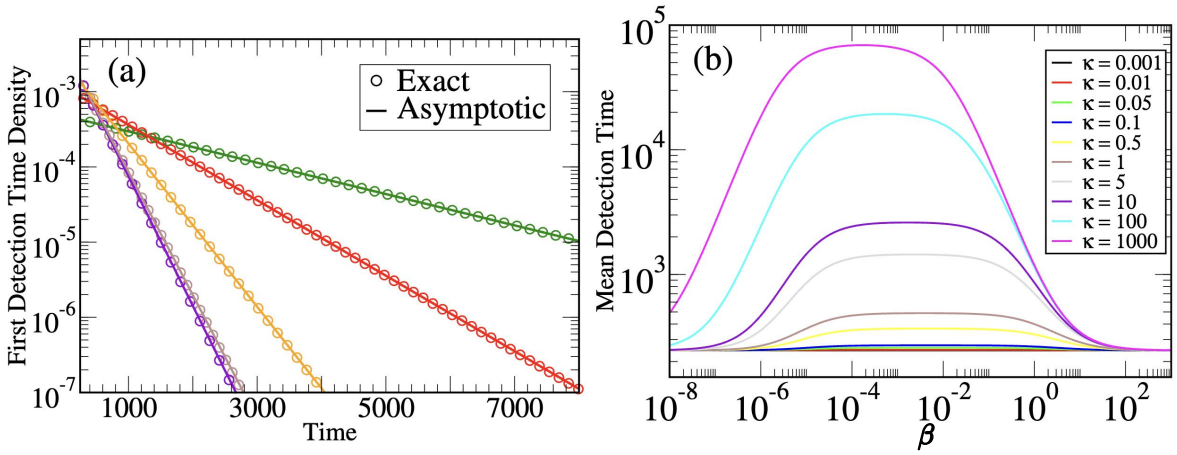


Figure 2.3: (a) Asymptotic first detection time distribution for $t >> 1$ with $x^* = 5$ for $(\alpha, \beta)$ = $(1,1), (0.1,1), (1,0.1), (10,1)$, and $(1,10)$. Other parameters are the same as in Fig. 2.2. (b) Mean detection time as a function of $\beta$, where along each curve $\kappa = \frac{\alpha}{\beta}$ is held constant.

$W_-(j) = kj$, with $j \in \{0, 1, 2, \cdots, N\}$. These rates were previously used to model threshold crossing processes [54] in the context of triggering of biochemical reactions [53]. Figure 2.2 shows the first detection time distribution for this process with parameters $x_0 = 0, N = 20, \gamma = 0.1$ and $k = 1$, for threshold values $x^* = 3, 5$ and 7, and $(\alpha, \beta) = (1,1), (10,1)$ and $(1,10)$. This figure shows analytical results (solid lines) for which inverse Laplace transform of Eq. 2.14 has been numerically performed, and simulations (open triangles) were generated by performing $10^7$ realizations of the stochastic process. An excellent agreement is observed between the analytical result and the simulations. For comparison, the case of the sensor being always-on is also shown (as dashed lines), and it effectively corresponds to the first-passage time distribution. If the sensor is initially active, then for $t << \frac{1}{\alpha}$, the first detection time distribution matches with the first-passage time distribution. This is because, in this limit, the threshold is crossed earlier than the typical timescale for the inactivation of the sensor. Starting from around $t \approx \frac{1}{\alpha}$, the first detection time distribution deviates from the first-passage time distribution, a feature captured by the analytical result. For $t >> \frac{1}{\alpha}$, both the first detection time distribution and first-passage time distribution show an exponential tail with different decay rates.

The Laplace transform obtained in Eq. 2.14 is of utmost importance as it allows us to systematically obtain the moments of the first detection time density. The mean first detection time can be computed as

$$\langle T_d(x_0, \sigma_0) \rangle = -\frac{d}{ds} \widetilde{D}_s(x_0, \sigma_0) \Big|_{s=0}. \tag{2.19}$$

The Laplace transform also contains valuable information about the tail of the first detection time distribution. For a BDP, with the same parameters as for Fig. 2.2, the first detection time distribution takes the asymptotic form $\frac{1}{\langle T_d \rangle} e^{-t/\langle T_d \rangle}$ for $t >> 1$. In Fig. 2.3(a) for a threshold of $x^* = 5$, and for several pairs of $(\alpha, \beta)$, this asymptotic result stands validated. Note that, in general, the asymptotic tail need not be Poisson-like. A detailed discussion on these asymptotics is given in Refs. [72–74].

Further, we define $\kappa = \alpha/\beta$, which is the fraction of time the sensor spends in the inactive state. If $\kappa << 1$, then the sensor is active nearly all the time. The mean detection time $\langle T_d \rangle$ is plotted as a function of $\beta$ for a constant value of $\kappa$ in Fig. 2.3(b). As this figure reveals, the $\langle T_d \rangle \approx \langle T_f \rangle$ for small and large values of $\alpha$. For intermediate values of $\alpha$, the mean first-passage and detection times can differ from one another by several orders of magnitude depending on the value of $\kappa$ – larger $\kappa$ leads to larger $\langle T_d \rangle$. This has a surprising outcome for event detections. Physically, this implies that even if $\kappa >> 1$, where the sensor spends most of its time in the inactive state, the detection can happen at timescales comparable to $\langle T_f \rangle$ as long as the time scales of the sensor switching is much faster than the intrinsic time scale of the underlying process. This effectively renders the switching to have little effect on the detection times. Though seemingly counterintuitive, a similar result was also noted in a different scenario of diffusing particles searching for an intermittent target [75].

#### 2.3.1.2 Splitting Probabilities

A key feature in the problem of detecting threshold crossing events under intermittent sensing is that the detection of the threshold crossing event does not necessarily happen at state $x^*$ of the BDP, but can happen at any state $\zeta \in \{x^*, x^*+1, \cdots, N\}$. This crucial information is contained in the *splitting probabilities* $H_\zeta$, defined as the probability that the event is detected in state $\zeta$.

For brevity, the following quantities are defined:

$$h_1(t) = F_t(x^* - 1|x^*)e^{-\beta t}, \tag{2.20}$$

$$h_2(k, x^*, t) = \beta e^{-\beta t}\, \hat{P}_t(k|x^*), \tag{2.21}$$

for $k \in \{x^*, x^*+1, \cdots, N\}$, where $\hat{P}_t(k|x^*)$ denotes the probability that the underlying BDP is found in state $k$ at time $t$, starting from state $x^*$ without visiting the state $x^* - 1$ during this

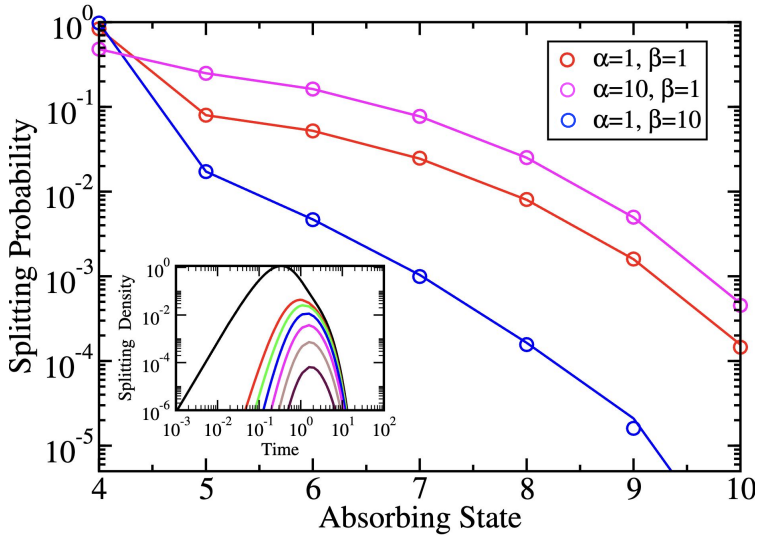


Figure 2.4: Splitting probability for states of the underlying process (lines), for $\gamma = 1$, $k = 1$, $N = 10$, $x_0 = 0$, $x^* = 4$, and three different pairs of $(\alpha, \beta)$ = $(1, 1)$, $(1, 10)$, and $(10, 1)$. Symbols are from simulations. (Inset) Splitting probability density $H_t(\zeta)$ with $\zeta$ taking values from 4 to 10, as a function of time, for $(\alpha, \beta) = (1, 1)$.

process. By performing an analysis similar to the computation of the first detection time density, the density $H_t(\zeta)$ of the threshold crossing event being detected at $\zeta$ at time $t$ can be obtained. Summing over the weights of all trajectories that lead to the threshold crossing event at $\zeta = x^*$ at time $t$, the Laplace transform of splitting probability density $\widetilde{H}_s(x^*)$ is

$$\widetilde{H}_s(x^*) = \widetilde{f}_1(s) + \frac{\widetilde{f}_2(s)\left(\widetilde{h}_1(s)\widetilde{f}_4(s) + \widetilde{h}_2(x^*, x^*, s)\right)}{1 - \widetilde{h}_1(s)\widetilde{f}_5(s)} \tag{2.22}$$

and for $\zeta = x^* + r$, where $r \in \{1, 2, \cdots, N - x^*\}$, we obtain

$$\widetilde{H}_s(x^* + r) = \frac{\widetilde{f}_2(s)\widetilde{h}_2(x^* + r, x^*, s)}{1 - \widetilde{h}_1(s)\widetilde{f}_5(s)}. \tag{2.23}$$

The splitting probability $H_\zeta$ can thus be obtained as $H_\zeta = \int_0^\infty dt\, H_t(\zeta)$, and is equal to the $s \to 0$ limit of $\widetilde{H}_s(\zeta)$. Figure 2.4 shows the splitting probabilities $H_\zeta$ for different values of $\zeta$, for the parameter values $\gamma = 1$, $k = 1$, $N = 10$, $x_0 = 0$, $x^* = 4$ and three different pairs of $(\alpha, \beta)$ – $(1, 1), (10, 1)$ and $(1, 10)$. This demonstrates an excellent agreement between the analytical and simulation results. Furthermore, the inset in Fig. 2.4 shows the analytically computed splitting probability density for $(\alpha, \beta) = (1, 1)$.

#### 2.3.1.3 First-Passage Time Distribution Conditioned on a Detection Event

If the first detection of a threshold crossing event happens at time $T_d$, what can we say about the first-passage time $T_f$? This has practical value as it estimates the first occurrence time for an event that possibly went undetected. In sensors that detect abnormal voltage fluctuations (with potential for damage), $T_f$ corresponds to the time until when the device being monitored was fully functional, and $T_d$ denotes the time when the sensor detects the large fluctuation.

We define $F_{T_f}(m|n_0, \sigma_0, T_d)$ to be the density that the first-passage to the threshold $x^*$ happens at time $T_f$, conditioned on the fact that the first detection of the threshold crossing event happens at $T_d$, and that the underlying process starts from a state $x_0$ whereas the sensor starts from state $\sigma_0$. Clearly, for $T_f > T_d$, $F_{T_f}(x^*|x_0, \sigma_0, T_d) = 0$.

For $T_f < T_d$, we are interested in the trajectories that reach the threshold $x^*$ for the first time at $T_f$, but go undetected, and eventually, the threshold crossing event is detected at time $T_d$. We can break each such trajectory into two parts: the evolution up to time $T_f$ and the evolution up to time $T_d$, starting from time $T_f$. The first part of each trajectory is a *first-passage trajectory*, *i.e.,* one which reaches the threshold for the first time at time $T_f$. We can immediately also conclude that at time $t = T_f$, the state of the underlying birth-death process must be equal to the threshold, and the state of the sensor must have been inactive. Furthermore, the second part of each trajectory is a *first detection trajectory*, which starts from an initial state such that the birth-death process is at the threshold and the sensor is inactive, and subsequently, the first detection of the threshold crossing event happens at time $T_d$. Putting this together, we have

$$F_{T_f}(x^*|x_0, \sigma_0, T_d) = F_{T_f}(x^*|x_0) \cdot p_{T_f}(I|\sigma_0) \frac{D_{T_d - T_f}(x^*, I)}{D_{T_d}(x_0, \sigma_0)} \tag{2.24}$$

where the denominator $D_{T_d}(x_0, \sigma_0)$ is due to the fact that we are looking at the subset of trajectories, which are conditioned to undergo the first detection event at time $T_d$. This shows that the first-passage time distribution conditioned on detection at a specific time $F_{T_f}(x^*|x_0, \sigma_0, T_d)$ can be expressed explicitly as the unconditioned first-passage time distribution $F_{T_f}(x^*|x_0)$, multiplied by additional *tilting* factors which ensure that the threshold crossing event is detected exactly at $T_d$, after it goes undetected at $T_f$.

A similar argument enables us to see that for $T_f = T_d$, we have

$$F_{T_f}(x^*|x_0, \sigma_0, T_d = T_f) = F_{T_f}(x^*|x_0)\frac{p_{T_f}(A|\sigma_0)}{D_{T_f}(x_0, \sigma_0)}. \tag{2.25}$$

We emphasize again that the calculation of $F_{T_f}(x^*|x_0, \sigma_0, T_d)$ which is the conditioned first-passage time density is extremely important as it allows us to take in the available information (the time of first detection of the threshold crossing event) and improve our estimate of when the first-passage event could have occurred based on that. This calculation falls under the theme of the study of the statistics of *stochastic bridges* – where the initial and final states of the process are known, and we are interested in the computation of the statistics of events in between the final and initial states. The ideas discussed here and the general notion of stochastic bridges will appear again in Sec. 4.3 where we will demonstrate how these ideas can be used to infer missing statistics in real-world time-series data.

#### 2.3.1.4 Applications

These results can be applied to threshold crossing events in processes with other absorbing states. Important examples are models of population dynamics and compartmental models for disease propagation. These models can estimate the time taken for the size of a population or the infected caseload to cross a threshold, and such models contain an absorbing state where the size of the population or number of infected individuals goes to zero. During a pandemic, while the dynamics of the number of infected individuals follows a continuous time BDP, they are intermittently reported in specific time windows. Thus, the formalism developed in this work has practical relevance as well. In Fig. 2.5, the analytical first detection time distribution for the SIS model and the logistic model are shown along with simulation results.

Our work can further be extended to processes with stochastic resetting [76–81], in which some observable such as the accumulated stress or damage can undergo burst-like relaxations. Recently, this process has received considerable research attention with extensive applications that include population dynamics under stochastic catastrophes [82–84] to the dynamics of queues subject to intermittent failure. In Fig. 2.5, the first detection time density under intermittent sensing is shown for two cases: a BDP with simple resets, and with resets that include a refractory period [85]. In both cases, analytical and simulation results are in agreement.

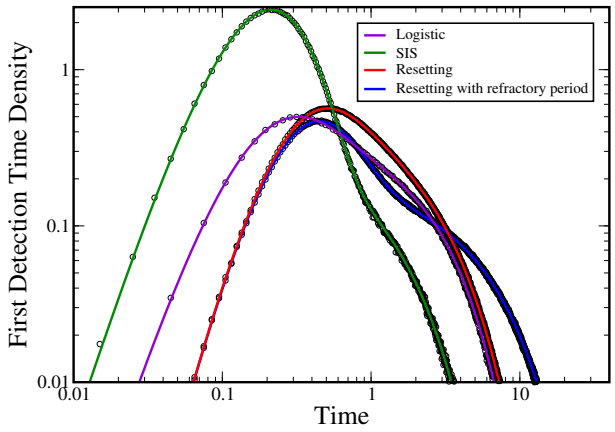


Figure 2.5: First detection time distributions for various processes – Logistic model (violet), SIS epidemiological model (green), BDP with stochastic resets (red) and that with a refractory period (blue) – showing an excellent agreement with numerical simulations of these processes (circles).

## Simulation Details for Fig. 2.5

### SIS Model

The susceptible-infected-susceptible (SIS) model [86] of disease propagation is a stochastic model that describes the spread of a disease in a population, which we consider to be well-mixed. The population consists of two types of individuals: those that are susceptible to the infection and those that are currently infected. The rate at which the disease is transmitted between individuals is $\gamma$, and the recovery rate for each infected individual is $\mu$. If $j$ represents the number of infected individuals, there are $j(N-j)$ pairwise contacts between infected and susceptible people in a well-mixed population. Each of the $j$ infected individuals recovers at rate $\mu$. The rates of increase and decrease of the number of infected individuals is given by

$$W_+(j) = \gamma j(N-j), \qquad W_-(j) = \mu j. \tag{2.26}$$

The parameter values chosen to obtain the curve for Fig. 2.5 are $N = 15, x^* = 7, x_0 = 1, \gamma = 0.1$, and $\mu = 0.4$.

**Extension to SIS models on networks:** It is of great interest to go beyond the fully connected graph (well-mixed limit), and study models of epidemics, like the SIS model, on arbitrary networks – which better describe the heterogeneous connection patterns observed among people in a society. However, analytical calculations for such processes are difficult. In particular, the explicit computation of the probability distributions of the time taken for $x^*$ individuals to be

infected for the first time in a population of $N$ agents has not yet been possible. A difficulty associated with analytical calculations for processes on networks is highlighted in Fig. 2.6.

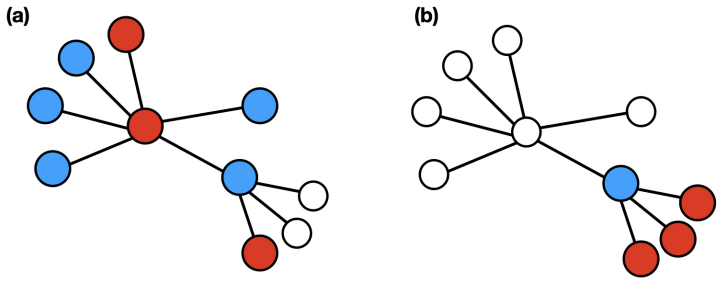


Figure 2.6: A schematic of two scenarios in the SIS model, both of which have 3 infected (red) individuals. The blue circles denote the agents which are at risk of getting infected. While the effective rate at which the number of infected individuals will drop from 3 to 2 is $3\mu$ in both the configurations, the rate for the number of infected people to go from 3 to 4 is different for both configurations – (a) $6\gamma$ and (b) $3\gamma$. Thus, it is difficult to theoretically define a single effective rate by which the number of infected individuals in the population changes from $n$ to $n+1$, as the rates depend on the specific configuration that the process is in.

In order to build a better theoretical understanding of these problems, an approximate scheme has been developed [67–69], wherein the dynamics of the number of infected people in a population is mapped to a birth-death process, whose rates are inferred from stochastic simulations of the exact dynamics on the network of choice. Encoded in these rates is the information of the epidemic parameters, as well as some information about the network structure. In particular, the choice of rates for $W_+(j)$ was chosen to be

$$W_+(j) = \gamma \frac{\sum_q q t_{q,j}}{\sum_q t_{q,j}}, \; 1 \leq j \leq N, \tag{2.27}$$

where $t_{q,j}$ keeps track of how often a state with $j$ infected nodes and $q$ S-I links is visited in the evolution. As mentioned earlier, the rate $W_-(j)$ is already known to be exactly $\mu \cdot j$. Once these rates are numerically determined through stochastic simulations, the formalism we have developed for birth-death processes can be used to estimate the first detection time distribution for the number of infected individuals to cross a threshold.

We note that while the above prescription will allow us to build an approximate scheme for studying threshold crossing events for observables linked to dynamical processes on networks under perfect and imperfect (intermittent) sensing, using recent advances in the study of stochastic processes with memory on networks [87], future works should be dedicated towards obtaining the

first-passage time distribution and first detection time distribution of such observables exactly.

### Logistic Model

The stochastic version of the logistic model describes the dynamics of a population of mortal agents who can reproduce. A constant rate $B$ is assumed for each agent, which means that in a small time interval $dt$, each individual gives birth to a new individual with probability $Bdt$. For each agent, there is a constant death rate (set to $1$) when the population size is low. However, for larger population sizes, the death rate increases by an amount that is quadratic in the size of the population. In the birth-death formulation, the transition rates are

$$W_+(j) = Bj, \qquad W_-(j) = j + Kj^2/N, \tag{2.28}$$

where $K$ determines the strength of influence of competition towards the death rates. The parameter values chosen to obtain the curve for Fig. 2.5 from the main text are $N = 15, x^* = 8, x_0 = 4, B = 1.5$, $K = 0.1$, $\alpha = \beta = 1$.

### Stochastic Resets

In the birth-death process with stochastic resets, apart from the simple birth-death dynamics, with a rate $r$, the underlying process can be *reset* to the state $0$. This dynamics is reminiscent of fluctuating observables that undergo burst-like relaxations. Furthermore, one can also consider the process, where the reset happens to a dormant state, at rate $r$. When this reset happens, the underlying process spends some refractory time in this dormant state and resumes its birth-death dynamics at a rate $y$ from the state $0$. Following similar steps as outlined in the previous sections, the survival probability for a birth-death process with stochastic resets under intermittent sensing can be obtained as

$$\widetilde{S}_s(x_0, A) = \widetilde{Q}(s) + \frac{\widetilde{q}_1(s)\widetilde{q}_2(s)\widetilde{q}_4(s) + \widetilde{q}_1(s)\widetilde{q}_6(s)\widetilde{q}_8(s) + \widetilde{q}_1(s)\widetilde{q}_5(s)}{1 - \widetilde{q}_2(s)\widetilde{q}_3(s) - \widetilde{q}_6(s)\widetilde{q}_7(s)} \tag{2.29}$$

where the following functions are defined:

$$Q(t) = \int_t^\infty dt' F_{t'}^{(r)}(x^*|x_0) \tag{2.30}$$

$$q_1(t) = F_t^{(r)}(x^*|x_0)\, p_t(I|A) \tag{2.31}$$

$$q_2(t) = F_t(x^* - 1|x^*)\, e^{-(\beta+r)t} \tag{2.32}$$

$$q_3(t) = F_t^{(r)}(x^*|x^* - 1)\, p_t(I|I) \tag{2.33}$$

$$q_4(t) = \int_t^\infty dt' F_{t'}^{(r)}(x^*|x^* - 1) \tag{2.34}$$

$$q_5(t) = e^{-(\beta+r)t} \int_t^\infty dt' F_{t'}(x^* - 1|x^*) \tag{2.35}$$

$$q_6(t) = r q_5(t) \tag{2.36}$$

$$q_7(t) = F_t^{(r)}(x^*| - 1)\, p_t(I|I) \tag{2.37}$$

$$q_8(t) = \int_t^\infty dt'\ F_{t'}^{(r)}(x^*| - 1) \tag{2.38}$$

where $F_t^{(r)}(x^*|x_0)$ denotes the first-passage time density from $x_0$ to $x^*$ for the birth-death process with resets being considered, and the state '$-1$' denotes the state in which the birth-death process spends a refractory period, before resuming its dynamics. The survival probability can be leveraged to obtain the detection statistics using the relation

$$\widetilde{D}_s(x_0, \sigma_0) = 1 - s\widetilde{S}_s(x_0, \sigma_0) \tag{2.39}$$

The parameter values chosen to obtain the curve for Fig. 2.5 from the main text are $N = 10, x^* = 5, x_0 = 0, r = \alpha = \beta = 1$ while the birth-death rates were chosen to be the same as the ones for the curves in Fig. 2. In the case where a refractory period is also considered, we choose $y = 1$.

### 2.3.2 Why does this formalism fail to generalize to continuous stochastic processes?

A quick look at Eq. (2.8) reveals the presence of the term $F_t(x^*-1|x^*)$. In the case of a continuous process, e.g., simple diffusion, this term is ill-defined and extremely tricky to deal with. This is due to the fact that for a continuous process, transitions happen from state a $x$ to states $x \pm \epsilon$ where $\epsilon \to 0$. Thus, one is often confronted with terms like $F_t(x^* - \epsilon|x^*)$, which are singular in the limit $\epsilon \to 0$ and thus are tricky to deal with. A diffusing particle starting from $x$ is guaranteed

to immediately hit $x - \epsilon$. In fact, the particle crosses $x - \epsilon$ infinitely many times within an infinitesimally short time period. Does this mean that the statistics of detection times of gated first-passage processes cannot be written in terms of the properties of the ungated process? As we will explain in the next section, this is not true.

## 2.4 Continuous State Markov Processes

In this section, we discuss the computation of the first detection time statistics for continuous Markov processes. The presentation in this section differs from the previous section in two ways.

1. In the previous section, we focused on equations that the distributions of the first detection time and first-passage time satisfied. In this section, however, we will shift our focus to the relations between the random variables themselves. Despite this change in presentation, we note that the two approaches are equivalent.

2. Given that we are working with continuous processes now, it allows us to establish more concrete connections with the gated chemical reactions literature, which has understandably largely focused on continuous processes. Thus, we generalize our analysis (discussed in Sec. 2.4.1) such that the problem of gated chemical reactions and detecting threshold crossing events under intermittent sensing emerge as limiting cases of the model. Moreover, the terms "reaction time" and "detection time" are interchangeable, and their use is context-dependent. Thus, in this chapter, we may often interpret $X_{x_0}(t)$ as the position of a particle stochastically evolving in time, which may 'react' when it is in the target region in its 'reactive' state. The reactive state is akin to the sensor being active, whereas the non-reactive state is like the sensor being inactive.

### 2.4.1 A Generalized Setup

Consider a continuous one-dimensional stochastic process $X_{x_0}(t)$ that undergoes Markovian evolution, with $X_{x_0}(0) = x_0$, and a gated interval $[a, b]$, that stochastically switches between active ($A$) and inactive ($I$) states. It is imperative to note that this generalized formalism of detecting the underlying process in an interval readily yields the limiting cases of gated reactions with point-like targets (when $\lim b \to a$) and threshold crossing under intermittent sensing (when

$\lim b \to \infty$). Thus, this approach provides a unifying framework as illustrated in Fig. 2.7.

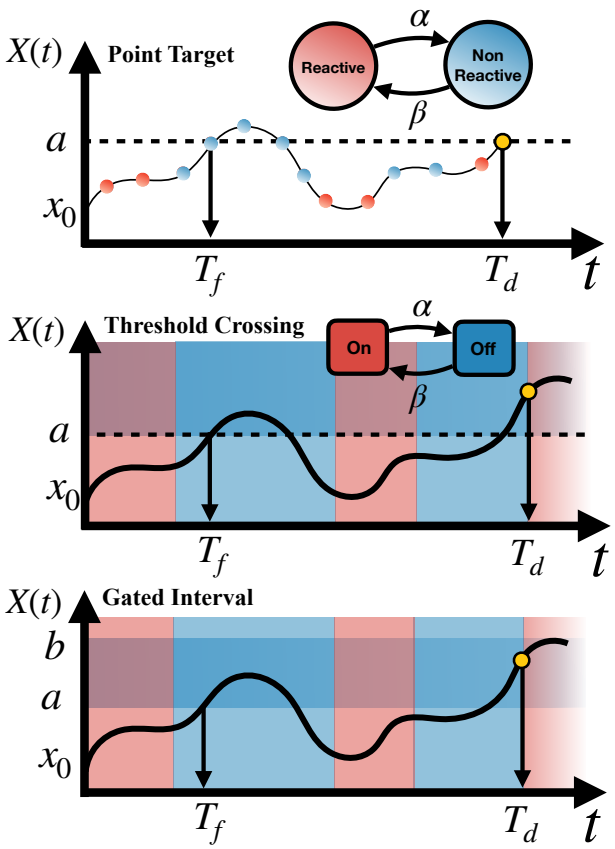


Figure 2.7: Continuous gated first-passage processes. Two central examples of such processes are gated chemical reactions (top panel) and the detection of threshold crossing by intermittent sensing (middle panel). Red represents the molecule being in the reactive state or, respectively, the sensor being on. Blue represents the molecule being in the non-reactive state or, respectively, the sensor being off. The corresponding first-passage times of these processes are denoted by $T_f$, while the reaction/detection times are denoted by $T_d$. The point target (top) and threshold crossing (middle) scenarios can both be seen as special cases of the gated interval problem (bottom).

We define the random variable $T_d(x_0, \sigma_0)$, with $\sigma_0 \in \{A, I\}$, to be the detection time starting from the composite state $(x_0, \sigma_0)$. Namely, $T_d(x_0, \sigma_0)$ is the first time the underlying process $X_{x_0}(t)$ is in the interval $[a, b]$, *while* the gate is in its active state $A$. Let us define the shorthand notation

$$\rho = \begin{cases} a, & \text{if } x_0 \leq a, \\ b, & \text{if } x_0 \geq b. \end{cases} \tag{2.40}$$

We can express the random variable $T_d(x_0, \sigma_0)$ recursively in the following manner

$$T_d(x_0, \sigma_0) = T_f(\rho \mid x_0) + \begin{cases} 0, & \text{if } \sigma_{T_f(\rho|x_0)} = A \\ T_d(\rho, I), & \text{otherwise,} \end{cases} \tag{2.41}$$

where $T_f(\rho \mid x_0)$ is a random variable that denotes the simple ungated first-passage time to $\rho$, starting from $x_0$, and $\sigma_{T_f(\rho|x_0)}$ denotes the state of the gate at this time.

In turn, the recursive relation satisfied by $T_d(\rho, I)$ follows a different logic. Instead of analyzing the renewal of the process when the *first return* to the gated interval happens, we consider the event where the gate state switches from the state $I$ to $A$ for the first time. This allows us to write

$$T_d(\rho, I) = W_\beta + \begin{cases} 0, & \text{if } X_\rho(W_\beta) \in [a, b], \\ T_d(y, A), & \text{if } X_\rho(W_\beta) = y \in (-\infty, a), \\ T_d(y, A), & \text{if } X_\rho(W_\beta) = y \in (b, \infty), \end{cases} \tag{2.42}$$

where $W_\beta$ is the exponentially distributed random variable that denotes the time taken to switch from state $I$ to $A$. The structure of Eq. (2.42) embodies the crucial difference between continuous and discrete-space gated processes.

To circumvent the ill-defined first-return time, we break the subsequent trajectory in Eq. (2.42) into two: (i) First, we let the underlying process evolve as if there is no target for the time $W_\beta$ it takes the sensor to become active. The probability of finding the underlying process at some point $y$ after $W_\beta$ is given by the conserved propagator $C(y, W_\beta \mid \rho)$, i.e., the propagator for the corresponding problem in the absence of any gating or absorbing boundaries. (ii) The process then continues from position $y$ and state $A$. If $y$ happens to fall inside the target interval, we are done. Otherwise, the particle is either above or below the target. The detection time from that state is respectively given by plugging $x_0 = y$ in Eq. (2.41) and the corresponding value of $\rho$ according to Eq. (2.40).

Two things are immediately apparent. First, for this trick to work, we require Markovianity of the underlying process – the exact trajectory that the process has taken to reach $y$ in stage (i) is irrelevant when stage (ii) begins. Second, to know the statistics of the point $y$, knowledge of the corresponding conserved propagator is required. In turn, there is no way to express the first detection time solely in terms of the ungated first-passage time and transition rates $\alpha$ and $\beta$, and

the propagator is carried into this relation. These two realizations are in contrast to the analogue theory of discrete-space gated processes, which do not require a knowledge of the propagator and can also be extended beyond Markov processes (to include renewal processes). Nonetheless, the additional requirements in continuous space are a necessary price to pay for the solution of a much more complex gated problem.

## 2.4.2 Results

We now leverage the above set of equations to compute statistics of the gated first-passage time.

### 2.4.2.1 Mean detection time

Let us assume that the mean detection time is finite, later on we will deal with cases of diverging mean. Taking expectations of both sides of Eq. (2.41), we obtain

$$\langle T_d(x_0, \sigma_0)\rangle = \langle T_f(\rho \mid x_0)\rangle + \langle I_f\rangle \langle T_d(\rho, I)\rangle \,, \tag{2.43}$$

where $I_f$ is an indicator random variable that receives the value $1$ if the particle first arrived at $\rho$ in the inactive state and $0$ otherwise. In Eq. (2.43) we have used the independence of $I_f$ and $T_d(\rho, I)$: $\langle I_f T_d(\rho, I)\rangle = \langle I_f\rangle \langle T_d(\rho, I)\rangle$. For this, we have noted that $T_d(\rho, I)$ is the additional time it takes the reaction to complete in a scenario where the particle arrived at $\rho$ in the inactive state, i.e., conditioned on $I_f = 1$. Thus, while $I_f$ determines if an additional time $T_d(\rho, I)$ should be added or not, it is uncorrelated with the duration of this time. The duration of $T_d(\rho, I)$ does not depend on whatever happened prior to arriving at the interval boundary. The expectation of the indicator function is

$$\langle I_f\rangle = \left\langle p_{T_f(\rho|x_0)}(I \mid \sigma_0)\right\rangle . \tag{2.44}$$

Recalling Eq. (2.3), when $\sigma_0 = I$ we have

$$\langle I_f(\sigma_0 = I)\rangle = \pi_{\mathrm{I}} + \pi_{\mathrm{A}}\widetilde{F}_\lambda(\rho|x_0), \tag{2.45}$$

where $\widetilde{F}_\lambda(\rho|x_0)$ is the Laplace transform of $F_t(\rho \mid x_0)$ evaluated at $s = \lambda$. Similarly, when $\sigma_0 = A$, we have

$$\langle I_f(\sigma_0 = A)\rangle = \pi_{\mathrm{I}}\Big[1 - \widetilde{F}_\lambda(\rho \mid x_0)\Big]. \tag{2.46}$$

Equations (2.45) or (2.46) can, in turn, be plugged into Eq. (2.43) in accordance with the initial condition $\sigma_0$. Note that if the initial state of the gating dynamics is the equilibrium occupancy probabilities, denoted here by $\sigma_0 = E$, we simply have

$$\langle I_f(\sigma_0 = E)\rangle = \pi_{\mathrm{I}}. \tag{2.47}$$

Moving on, taking expectations of both sides of Eq. (2.42) we obtain

$$\langle T_d(\rho, I)\rangle = \beta^{-1} + \int_{-\infty}^{\infty} \widetilde{\Phi}_\rho(\beta)\, \langle T_d(y, A)\rangle \Big[\Theta_-(y) + \Theta_+(y)\Big] dy \tag{2.48}$$

where $\widetilde{\Phi}_\rho(z) := \beta\widetilde{C}(y, z \mid \rho)$, such that $\widetilde{C}(y, \beta \mid \rho)$ is the Laplace transform of $C(y, t \mid \rho)$ evaluated at $\beta$, and where $\Theta_-(y)$ is a step function that equals 1 for all $y < a$ and 0 otherwise, and $\Theta_+(y)$ equals 1 for all $y > b$ and 0 otherwise. In deriving Eq. (2.48) we have used the independence of stages (i) and (ii) that were described below Eq. 2.42, which requires Markovianity of the propagator. Note that we have also used $\langle C(y, W_\beta \mid \rho)\rangle = \beta\widetilde{C}(y, \beta \mid \rho) = \widetilde{\Phi}_\rho(\beta)$.

We can now plug Eq. (2.43) into Eq. (2.48) while noting that $\langle T_d(\rho, I)\rangle$ of Eq. (2.43) is independent of $y$ in the integral of Eq. (2.48), and so can be taken out of the integral. This gives

$$\langle T_d(\rho, I)\rangle = \beta^{-1} + \tau_\rho + p_\rho^- \langle T_d(a, I)\rangle + p_\rho^+ \langle T_d(b, I)\rangle \tag{2.49}$$

where we have defined

$$\tau_\rho = \int_{-\infty}^{\infty} \widetilde{\Phi}_\rho(\beta)\, \langle T_f(\iota_\pm \mid y)\rangle \Big[\Theta_-(y) + \Theta_+(y)\Big] dy, \tag{2.50}$$

such that $\iota_- = a$ for $y < a$ and $\iota_+ = b$ for $y > b$, and

$$p_\rho^\pm = \int_{-\infty}^{\infty} \widetilde{\Phi}_\rho(\beta)\, \big\langle p_{T_f(\iota_\pm|y)}(I \mid A)\big\rangle\, \Theta_\pm(y) dy, \tag{2.51}$$

where $\big\langle p_{T_f(\iota_\pm|y)}(I \mid A)\big\rangle = \pi_I\Big[1 - \widetilde{F}_\lambda(\iota_\pm \mid y)\Big]$. Note that Eq. (2.49) is actually a shorthand notation for a system of two equations, for the two unknowns $\langle T_d(a, I)\rangle$ and $\langle T_d(b, I)\rangle$, which one gets by substituting the two possible values of $\rho = \{a, b\}$.

Each term on the right-hand side of Eq. (2.49) gives us insight into the different mechanisms through which a detection event can take place. For instance, the first term $\beta^{-1}$ denotes the mean time taken for the particle to turn active ($A$), starting from the inactive state ($I$). It is easy to see

that the mean detection time $\langle T(\rho, I)\rangle$ satisfies $\langle T(\rho, I)\rangle \geq \beta^{-1}$ where the equality holds only in the extreme cases where the particle is always detected as soon as it turns reactive. However, in almost all practically relevant scenarios, this will not be the case. Namely, there will be a non-zero probability for a particle that starts at the boundary of the gated interval to be found *outside* the interval when it turns reactive. In this case, the additional time taken for detection is captured by the other three terms in Eq. (2.49).

If detection did not happen when the particle turned reactive, it can happen later in two different ways. Suppose that when the particle turns reactive, it is at $y \notin [a, b]$. For a detection event to take place, the particle now has to reach the boundary nearest to it, starting from position $y$. If at the moment when the particle reaches the nearest boundary, it is found reactive, then it is detected right away. In Eq. (2.49), $\tau_\rho$ captures the weighted contribution of such events, starting from different values of $y$, to the mean detection time. However, if upon reaching the boundary closest to it, the particle is non-reactive, the dynamics is renewed, and the mean additional time taken for detection is either $\langle T_d(a, I)\rangle$ or $\langle T_d(b, I)\rangle$, depending on whether $y$ was closer to boundary point $a$ or $b$.

The identification of a renewal moment provides us with the needed closure that allows us to obtain the exact formula for the mean detection time. In particular, by solving the system of equations in (2.49) for the two unknowns $\langle T_d(a, I)\rangle$ and $\langle T_d(b, I)\rangle$, we obtain

$$\langle T_d(a, I)\rangle = \frac{(\beta^{-1} + \tau_a)(1 - p_b^+) + p_a^+(\beta^{-1} + \tau_b)}{1 - p_a^- - p_b^+ + p_a^- p_b^+ - p_b^- p_a^+}, \tag{2.52}$$

and

$$\langle T_d(b, I)\rangle = \frac{(\beta^{-1} + \tau_b)(1 - p_a^-) + p_b^-(\beta^{-1} + \tau_a)}{1 - p_a^- - p_b^+ + p_a^- p_b^+ - p_b^- p_a^+}. \tag{2.53}$$

For the symmetric case in which the dynamics and the boundary conditions to the left and the right of the target center are the same (e.g., diffusion on the infinite line), Eqs. (2.52) and (2.53) are equal and simplify considerably. Setting $\tau_a = \tau_b := \tau$ and $p_a^\pm = p_b^\pm := p^\pm$, we obtain

$$\langle T_d(\rho, I)\rangle = \frac{\beta^{-1} + \tau}{1 - p^- - p^+}. \tag{2.54}$$

The above exact equation for the mean detection time admits a simple interpretation in the form of Bernoulli trials. We define each trial as an independent attempt at detection when the particle is initially non-reactive at one of the target's boundaries. Each attempt takes on average $\beta^{-1} +$

$\tau$, where $\beta^{-1}$ is the mean time for the particle to turn reactive, and $\tau$ denotes the additional contribution coming from events where the particle is found outside the interval when it turns reactive, and thus has to return to its nearest boundary. The number of trials until detection follows a geometric distribution, and the mean number of trials is given by $(1 - p_a - p_b)^{-1}$. This acts as a multiplicative factor to the mean time taken for one trial and altogether yields the mean detection time.

#### 2.4.2.2 Distribution of the First Detection Time

We now turn to compute the full distribution of the first detection time. This is required to complement the limited information provided by the mean. The calculation of the Laplace transforms of the distributions of the random variables in Eqs. (2.41) and (2.42) is done along the lines followed for their respective means (Sec. 2.4.2.1). We have thus delegated the details of this calculation to Appendix A, and will only quote the results here. The Laplace transform of Eq. (2.41) is

$$\widetilde{D}_s(x_0, \sigma_0) = \widetilde{F}_s(\rho \mid x_0) \left[\pi_A + \pi_I \widetilde{D}_s(\rho, I)\right] \pm (1 - \pi_{\sigma_0}) \widetilde{F}_{s+\lambda}(\rho \mid x_0) \left[\widetilde{D}_s(\rho, I) - 1\right], \quad (2.55)$$

where we have a plus sign if $\sigma_0 = I$, and a minus sign if $\sigma_0 = A$. For $\sigma_0 = E$, the second term vanishes, and we retain only the first term.

The Laplace transform of Eq. (2.42) for the case $\rho = a$ is

$$\widetilde{D}_s(a, I) = \frac{(\widetilde{\phi}_a + \widetilde{\chi}_a)(1 - \widetilde{\psi}_b^+) + \widetilde{\psi}_a^+ (\widetilde{\phi}_b + \widetilde{\chi}_b)}{1 - \widetilde{\psi}_a^- - \widetilde{\psi}_b^+ + \widetilde{\psi}_a^- \widetilde{\psi}_b^+ - \widetilde{\psi}_b^- \widetilde{\psi}_a^+}, \quad (2.56)$$

and for the case $\rho = b$ is

$$\widetilde{D}_s(b, I) = \frac{(\widetilde{\phi}_b + \widetilde{\chi}_b)(1 - \widetilde{\psi}_a^-) + \widetilde{\psi}_b^- (\widetilde{\phi}_a + \widetilde{\chi}_a)}{1 - \widetilde{\psi}_a^- - \widetilde{\psi}_b^+ + \widetilde{\psi}_a^- \widetilde{\psi}_b^+ - \widetilde{\psi}_b^- \widetilde{\psi}_a^+}, \quad (2.57)$$

where we have defined

$$\widetilde{\phi}_\rho(s) \equiv \beta \int_a^b \widetilde{C}(y, s + \beta \mid \rho) dy \equiv \int_a^b \widetilde{\Phi}_\rho(s + \beta) dy, \quad (2.58)$$

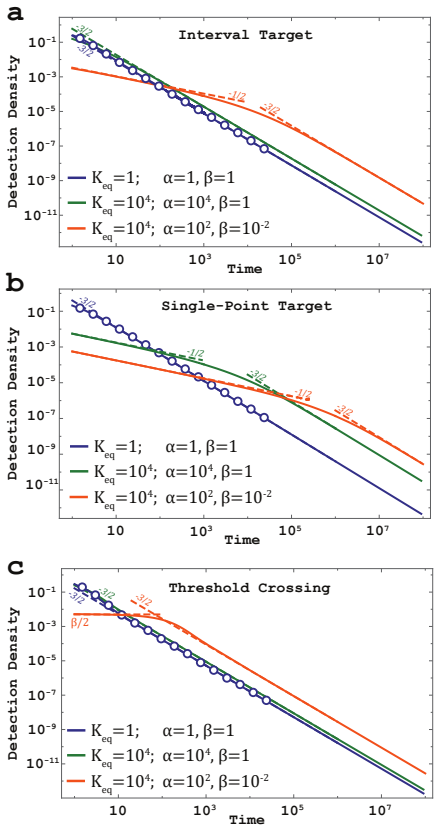


Figure 2.8: A comparison of the detection time distribution and its dependence on the transition rates between models of (a) a gated interval of length $b - a = 1$, (b) a gated point, and (c) gated threshold crossing. In all cases, we set $\mathcal{D} = 1$ for the diffusion coefficient, a non-reactive initial gate state, and $a$ for the initial position of the particle. In each panel, we plot three color-coded curves, where each color represents a different choice of values for the transition rates $\alpha$ and $\beta$. For each choice of parameters, the lines represent numerical Laplace inversion of Eq. (2.68), and the dashed lines are the corresponding transient and asymptotic power laws according to Eqs. (2.69) and (2.71), and circles come from Monte-Carlo simulations with $10^5$ particles and a simulation time step $\Delta t = 10^{-4}$.

$$\widetilde{\chi}_\rho(s) \equiv \int_{-\infty}^{\infty} \widetilde{\Phi}_\rho(s+\beta)\Big[\pi_A \widetilde{F}_s(\iota_\pm \mid y) + \pi_I \widetilde{F}_{s+\lambda}(\iota_\pm \mid y)\Big]\Big[\Theta_-(y) + \Theta_+(y)\Big]dy, \tag{2.59}$$

and

$$\widetilde{\psi}^\pm_\rho(s) \equiv \int_{-\infty}^{\infty} \widetilde{\Phi}_\rho(s+\beta)\pi_I\Big[\widetilde{F}_s(\iota_\pm \mid y) - \widetilde{F}_{s+\lambda}(\iota_\pm \mid y)\Big]\Theta_\pm(y)dy, \tag{2.60}$$

where again $\iota_- = a$ and $\iota_+ = b$. As happened for the formulas for the mean, for the symmetric case in which the dynamics and the boundary conditions to the left and the right of the target center are the same Eqs. (2.56) and (2.57) are equal and simplify considerably. Setting $\phi_a =$

$\phi_b := \phi$, $\chi_a = \chi_b := \chi$ and $\psi_a^{\pm} = \psi_b^{\pm} := \psi^{\pm}$, we obtain

$$\widetilde{D}_s(\rho, I) = \frac{\widetilde{\phi} + \widetilde{\chi}}{1 - \widetilde{\psi}^{-} - \widetilde{\psi}^{+}}. \tag{2.61}$$

#### 2.4.2.3 Long Time Asymptotics – Inheritance of Power-Laws

For simplicity, let us assume the symmetric case in which both the dynamics and the boundary conditions to the left and the right of the target are the same. We focus on processes for which the first-passage time distribution of the underlying ungated process has an asymptotic power-law behavior of the form

$$F_t(\rho \mid y) \simeq \frac{\theta}{\Gamma(1-\theta)} \frac{\tau_f^{\theta}}{t^{1+\theta}}, \quad 0 < \theta < 1, \tag{2.62}$$

where $\tau_f > 0$. Note that in this case, the mean first-passage time diverges. Using the Tauberian theorem, it can be shown that the small $s$ asymptotics of the Laplace transform of the first-passage time is given by $\widetilde{F}_s(\rho \mid y) \simeq 1 - (\tau_f s)^{\theta}$ (see pp. 43-45 in Ref. [17]). Note that $\tau_f$ is a function of the distance to the closest boundary of the interval target.

In Appendix B, we show that corresponding gated processes inherit the above asymptotics. That is to say, the first detection time density also decays as a power law, and the power law exponent $\theta$ remains the same. The asymptotics differ only in the corresponding prefactor, which is determined exactly

$$D_t(\rho, I) \simeq \frac{\theta}{\Gamma(1-\theta)} \frac{\left(\pi_I^{-1} \frac{B}{A}\right)}{t^{1+\theta}}, \tag{2.63}$$

where $A$ and $B$ are given in Appendix B.

We thus see that, for the cases studied here, the gated detection time has a power law behavior with the same $\theta$ of the corresponding ungated process but with a different prefactor, which can be determined exactly based on descriptors of the corresponding ungated process. In particular, for a single-point target ($b \to a$), we find

$$D_t(a, I) \simeq \frac{1}{t^{1+\theta}} \frac{\theta}{\Gamma(1-\theta)} \times \frac{\int_{-\infty}^{\infty} \widetilde{\Phi}_{\rho}(\beta) \tau_f^{\theta}(y) dy}{\pi_A + \pi_I \int_{-\infty}^{\infty} \widetilde{\Phi}_{\rho}(\beta) \widetilde{F}_{\lambda}(a \mid y) dy}, \tag{2.64}$$

where we recall that $\pi_{\mathrm{A}} = \beta/\lambda$ and $\pi_{\mathrm{I}} = \alpha/\lambda$. In the converse limit of threshold crossing

$(b \to \infty)$ we obtain

$$D_t(a, I) \simeq \frac{1}{t^{1+\theta}} \frac{\theta}{\Gamma(1-\theta)} \times \frac{\int_{-\infty}^{a} \widetilde{\Phi}_\rho(\beta) \tau_f^\theta(y) dy}{\pi_A + \pi_I \Big[ \int_a^\infty \widetilde{\Phi}_\rho(\beta) dy + \int_{-\infty}^{a} \widetilde{\Phi}_\rho(\beta) \widetilde{F}_\lambda(a \mid y) dy \Big]}.$$

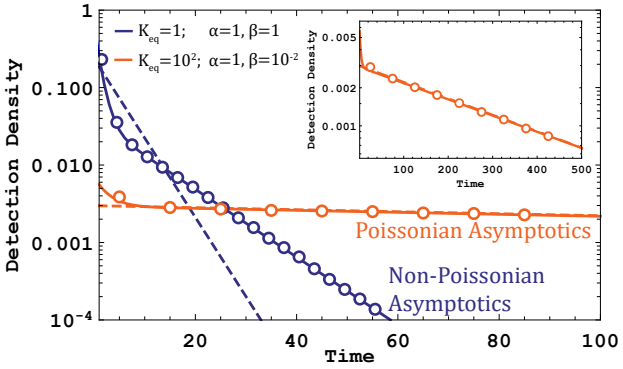


Figure 2.9: The first detection time distribution at a gated interval $[a, b]$, for a diffusing particle restricted to a box $[0, L]$ with reflecting boundaries. The lines are numerical Laplace inversions of Eq. (2.61), where $\phi$, $\chi$ and $\psi^{\pm}$ are calculated using the results of Appendix D. The circles are the results of Monte-Carlo simulations with $10^5$ particles and a simulation time step $\Delta t = 10^{-4}$. Here, we take: $\alpha = 1$, $L = 10$, $D = 1$ and $l = 1$ where $a = (L - l)/2$ and $b = (L + l)/2$. The gate is initially in the non-reactive state, and we set $a$ for the initial position of the particle. The blue line is drawn for the case $\beta = 1$ and $K_{eq} = 1$, and the orange line is drawn for the case $\beta = 10^{-2}$ and $K_{eq} = 10^2$. The dashed lines represent exponential distributions whose means are taken to be the mean detection times according to Eq. (2.54). While a single exponential is not expected a priori, it is observed for the case of high-crypticity (orange). It can be appreciated that the distribution is well described by the dashed line (also see inset).

#### 2.4.2.4 Transient behavior under high crypticity

In the work of Mercado-Vásquez and Boyer [47], a freely diffusing particle in search of a gated *single-point target* was considered. The authors showed that when $K_{eq} = \frac{\alpha}{\beta} \gg 1$ an interim regime of slower power-law decay emerges before the asymptotic regime. In particular, the asymptotic decay of the first detection time density of $t^{-3/2}$ that is seen for simple diffusion is preceded by a long stretch of time where the density decays as $t^{-1/2}$. A detection process for which $K_{eq} \gg 1$ was termed highly cryptic since it spends most of its time in the non-reactive (inactive) state.

Yet, there remains a question: Is the condition $K_{eq} \gg 1$ sufficient to guarantee a slower transient regime for any gated process, provided that the underlying ungated process has the

asymptotic power-law behavior of Eq. (2.62)? In appendix C, we show that the answer to this question is no. Specifically, we show that whenever there is a possibility to spend some time in the target region while being in the non-reactive state, an additional condition is required to guarantee a slower pre-asymptotic power-law decay.

Simply put, the time spent in the non-reactive state before transitioning to the reactive state must be considerably larger than the time spent on the target upon arrival. For the problem of a gated interval considered in this work, there is certainly a probability to spend time within the interval $[a, b]$ while being in the non-reactive state. In appendix C, we show that, in this case, the additional requirement translates to

$$\frac{b-a}{\tau_r^\theta} \ll \beta^{\theta-1}, \tag{2.65}$$

with $\tau_r$ set by the small $s$ asymptotics of the propagator $\widetilde{C}(y, s \mid y) \simeq (\tau_r s)^{-\theta}$, and where we have assumed that $\widetilde{C}(y, s \mid a) \simeq s^{-\theta} H(|y-a| s^\theta)$, where $H$ is some function. Simple diffusion is just one example of a process that belongs to this group. In Appendix C, we also show that for such processes $\tau_f$ and $\tau_r$ are related by

$$\tau_r = \left( \frac{|y-a| \frac{d\widetilde{C}(y,s|a)}{dy}}{\tau_f^\theta} \right)_{y=a}^{-1/\theta}. \tag{2.66}$$

Examining Eq. (2.65), it is thus clear that in the limit of a single-point target, $b \to a$, the left-hand side of Eq. (2.65) is zero. The additional requirement is then fulfilled for every finite transition rate $\beta$. From the qualitative understanding above, this is anticipated. Indeed, when the target is of measure zero, the particle spends no time on the target and can react with it only by crossing it while being in the reactive state. Thus, in such cases, we only care about the equilibrium occupancies of the reactive and non-reactive states. Namely, the rates can be arbitrarily large as long as the rate to become reactive is much slower than its converse. On the other hand, Eq. (2.65) will never be satisfied in the case of threshold crossing, where $b \to \infty$. This means that the cryptic transient regime will never be observed in gated threshold crossing problems of the type analyzed herein.

In appendix C, we show that when $K_{eq} \gg 1$ and the condition in Eq. (2.65) is satisfied, the

transient regime of the first detection time density scales like

$$D_t(\rho, I) \simeq \frac{1}{\Gamma(\theta)} \frac{A}{B} t^{\theta-1}, \tag{2.67}$$

where $A$ and $B$ are the same as in the previous subsection (definitions can be found in Appendix B). Thus, under these conditions, we indeed see a transient regime with a different power law than the asymptotic. Furthermore, we can exactly determine this power-law, and its prefactor.

The findings presented in this subsection call for a refined definition of high-crypticity, which takes into account the time spent on the target: A process is highly-cryptic if it spends most of its time in the non-reactive state *and* the time spent in the non-reactive state before transitioning to the reactive state is considerably larger than the time spent on the target upon arrival to it.

#### 2.4.2.5 Diffusion to a Gated Interval

In this section, we show how to apply the framework developed above to obtain explicit solutions for the first detection time of a diffusing particle by a gated interval. We first solve for free diffusion and then consider the effects of confinement and drift.

**Freely diffusing particle**

Consider the gated interval problem illustrated in (Fig. 2.1, bottom); and further assume that the particle, initially at $x_0$ at state $\sigma_0 \in \{\mathrm{A}, \mathrm{I}\}$, is not restricted and free to diffuse on the entire one-dimensional line. The gated target is the interval $[a, b]$.

The free-diffusion conserved propagator is a Gaussian and its Laplace transform is given by $\widetilde{C}(y, s|x_0) = \frac{1}{\sqrt{4\mathcal{D}s}} e^{-\sqrt{\frac{s}{\mathcal{D}}}|y-x_0|}$. Also, the Laplace transform of the first-passage time distribution from an arbitrary point $y$ to an arbitrary point $\rho$ is $\widetilde{F}_s(\rho \mid y) = e^{-\sqrt{\frac{s}{\mathcal{D}}}|\rho-y|}$ [1]. In fact, these two classical results are all we need in order to solve the gated problem, using the renewal formalism established in Sec. 2.4.1.

For any $x_0 \notin [a, b]$ we can break the trajectory of the gated problem into two parts. A first-passage trajectory to $\rho \in \{a, b\}$ that is followed, if the particle was not detected upon arrival, by a first detection process starting from the state $(\rho, I)$. Because the first part of the trajectory is a first-passage process that is well understood, from now on, we will focus on the second part, i.e., a detection process with initial state $(\rho, I)$. It is important to note that accounting for the entire trajectory by adding its first-passage part is then a simple task that can generally be done via Eqs.

(2.43) and (2.55).

It can be easily appreciated that in this example, the dynamics and the boundary conditions to the left and right of the target are the same, and we can use Eq. (2.61) to calculate the Laplace transform of the first detection time distribution. Plugging $\widetilde{C}(y,s \mid x_0)$ and $\widetilde{F}_s(\rho \mid y)$ into Eq. (2.61) we obtain

$$\widetilde{D}_s(\rho,I)=\frac{\frac{1}{\omega_1^+}-\frac{e^{-(b-a)\sqrt{\frac{s+\beta}{D}}}\left(\lambda+\omega_1^-\right)-\lambda}{\omega_2}}{2\beta^{-1}+\frac{\left(1+e^{-(b-a)}\sqrt{\frac{s+\beta}{D}}\right)\alpha\omega_1^-}{\omega_2\left(\sqrt{\beta+s}+\sqrt{s}\right)\left(\sqrt{\beta+s}+\sqrt{\lambda+s}\right)}}, \tag{2.68}$$

where we have defined $\omega_1^{\pm}=\sqrt{s+\beta}(\sqrt{s}\pm\sqrt{s+\lambda})$ and $\omega_2=(s+\beta)\lambda$. Similarly we can get the long-time asymptotics by plugging $\widetilde{C}(y,s|x_0)$ and $\widetilde{F}_s(\rho \mid y)$ into Eq. (2.63). Noting that $\tau_f=\frac{|y-x_0|^2}{\mathcal{D}}$, we obtain

$$D_t(\rho,I)\simeq\frac{1}{2\sqrt{\pi}}t^{-3/2}\frac{\left(1+e^{-(b-a)\sqrt{\frac{\beta}{\mathcal{D}}}}\right)(\sqrt{\beta}+\sqrt{\lambda})\lambda}{2\alpha\beta+\left(1-e^{-(b-a)\sqrt{\frac{\beta}{\mathcal{D}}}}\right)\alpha\sqrt{\beta\lambda}+2\left(\beta^2+\sqrt{\beta^3\lambda}\right)}. \tag{2.69}$$

Finally, in the previous section, we have seen that for a finite-sized target, high-crypticity requires the condition in Eq. (2.65) as well as $K_{eq}=\frac{\alpha}{\beta}\gg 1$. For our example here $\tau_r=4\mathcal{D}$ and so the condition in Eq. (2.65), after squaring both sides of the equation, translates to

$$\frac{(b-a)^2}{4\mathcal{D}}\ll\beta^{-1}, \tag{2.70}$$

namely, the time spent in the non-reactive state before transitioning to the reactive state must be considerably larger than the time it takes the particle to diffuse a distance comparable to the size of the target. If both $K_{eq}\gg 1$ and Eq. (2.70) hold, a transient regime emerges before the asymptotic regime of Eq. (2.69). In this regime, according to Eq. (2.67), we have

$$D_t(\rho,I)\simeq\frac{1}{\sqrt{\pi}}t^{-1/2}\sqrt{\beta}\left(\frac{2}{1+e^{-(b-a)\sqrt{\frac{\beta}{\mathcal{D}}}}}-\frac{1}{1+\sqrt{K_{eq}^{-1}}}\right). \tag{2.71}$$

In Fig. 2.8 there are three panels corresponding to: (a) the gated interval problem, and its two extreme limits (b) the gated single-point target problem, and (c) the gated threshold crossing problem, which was illustrated in Fig. 2.1. In each panel, we plot three color-coded curves, where each color represents a different choice of values for the transition rates $\alpha$ and $\beta$. Purple curves represent $\alpha=\beta=1$ such that $K_{eq}=\alpha/\beta=1$. Green curves represent $\alpha=10^4$ and $\beta=1$

such that $K_{eq} = 10^4$. Orange curves represent $\alpha = 10^2$ and $\beta = 10^{-2}$ such that again $K_{eq} = 10^4$. The green and orange curves have the same ratio of transition rates ($K_{eq} = 10^4$), but the latter transitions are much slower, and specifically, $\beta$ is much smaller.

In panel (a), the case of an interval target, we see that the purple and green curves are similar in shape — an asymptotic $\sim t^{-3/2}$ power-law kicks in rather early. In contrast, the orange curve possesses a prolonged transient regime of $\sim t^{-1/2}$ before the asymptotic regime enters. This is because the orange curve fulfills both conditions for high-crypticity, i.e., $K_{eq} \gg 1$ *and* Eq. (2.70).

In panel (b), the case of a single-point target, the green curve is actually similar in shape to the orange curve. In this limit, the condition in Eq. (2.70) is always met, and it is sufficient to require that $K_{eq} \gg 1$. Note, however, that while the ratio of the transition rates alone determines whether a prolonged transient regime exists, the duration of this regime is affected by the magnitude of the rates through $\lambda = \alpha + \beta$. More specifically, the transition between the transient and asymptotic regimes occurs at $K_{eq}^2/\lambda$ [47].

Finally, in panel (c), we present the case of threshold crossing. There, we see that none of the curves possess a prolonged transient regime, as the condition in Eq. (2.70) is never met. Furthermore, for short times (up to $\beta^{-1}$) the detection probability density is constant with a value of $\beta/2$. This can be easily understood by the following argument: With probability $\beta e^{-\beta t} \simeq \beta$, the particle becomes reactive after a short time $t$. Since the motion is symmetric, upon becoming reactive, the particle has a probability half to be found above its starting position. Recalling the particle started on the threshold, it has a probability half of being detected upon becoming reactive. In total, the first detection probability density at short times is $\beta/2$.

**Diffusion in confinement**

Let us now restrict the particle to diffuse inside a box $[0, L]$ with reflecting boundaries, such that the gated target is inside the box ($0 < a \leq b < L$). The confinement renders the first-passage asymptotics exponential, so the results derived for heavy-tailed distributions are no longer valid. However, it also renders the mean first-passage time finite, and so one can use Eq. (2.43) together with Eqs. (2.52) and (2.53) to obtain the mean detection time.

Furthermore, as we did for the freely diffusing particle, we can, of course, calculate the entire Laplace transform of the reaction time. Let us again focus on a reaction with initial state $(\rho, I)$, i.e., assume the particle starts on the boundary in the non-reactive state. For simplicity, let us

further assume that the center of the gated interval is situated exactly at the center of the confining box: $a = (L - l)/2$ and $b = (L + l)/2$, such that $l = b - a$. We can thus use Eq. (2.61). All we require for this calculation is the conserved propagator for diffusion restricted to a box $[0, L]$, and the first-passage time to $a$, starting from some $x \in [0, a]$ (which in our case is equal to the first-passage time to $b$ starting from $L - x$). These quantities are calculated in Appendix D.

In Fig. 2.9, we set $\alpha = 1$, $L = 10$, $l = 1$ and $D = 1$, and plot the detection time density for $\beta = 1$ (blue line, $K_{eq} = 1$) and for $\beta = 10^{-2}$ (orange line, $K_{eq} = 10^2$). For each case, we also plot an exponential distribution with the mean taken to be the mean detection time calculated according to Eq. (2.54) (dashed lines of corresponding colors). For $\beta = 1$ the distribution is clearly non-exponential, there are two distinct phases. Therefore, despite having an exponential tail, the gated distribution cannot be captured by a single exponent, which is to be expected since multiple time scales are involved in the problem. However, for $\beta = 10^{-2}$ high-crypticity conditions are met, and we observe Poisson-like asymptotics [72]. This is to say that the distribution is well approximated by an exponential distribution whose mean is simply the mean detection time. This can be understood by noting that the time it takes for the diffusing particle's position to equilibrate over the box is much shorter than the time it takes the particle to turn reactive. The latter then becomes the rate-limiting step, which dominates the distribution of detection times. This example warrants caution — Poisson kinetics is not guaranteed in the general case but does emerge in the cryptic regime.

### Diffusion with drift

As we discussed above, the mean first-passage time of a freely diffusing particle diverges, and this property is inherited by the corresponding gated problem. Confinement can regularize the mean and make it finite. This can also be done by introducing a constant drift velocity $v$ in the target's direction. The mean first-passage time of the ungated problem is then simply given by $\ell/v$, where $\ell$ denotes the distance between the initial position of the particle and the point target. However, considering the gated counterpart of this problem, we observe that the mean detection time diverges despite the constant drift. This fact can be intuitively understood through the following argument: when the drift drives the particle downhill towards the target, there is a non-zero probability that the particle will arrive at the target in the non-reactive state. Subsequently, by the time

it turns reactive again, the particle is likely to be on the other side of the target, and it now has to travel "uphill" for the detection to occur. This renders the mean detection time infinite. It is thus clear that the mean detection time under stochastic gating can be remarkably different from its ungated counterpart.

A slight variation of the drift-diffusion model discussed above can nevertheless render the gated mean finite. In particular, consider a particle diffusing under a constant drift velocity $v$ towards the origin, with the origin also being a reflective boundary. For $0 < a < b$, we consider a gated interval $[a, b]$, where the particle can get detected and absorbed in its reactive state. Despite the constant drift, the reflecting boundary at the origin ensures that the mean first-passage time to the boundaries of the interval remains finite, irrespective of whether the particle has to travel uphill or downhill. Consequently, the mean detection time is also finite. A schematic of this setup is provided in Fig. 2.10a.

The formalism developed in Sec. 2.4.1 asserts that knowing certain ungated observables is enough in order to obtain the first detection time statistics. In particular, a key quantity is the conserved propagator for the diffusion equation with drift. This obeys

$$\frac{\partial C(x,t|x_0)}{\partial t} = \mathcal{D}\frac{\partial^2 C(x,t|x_0)}{\partial^2 x} + v\frac{\partial C(x,t|x_0)}{\partial x}, \tag{2.72}$$

with the initial condition $C(x, t = 0|x_0) = \delta(x - x_0)$ and boundary conditions $\frac{dC(x,t|x_0)}{dr}\big|_{x=0} = 0$ and $C(x \to \infty, t|x_0) = 0$. The drift is $v > 0$ and its direction is towards the reflecting boundary at zero. In appendix E, we obtain $\widetilde{C}(x, s|x_0)$ in Eq. (E.2). The Laplace transform of the first-passage probability $\widetilde{F}_s(x|x_0)$ and its mean $\langle T_f(x|x_0)\rangle$ can also be obtained and we give them in Eqs. (E.11) and (E.12). Assuming for simplicity that the particle starts at the boundary $b$, one can utilize Eq. (2.53) to obtain the mean detection time $\langle T_d(b, I)\rangle$ by plugging in the ungated quantities obtained above.

For intermediate values of $v > 0$, it is clear that drift can speed up detection as it helps avoid situations where the particle drifts away from the interval. However, if $v$ is sufficiently large, a significant contribution to the detection time comes from trajectories where the diffusing particle crosses over to the other side of the interval (with its position somewhere between 0 and $a$), and then travels uphill against the drift, for the eventual detection (see Fig. 2.10a and the associated caption). Thus, one would expect the mean detection time $\langle T_d(b, I)\rangle$ to vary non-monotonically

as a function of $v$. This expectation is indeed verified in Fig. 2.10(b), where we fix $\alpha = \mathcal{D} = 1$, $a = 1$ and $b = 3$ and plot $\langle T_d(b, I)\rangle$ vs. $v$ for $\beta = 0.25, 0.5, 1, 2, 4$. For small values of $v$, the mean detection time decreases linearly as the drift is increased. However, for large $v$, it increases rapidly, indicating that detection is much more difficult.

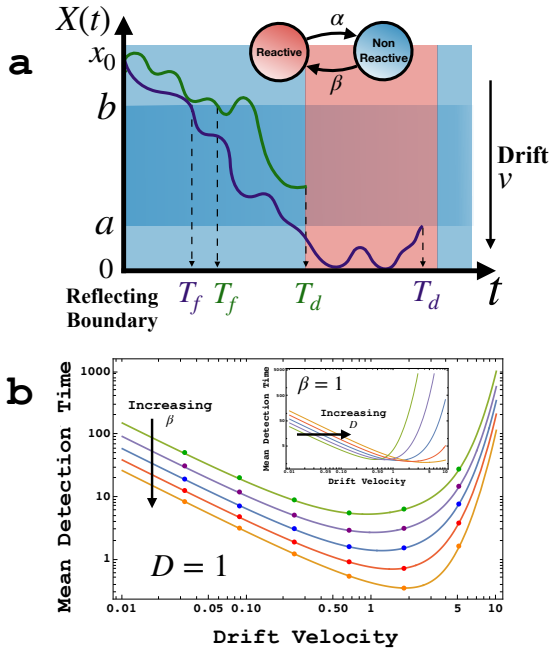


Figure 2.10: Detecting a particle diffusing with drift by a gated interval. (a) Schematics of the process where a particle, initially at $x_0$ while the gate is in the non-reactive state, is diffusing on the positive ray $(0, \infty)$ with a drift velocity $v$ towards the origin. The gated interval is $[a, b]$, and the origin is considered reflective. The two trajectories represent two different types of detection events. The purple trajectory illustrates a scenario likely to happen when $v$ is large. Namely, if the particle arrives at the upper boundary $b$ when the gated interval is non-reactive, then the particle may be able to cross the interval without being detected. It will subsequently need to go against the drift for a detection event to occur. The green trajectory is representative of low $v$, where a particle that arrives at the upper boundary when the interval is non-reactive is unlikely to cross the interval without being detected. (b) Mean detection time $\langle T(b, I)\rangle$ vs. $v$ for $\beta = 0.25, 0.5, 1, 2,$ and 4, at $\alpha = \mathcal{D} = 1$ . The mean detection time displays a non-monotonic dependence on $v$, and achieves a minimum for some $v = v^*$. Inset shows plots for $\mathcal{D} = 0.25, 0.5, 1, 2,$ and 4, at $\alpha = \beta = 1$, showing that $v^*$ also depends on $\mathcal{D}$.

This naturally leads to the question of finding the optimal drift velocity which minimizes the mean detection time. From Fig. 2.10(b), it is evident that the value of $v^*$, which is the value of $v$ for which $\langle T_d(b, I)\rangle$ achieves its minimum value, increases as $\beta$ increases. This is expected as increasing $\beta$ increases the amount of time the particle spends in the reactive state. This, in turn, reduces the chance that the particle will cross the interval undetected, which allows for higher

drift velocities. Naively, one could formulate the following argument to find $v^*$: the mean time taken for the particle to turn reactive is $\beta^{-1}$, while the particle travels an average distance of $v/\beta$ during this time. So, one could give a preliminary estimate of $v^* \approx (b-a)\beta$. However, as we show in the inset of Fig. 2.10(b), $v^*$ also depends on the diffusion coefficient, with smaller values of $\mathcal{D}$ corresponding to higher values of $v^*$. This highlights the importance of the exact result obtained in Eq. (2.53), which captures the explicit dependence of the mean detection time on $\mathcal{D}$, along with other relevant parameters, and allows us to analytically study this optimization problem.

## 2.5 Discussion

Gated first-passage processes, which arise in various situations ranging from analysis of time-series data to several chemical reactions, were the focal point of this chapter. We presented a novel framework that yields closed-form solutions for the statistics of the detection time density in terms of the properties of the ungated first-passage process. In particular, our approach allowed us to obtain the Laplace transform of the detection time density and all its moments.

Crucially, we showed that the exact results derived herein shed light on universal features of gated first-passage processes. Namely, in situations where the ungated first-passage time density is characterized by power-law asymptotics, the corresponding detection time density inherits the same power-law decay, albeit with a different prefactor. The long-time power-law tail may be preceded by a slower transient power-law decay with a different exponent. Our formalism reveals that, in the case of point targets, such a transient power-law decay is a generic feature of Markovian gated first-passage processes. Yet, an additional condition is required to guarantee its existence for targets of non-zero volume. In Appendix F, we also discuss the generalization of our results to higher dimensions.

In this section, we focused on continuous processes. Yet, in fact, our formalism can also treat processes with discontinuous trajectories (albeit still in continuous space). An interesting example is stochastic jump processes, which can be treated by our formalism as long as jumps cannot be made into the gated target itself. Consider, for example, continuous stochastic processes that undergo stochastic resetting. We note that for the gated point target search and threshold crossing problems, the formulas derived in this section hold without change, even in the presence

of resetting. Generalization to the case of a gated interval is also straightforward but requires careful consideration since restart can teleport the particle from one side of the interval to another without the need to cross the interval itself.

Finally, an important generalization of the framework considered herein is to the case of non-Markovian gating. Indeed, it is often the case that the dynamics of molecular gates are governed by binding and unbinding events of ligands. In turn, these events themselves are governed by first-passage processes whose first-passage times distributions need not be exponential. This highlights the importance of understanding the role non-Markovianity plays in determining the statistics of gated detection times. Non-Markovian gating also plays a central role when considering periodically sampled time-series, which have been recently shown to have interesting and distinct behaviors compared to their ungated counterparts. Developing an analytical framework to address these questions is an important direction for future research.

# CHAPTER 3

# Inference from Gated First-Passage Times

First-passage times provide invaluable insight into the fundamental properties of stochastic processes. However, as we have discussed throughout the thesis so far, various forms of gating mask first-passage times and differentiate them from actual detection times. For instance, imperfect conditions may intermittently gate our ability to observe a system of interest such that exact first-passage instances might be missed. In other cases, e.g., certain chemical reactions, direct observation of the molecules involved is virtually impossible, but the reaction event itself can be detected. However, this instance need not coincide with the first collision time since some molecular encounters are infertile and hence, gated.

Motivated by the challenge posed by such real-life situations, in this chapter, we present a universal — model-free — framework for the inference of first-passage times from the detection times of gated first-passage processes. Furthermore, when the underlying laws of motions are known, our framework also provides a way to infer physically meaningful parameters. In this chapter, we aim to demonstrate the robustness of our approach and its insensitivity to underlying details through several settings of physical relevance.

## 3.1 Motivation and Problem Statement

In this thesis thus far, our focus was on uncovering the statistics of the detection times. We did so by primarily connecting its statistics to the statistics of the first-passage times. In many examples, however, that may not be feasible as the experimentally accessible quantities are the first detection times and the prime challenge at hand is to uncover properties about the underlying process from the gated measurements.

Figure 3.1 exemplifies two instances where gating arises naturally: (a) Single particle tracking of an intermittently observed particle, which transitions between a visible state and an invisible state. For example, a wide class of fluorophores undergo photoblinking in single-particle measurement [88–97]. Other reasons for such gating can be the intermittent loss of focus on a moving

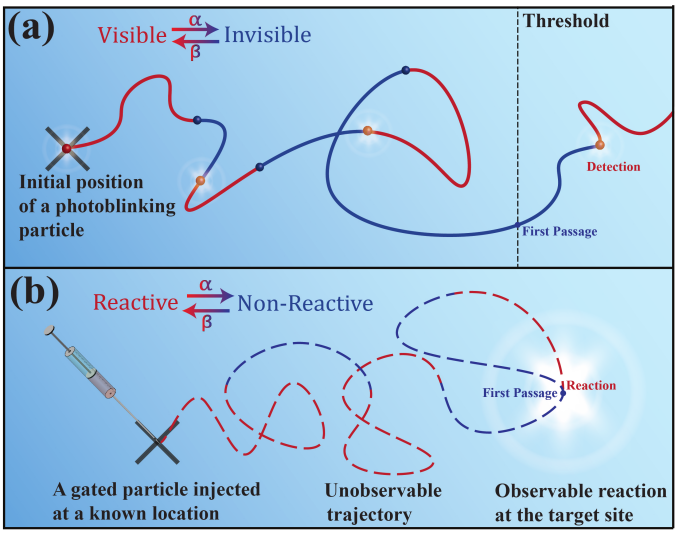


Figure 3.1: Instances highlighting the need for inference in gated first-passage processes. (a) Detection of threshold crossing under intermittent sensing. Consider single particle tracking of a photoblinking particle. The first-passage properties of the particle can be mischaracterized as the particle can cross the threshold while being in its invisible state. (b) Gated chemical reaction or target search. Imagine a situation where tracking of the particle is not possible, and the only observable is the reaction time. For such processes, we show how the first-passage time distribution and further relevant observables can be inferred from the detection time distributions.

particle in 3-dimensions [98] or slow frame acquisition rate [99]; (b) A gated chemical reaction or target search, where tracking of the particle is not possible, and the reaction time is the only measurable quantity. Such instances may arise in cellular signalling driven by narrow escape [100, 101] and among fluorescent probes [102]. In both the examples illustrated in Fig. 3.1, the first-passage time statistics carry invaluable insight into the process, but are inaccessible to direct measurement. In such scenarios, a crucial challenge is to reliably *infer* the first-passage statistics and other fundamental properties of the system of interest. Our central objective in this chapter is to solve this challenge.

In this chapter, first, we will present exact results demonstrating how the first-passage time density can be obtained purely from gated statistics, and illustrate its applications in the inference of the diffusion coefficient. Second, using the joint knowledge of the gated and ungated first-passage time densities, we establish that the overlooked *short-time regime* of the first detection time distribution can be leveraged to obtain the gating rates. In what follows, we use $\langle T_z \rangle$ and $\widetilde{Z}_s \equiv \left\langle e^{-sT_z} \right\rangle$ to denote, respectively, the expectation and Laplace transform of the random variable $T_z$, and by $Z_t$ we denote its probability density function.

## 3.2 The Basic Setup

We recall our setup where a gated process is modeled consisting of two independent components. First, an underlying process $X_{x_0}(t)$, initially at $x_0$, modeled as a continuous-time Markov process. In this chapter, we note that several of our results directly apply to both discrete and continuous space processes, and can also be extended beyond Markov processes to include renewal processes. Second, a gate modeled by a two-state continuous-time Markov process, that intermittently switches between an 'open' active ($A$) state and a 'closed' inactive ($I$) state. The gate switches from state $A$ to $I$ at rate $\alpha$, and from $I$ to $A$ at $\beta$. For $\sigma_0, \sigma \in \{A, I\}$, we quickly recall that $p_t(\sigma|\sigma_0)$ denotes the probability that the gate is in state $\sigma$ at time $t$, given that it was in state $\sigma_0$ initially, and we define $\pi_A = \beta/\lambda$ and $\pi_I = \alpha/\lambda$ which are the equilibrium occupancy probabilities of states $A$ and $I$ respectively, where $\lambda = \alpha + \beta$ is the relaxation rate to equilibrium.

As is the case throughout this thesis, the central quantity of interest is the first-passage time $T_f(x^*|x_0)$, which is the time taken for $X_{x_0}(t)$ to reach state $x^*$ for the first time, and we denote its probability density by $F_t(x^*|x_0)$. In many scenarios the first-passage time is not directly measurable, and instead we can only measure the detection time $T_d(x_0, \sigma_0)$, of a reaction or threshold crossing event. We denote by $D_t(x_0, \sigma_0)$ the probability density of $T_d(x_0, \sigma_0)$, which is the first time the underlying process is *detected* in some target-set $\mathcal{Q}$, given that the initial state of the composite process (underlying + gate) is initially at $\{x_0, \sigma_0\}$.

In this work, we focus on two widely applicable settings: (i) the detection of threshold crossing events of a 1-dimensional intermittent time-series with nearest-neighbor transitions, where $\mathcal{Q}$ denotes all states above a certain threshold $x^*$ and $T_d(x_0, \sigma_0)$ is the first time when $X_{x_0}(t) \geq x^*$ while the detector is active (A), and (ii) gated reactions or target search on an arbitrary network in discrete space or in arbitrary dimension in continuous space. Here, $\mathcal{Q}$ is typically a single target state/point $x^*$, and $T_d(x_0, \sigma_0)$ denotes the first time the underlying process $X_{x_0}(t)$ is at $x^*$, while the gate is open (A).

## 3.3 Results

### 3.3.1 Inference of first-passage time distribution from gated observations

We begin our analysis by recalling Eq. (2.4) where for $x_0 \notin \mathcal{Q}$ we have

$$D_t(x_0,\sigma_0) = F_t(x^*|x_0)p_t(A|\sigma_0) + \int_0^t F_{t'}(x^*|x_0)p_{t'}(I|\sigma_0)D_{t-t'}(x^*,I)\,dt', \tag{3.1}$$

where the probability for a detection event occurring at time $t$ has two contributions: (i) the detection time coinciding with the first-passage time, and (ii) the gate being closed during the first-passage event (I), and detection happening strictly after this moment in time. The Laplace transform of Eq. (3.1), can be expressed in compact form as

$$\widetilde{D}_s(x_0,\sigma_0) = \left[\pi_A + \pi_I\widetilde{D}_s(x^*,I)\right]\widetilde{F}_s(x^*|x_0) + \mathbb{1}(\sigma_0)(1-\pi_{\sigma_0})\left[1-\widetilde{D}_s(x^*,I)\right]\widetilde{F}_{s+\lambda}(x^*|x_0), \tag{3.2}$$

where $\lambda = \alpha+\beta$, and $\mathbb{1}(\sigma_0)$ takes values $+1$ or $-1$ when $\sigma_0 = A$ or $I$, respectively.

Setting $\sigma_0 = A$ in Eq. (3.2) and rearranging, we have

$$\widetilde{D}_s(x_0,A) = \pi_A\widetilde{F}_s(x^*|x_0) + \pi_I\widetilde{F}_{s+\lambda}(x^*|x_0) + \pi_I\left(\widetilde{F}_s(x^*|x_0) - \widetilde{F}_{s+\lambda}(x^*|x_0)\right)\widetilde{D}_s(x^*,I), \tag{3.3}$$

or

$$\widetilde{D}_s(x_0,A) = \Big(\pi_A + \pi_I\widetilde{D}_s(x^*,I)\Big)\widetilde{F}_s(x^*|x_0) + \pi_I\Big(1-\widetilde{D}_s(x^*,I)\Big)\widetilde{F}_{s+\lambda}(x^*|x_0). \tag{3.4}$$

Similarly, the corresponding equation for $\sigma_0 = I$ reads

$$\widetilde{D}_s(x_0,I) = \Big(\pi_A + \pi_I\widetilde{D}_s(x^*,I)\Big)\widetilde{F}_s(x^*|x_0) - \pi_A\Big(1-\widetilde{D}_s(x^*,I)\Big)\widetilde{F}_{s+\lambda}(x^*|x_0). \tag{3.5}$$

It is easy to see that Eqs. (3.4) and (3.5) can be written in compact form as

$$\widetilde{D}_s(x_0,\sigma_0) = \left[\pi_A + \pi_I\widetilde{D}_s(x^*,I)\right]\widetilde{F}_s(x^*|x_0) + \mathbb{1}(\sigma_0)(1-\pi_{\sigma_0})\left[1-\widetilde{D}_s(x^*,I)\right]\widetilde{F}_{s+\lambda}(x^*|x_0), \tag{3.6}$$

where $\mathbb{1}(\sigma_0)$ takes values $+1$ or $-1$ when $\sigma_0 = A$ or $I$, respectively, yielding Eq. (3.2). Furthermore, the term containing $\widetilde{F}_{s+\lambda}(x^*|x_0)$ can be eliminated from Eqs. (3.4) and (3.5) by multiplying

them by $\pi_A$ and $\pi_I$ respectively, and adding the two resulting equations. This allows us to write

$$\widetilde{F}_s(x^*|x_0) = \frac{\pi_A \widetilde{D}_s(x_0, A) + \pi_I \widetilde{D}_s(x_0, I)}{\pi_A + \pi_I \widetilde{D}_s(x^*, I)}, \tag{3.7}$$

which is our first result. Equation (3.7) asserts that the first-passage density can be obtained exactly in terms of detection time densities and the gating rates. We note that Eq. (3.7) holds even when the underlying process in not Markovian, and instead is a renewal process. However, Eq. (3.7) implies that the inference of the first-passage time density $F_t(x^*|x_0)$, requires the detection statistics with initial conditions $\{x_0, A\}$, $\{x_0, I\}$, $\{x^*, I\}$ *and* the equilibrium probabilities $\pi_A$ and $\pi_I$. Such information may not be accessible in experimentally realizable scenarios where, e.g., it may not be possible to initialize a gated molecule in a specific internal state $\sigma_0 = A$ or $I$, and the values of $\pi_A$ and $\pi_I$ may also be unknown.

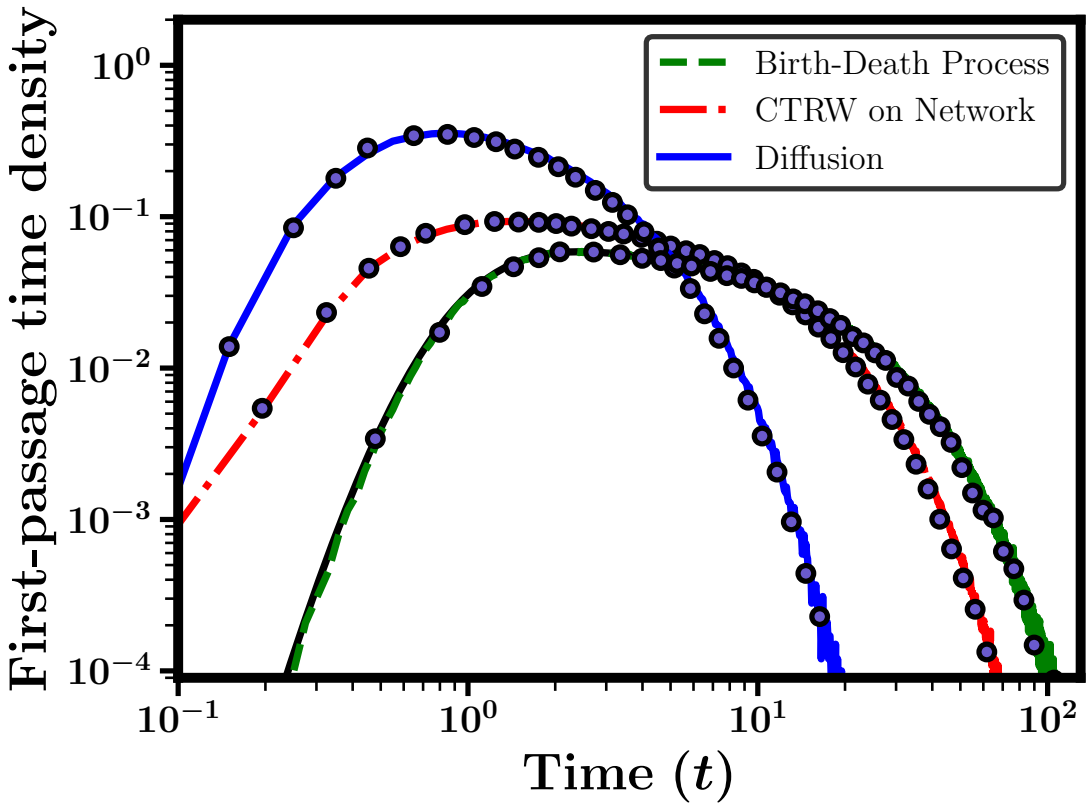


Figure 3.2: Inference of first-passage time distributions from gated observations. We consider the three different settings mentioned in the text and legend. Solid and dashed lines denote ungated first-passage time distributions obtained from theory and simulations, respectively. Circles are inferred using Eq. (3.8) from histograms of simulated gated detection times.

In such situations, the most practically realizable initial condition is the equilibrium $\sigma_0 \equiv E$,

where the gate is in the active state $A$ with probability $\pi_A$, and in the inactive state $I$ with probability $\pi_I$. Note that this initial condition is naturally achieved if the system is simply allowed to equilibriate. Interestingly, the detection time density starting from the initial condition $(x_0, E)$ is given by $D_t(x_0, E) = \pi_A \cdot D_t(x_0, A) + \pi_I \cdot D_t(x_0, I)$, whose Laplace transform is the numerator standing on the right-hand side of Eq. (3.7). Further noting that the Laplace transform of $D_t(x^*, E) = \pi_A \cdot \delta(t) + \pi_I \cdot D_t(x^*, I)$ gives the denominator on the right-hand side, we obtain an elegant reinterpretation of Eq. (3.7):

$$\widetilde{F}_s(x^*|x_0) = \frac{\widetilde{D}_s(x_0, E)}{\widetilde{D}_s(x^*, E)}. \tag{3.8}$$

Strikingly, Eq. (3.8) asserts that the first-passage time density can be inferred from the detection statistics, even without the explicit knowledge of $\pi_A$ and $\pi_I$, or control over the initial state of the gate.

The usefulness and validity of Eq. (3.8) is demonstrated in Fig. 3.2, with the help of three case studies of wide interest and applicability. First, a Markovian birth-death process which has been extensively used to model threshold activated reactions [53, 54, 56, 57] and the dynamics of chemical reactions on catalysts [103, 104]. Second, the paradigmatic continuous-space diffusion in a 1D confinement. Third, a gated chemical reaction/target search modeled by a non-Markovian continuous-time random walk (CTRW) [17, 105] on a network [106], which is e.g., used to model the motion of reactants, cells, or organisms in complex environments [49, 106–112]. The details of the parameters and models for preparing Fig. 3.2 are presented in Sec. H.3. In all of these settings, we show that the first-passage time distributions inferred from Eq. (3.8) (circles) using a procedure described in Sec. 3.3.1.2 are in excellent agreement with the true first-passage time distributions. We stress that this inference was performed solely using detection time histograms obtained from gated simulations, without assuming knowledge of their analytical expressions or model specific details (e.g. the network structure and the waiting time distribution in the CTRW example). However, when analytical expressions are available, like in the case of the birth-death process [30], one can directly perform the inference through Laplace inversion of Eq. (3.8).

Before moving forward, we note that Eq. (3.8) is reminiscent of the seminal renewal formula $\widetilde{F}_s(x^*|x_0) = \frac{\widetilde{C}(x^*,s|x_0)}{\widetilde{C}(x^*,s|x^*)}$ which relates, in Laplace space, the first-passage time density and the probability density $C(n_i, t|n_j)$ of finding the underlying process in state $n_i$ at time $t$, given its

initial state $n_j$ [1]. Clearly, the right-hand side of this formula and that of Eq. (3.8) are equal. In fact, we can obtain an even more general relation – considering two different initial states $x_0$ and $x_0'$, and after some algebra, we uncover the fundamental relation

$$\frac{\widetilde{D}_s(x_0, E)}{\widetilde{D}_s(x_0', E)} = \frac{\widetilde{C}(x^*, s|x_0)}{\widetilde{C}(x^*, s|x_0')}, \tag{3.9}$$

asserting that the ratio of the detection time densities (in Laplace space), starting from any two initial states $x_0$ and $x_0'$, is independent of the gating rates $\alpha$ and $\beta$. Note that this is true despite the fact that the detection time densities themselves depend on the gating rates. We remark that Eq. (3.9) holds in both settings: when $D_t(x_0, E)$ corresponds to gated target search and to the detection of threshold crossing events under intermittent sensing. In fact, this equality can be easily extended to give

$$\frac{\widetilde{D}_s(x_0, E)}{\widetilde{D}_s(x_0', E)} = \frac{\widetilde{C}(x^*, s|x_0)}{\widetilde{C}(x^*, s|x_0')} = \frac{\widetilde{F}_s(x^*|x_0)}{\widetilde{F}_s(x^*|x_0')}, \tag{3.10}$$

which constitute a novel and elegant set of relations between the propagator, and the first-passage and first detection time densities.

#### 3.3.1.1 Extension to renewal processes

In the above discussion we assumed that the underlying process is a continuous-time Markov process. However, this modelling assumption can be relaxed, and our results can be shown to be valid even when the underlying process is modelled as a renewal process.

To see this, we use as a starting point the following renewal structure [49]

$$T_d(x_0, \sigma_0) = T_f(x^*|x_0) + \begin{cases} 0, & \text{if } \sigma_{T_f(x^*|x_0)} = A \\ T_d(x^*, I), & \text{otherwise,} \end{cases} \tag{3.11}$$

where $T_d(x_0, \sigma_0)$, $T_d(x^*, I)$, and $T_f(x^*|x_0)$ denote random variables whose densities have been denoted by $D_t(x_0, \sigma_0)$, $D_t(x^*, I)$, and $F_t(x^*|x_0)$ in the main text. By $\sigma_{T_f(x^*|x_0)} = A$ in the above equation, we mean that the random variable denoting the state of the gate takes value $A$ at time $T_f(x^*|x_0)$, given that its state initially was $\sigma_0$. Equation (3.11) is valid even when the underlying spatial process is an arbitrary renewal process and thus allows us to relax the Markovian assumption.

Taking a Laplace transform of Eq. (3.11), and rearranging, we get

$$\widetilde{D}_s(x_0,\sigma_0) = \left[\pi_A + \pi_I \widetilde{D}_s(x^*, I)\right] \widetilde{F}_s(x^*|x_0) + \mathbb{1}(\sigma_0)(1-\pi_{\sigma_0}) \left[1 - \widetilde{D}_s(x^*, I)\right] \widetilde{F}_{s+\lambda}(x^*|x_0), \tag{3.12}$$

which is the same as Eq. (3.2).

#### 3.3.1.2 Inference of first-passage time distribution from data

Equation (3.8) allows us to represent the first-passage time distribution purely in terms of the observable detection time distributions. In this section, we show that this equation can be used to infer the first-passage time distribution directly from detection times data. This is of utmost importance, since in many practically relevant scenarios, analytical expressions for the detection time distributions are not known as we might not know the laws of motion or specific parameter values of the underlying process. First, we note that in the time domain Eq. (3.8) can be written as a convolution

$$D_t(x_0, E) = \int_0^t F_{t'}(x^*|x_0) D_{t-t'}(x^*, E)\, dt'. \tag{3.13}$$

This suggests that the problem of inferring the first-passage time distribution from gated detection times can be viewed as a deconvolution problem. In practice, when detection time data are obtained from simulations/experiments, we discretize the detection time distributions by binning the data in histograms. Thus, we discretize Eq. (3.13), and recast it as a matrix equation

$$\vec{D}_t(x_0, E) = \mathbb{D}_t(x^*, E)\vec{F}_t(x^*|x_0), \tag{3.14}$$

where $\mathbb{D}_t(x^*, E)$ is a matrix, which is interpretted as an operator that acts on the vector $\vec{F}_t(x^*|x_0)$ by performing a convolution and giving the vector $\vec{D}_t(x_0, E)$ as output. More specifically, we

have

$$\underbrace{\begin{bmatrix} D_0(x_0,E) \\ D_\Delta(x_0,E) \\ D_{2\Delta}(x_0,E) \\ D_{3\Delta}(x_0,E) \\ \vdots \\ D_{\mathcal{N}\Delta}(x_0,E) \end{bmatrix}}_{\vec{D}_t(x_0,E)} = \mathbb{D}_t(x^*,E) \underbrace{\begin{bmatrix} F_0(x^*|x_0) \\ F_\Delta(x^*|x_0) \\ F_{2\Delta}(x^*|x_0) \\ F_{3\Delta}(x^*|x_0) \\ \vdots \\ F_{\mathcal{N}\Delta}(x^*|x_0) \end{bmatrix}}_{\vec{F}_t(x^*|x_0)}, \tag{3.15}$$

where

$$\mathbb{D}_t(x^*,E) = \Delta \begin{bmatrix} D_0(x^*,E) & 0 & 0 & 0 & \dots & 0 \\ D_\Delta(x^*,E) & D_0(x^*,E) & 0 & 0 & \dots & 0 \\ D_{2\Delta}(x^*,E) & D_\Delta(x^*,E) & D_0(x^*,E) & 0 & \dots & 0 \\ D_{3\Delta}(x^*,E) & D_{2\Delta}(x^*,E) & D_\Delta(x^*,E) & D_0(x^*,E) & & \\ \vdots & \vdots & \vdots & & \ddots & \\ D_{\mathcal{N}\Delta}(x^*,E) & D_{(\mathcal{N}-1)\Delta}(x^*,E) & D_{(\mathcal{N}-2)\Delta}(x^*,E) & \dots & \dots & D_0(x^*,E). \end{bmatrix} \tag{3.16}$$

Here, $\Delta$ is the histograms' bin width and $\mathcal{N}+1$ as the total number of bins. Evidently, $\mathbb{D}_t(x^*,E)$ is a lower-triangular, Toeplitz, matrix whose entries are densities obtained from the histogram of $D_t(x^*,E)$, scaled by a factor of $\Delta$. Thus, we can write

$$\vec{F}_t(x^*|x_0) = \mathbb{D}_t(x^*,E)^{-1}\vec{D}_t(x_0,E), \tag{3.17}$$

implying that the problem of inferring the first-passage time distribution reduces to a problem of inverting a lower diagonal Toeplitz matrix with a non-zero determinant. In the main text, we demonstrated the validity and robustness of this approach using three distinct examples – a birth-death process, CTRW on network, and 1D confined diffusion, where we performed inference from detection time histograms generated from $10^6$ detection events. Further expanding on the diffusion example, in Fig. 3.3, we demonstrate the deconvolution method to infer the first-passage statistics from gated detection time data. In panel (a), we clearly note that the deconvoluted first-passage time density shows an excellent agreement with the first-passage time histogram computed from ungated simulations. A corresponding log-log plot in panel (b) reveals

some numerical errors in the tail of the inferred first-passage time distribution. In panel (c), we plot the inferred density after a logarithmic binning and we can see that the full circles (depicting the mean values of the values in each bin) match the true first-passage time histogram very well. The logarithmic binning helps in reducing the numerical errors from the tails, however it does not completely remove them. An alternate method to perform this inference could involve parametric inference which uses domain-specific knowledge (e.g., exponential tail of first-passage time distributions in confined systems) to improve upon this inference method.

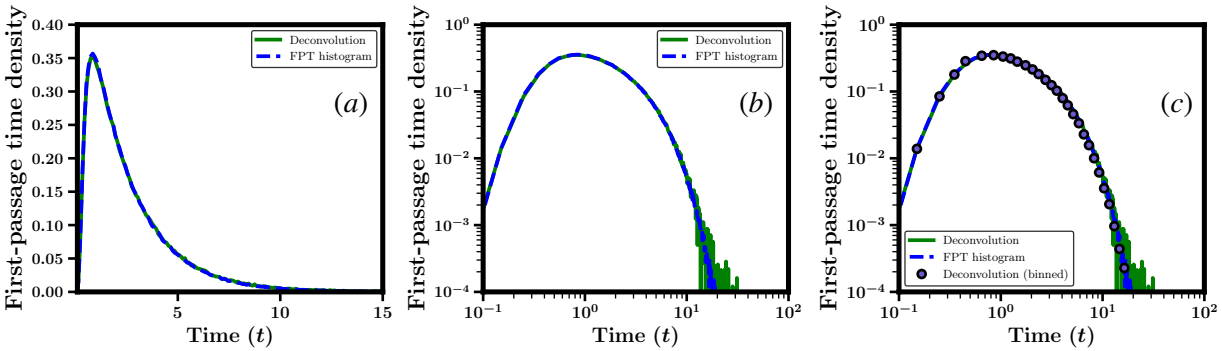


Figure 3.3: Illustration of the deconvolution method to infer the first-passage statistics from gated detection time data, using the example of a diffusing particle confined in a 1D box. (a) The deconvoluted first-passage time density overlaps almost perfectly with the first-passage time histogram computed from ungated simulations. (b) A log-log plot shows that there are numerical errors when estimating very small probabilities (the noisy green tail). However, by taking logarithmic bins and assigning the mean value of the densities within each bin to be the density for that bin, we show in panel (c) that the full circles (depicting the mean values of the values in each bin) match the first-passage time histogram well.

### 3.3.2 Inferring the mean first-passage time

The Laplace transform in Eq. (3.8) allows us to obtain all moments of the first-passage time in terms of moments of the detection time. Equation (3.8) further implies that all cumulants of the first-passage time can be expressed as differences between cumulants of detection times. For example, the mean first-passage time is given by

$$\langle T_f(x^*|x_0)\rangle = \langle T_d(x_0, E)\rangle - \langle T_d(x^*, E)\rangle. \tag{3.18}$$

While simple, Eq. (3.18) carries utmost importance in practical scenarios, where reliably estimating the full probability distribution is not a viable option, and only the mean can be accurately measured. Apart from setting an important time-scale for a wide class of chemical reactions in confinement, where the mean reaction time can be used to infer full reaction time statistics [113], the mean first-passage time can also shed light on fundamental properties of the system at hand [114, 115].

### 3.3.3 Inferring the gating rates $\alpha$ and $\beta$

Equation (3.8) states that the first-passage time density can be inferred from its gated counterparts, even without any prior knowledge of the gating rates $\alpha$ and $\beta$ or control over the initial internal condition. We will now illustrate how the inferred first-passage time distribution can be used together with the observed detection time distribution to infer the gating rates, thus providing insight into the dynamics of the gating process.

To proceed, we shift our focus to short-time asymptotics analysis which, despite several recent applications in stochastic thermodynamics [116–118] and chemical kinetics [119, 120], has not yet been used to further our knowledge on gated processes.

In the short-time limit, the dominant contribution to $D_t(x_0, E)$ comes from trajectories where the detection occurs upon first arrival. We recall that, for $\sigma_0 = E$, we have the relation,

$$D_t(x_0, E) = \pi_A F_t(x^*|x_0) + \pi_I \int_0^t F_{t'}(x^*|x_0) D_{t-t'}(x^*, I) dt', \tag{3.19}$$

which can be obtained from Eq. (3.2), by noting that $D_t(x_0, E) = \pi_A D_t(x_0, A) + \pi_I D_t(x_0, I)$. Furthermore, we have $D_t(x^*, E) = \pi_A \delta(t) + \pi_I D_t(x^*, I)$. Evidently, the short-time behaviour of $D_t(x^*, E)$ is governed by that of $D_t(x^*, I)$, which can in turn be expressed as

$$D_t(x^*, I) \simeq \beta(1 - \Delta(t)) \tag{3.20}$$

where $\Delta(t) \to 0$ in the $t \to 0$ limit. For example, in the case of gated chemical reactions where $x^*$ denotes a target state, the short-time expression for $D_t(x^*, I)$ is

$$D_t(x^*, I) \simeq \beta e^{-\beta t} e^{-\gamma_{x^*} t} \tag{3.21}$$

where $\gamma_{x^*}$ denotes the rate at which the reactant escapes the target state $x^*$. Equation (3.21)

expresses the fact that the dominant contribution to reaction events in the short-time limit comes from the events where the gate opens before the reactant leaves the target state $x^*$. Using the approximation $e^{-\lambda t} \simeq 1 - \lambda t$, it is easy to see that $\Delta(t) = (\beta + \gamma_{x^*})t + o(t)$, and in the $t \to 0$ limit, we have

$$\lim_{t\to 0} D_t(x^*, I) = \beta. \tag{3.22}$$

Equation (3.22) asserts that $D_t(x^*, I)$ tends to a constant ($\beta$) in the short-time limit. Similarly, the second term of the right-hand side in Eq. (3.19) can be safely ignored in the short-time limit, yielding

$$D_t(x_0, E) \simeq \pi_A F_t(x^*|x_0). \tag{3.23}$$

From here, we have

$$\pi_A = \lim_{t\to 0} \frac{D_t(x_0, E)}{F_t(x^*|x_0)}. \tag{3.24}$$

In a similar vein, the short-time asymptotics of $D_t(x^*, E)$ can be expressed as

$$D_t(x^*, E) \simeq \pi_I D_t(x^*, I). \tag{3.25}$$

Using Eq. (3.22), we arrive at

$$\pi_I = \lim_{t\to 0} \frac{1}{\beta} D_t(x^*, E). \tag{3.26}$$

We are now in the position to derive relations for the inference of $\alpha$ and $\beta$ from the limiting representations of $\pi_A$ and $\pi_I$ presented in Eqs. (3.24) and (3.26). To obtain these relations, we will use two identities: (i) $\pi_A + \pi_I = 1$, and (ii) $\pi_A \alpha = \pi_I \beta$. While the first identity is trivially the normalization of occupancy probabilities, the latter can be seen as a statement of detailed balance for the two-state Markov process which models our gate.

Writing Eq. (3.26) as $\pi_I\ \beta = \lim_{t\to 0} D_t(x^*, E)$, and using $\pi_A \alpha = \pi_I \beta$, we have

$$\pi_A\ \alpha = \lim_{t\to 0} D_t(x^*, E), \tag{3.27}$$

where, $\pi_A$ can be further substituted from Eq. (3.24), to obtain

$$\alpha = \lim_{t\to 0} \frac{D_t(x^*, E) F_t(x^*|x_0)}{D_t(x_0, E)}. \tag{3.28}$$

To obtain the corresponding inference relation for $\beta$, we note that Eq. (3.26) gives

$$\beta = \frac{1}{\pi_I} \lim_{t\to 0} D_t(x^*, E), \tag{3.29}$$

where $\pi_I = \frac{\alpha}{\alpha+\beta}$. This gives us

$$\beta = \frac{\alpha+\beta}{\alpha} \lim_{t\to 0} D_t(x^*, E), \tag{3.30}$$

which can be further simplified to obtain

$$\beta = \left(1 + \frac{\beta}{\alpha}\right) \lim_{t\to 0} D_t(x^*, E). \tag{3.31}$$

Substituting for $\alpha$ in the above equation from Eq. (3.28), we get

$$\beta = \lim_{t\to 0} \frac{D_t(x^*, E) F_t(x^*|x_0)}{F_t(x^*|x_0) - D_t(x_0, E)}. \tag{3.32}$$

Equations (3.28) and (3.32), which constitute the first set of relations that allow the inference of

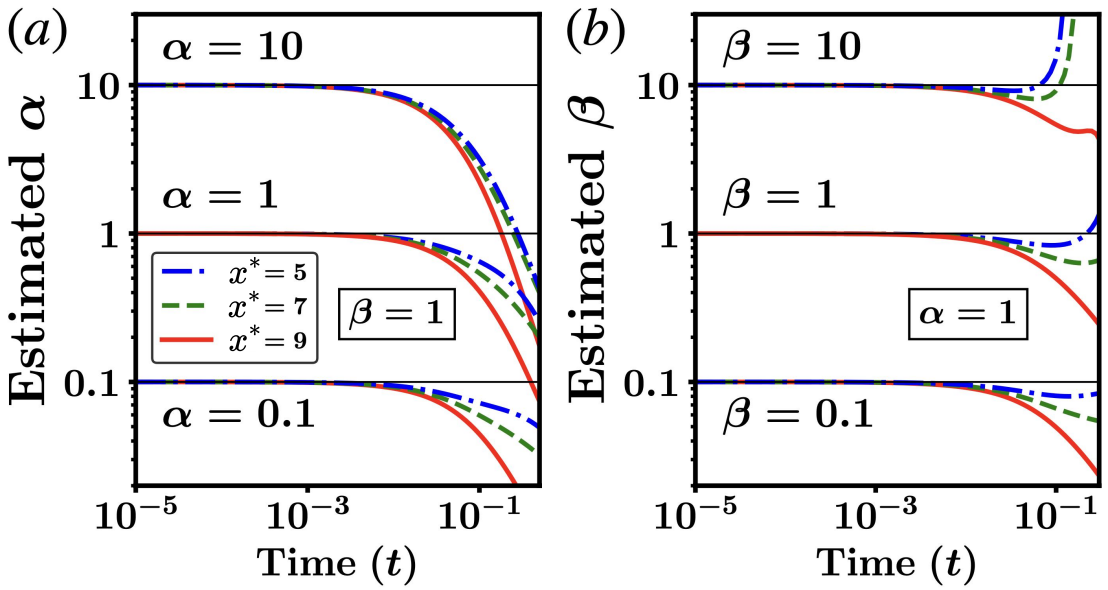


Figure 3.4: Inference of the gating rates $\alpha$ (panel a) and $\beta$ (panel b) from the short-time asymptotics of Eq. (3.28) and (3.32) respectively. Results are for the birth-death model used in Fig. 3.2, and various values of $\alpha$ and $\beta$. Details of the model and parameter values are in Appendix G.

gating rates in gated chemical reactions, are corroborated in Fig. 3.4, for the birth-death process with parameters described in Sec. H.3. Below, we show that these relations hold even for an arbitrary (non-equilibrium) initial condition of the gate. We then derive simpler inference relations

for the gating rates, which are obtained at the cost of perfect control over $\sigma_0$. Finally, we discuss the widely applicable case of simple diffusion and derive inference relations for $\alpha$ and $\beta$, which only differ by a factor of 2 from Eqs. (3.28) and (3.32).

#### 3.3.3.1 Inference for arbitrary initial condition of the gate

In this subsection, we demonstrate that Eqs. (3.28) and (3.32) hold more generally, and we can relax the condition that the gate is initially equilibriated.

Consider a situation where we do not have information about the initial conditions of the gate. Let us denote by $p_A$ and $p_I$ the unknown probabilities for the gate to be initially active $A$ and inactive $I$ respectively, for $p_A \in (0,1)$ and $p_I = 1 - p_A$. Note that we do not assume that $p_A = \pi_A$ and $p_I = \pi_I$. Following the intuition developed for Eq. (3.24) and Eq. (3.26), we have the following short-time asymptotic relations,

$$p_A = \lim_{t\to 0} D_t(x_0)/F_t(x^*|x_0) \tag{3.33}$$

and

$$p_I = \frac{1}{\beta}\lim_{t\to 0} D_t(x^*), \tag{3.34}$$

where we have dropped the notation for gate initialization ($D_t(x_0)$ denotes the detection time density given that the initial state of the underlying process is $x_0$, and the initial preparation of the gate is unknown). The normalization of probabilities dictates that $p_A + p_I = 1$. So, adding up the above two equations, we get,

$$1 = \lim_{t\to 0}\left(\frac{1}{\beta}D_t(x^*) + \frac{D_t(x_0)}{F_t(x^*|x_0)}\right) \tag{3.35}$$

yielding:

$$\beta = \frac{F_t(x^*|x_0)\; D_t(x^*)}{F_t(x^*|x_0) - D_t(x_0)} \tag{3.36}$$

which is the same as Eq. (3.32) from the main text. Similarly, Eq. (3.28) can be derived in this even more general setting.

#### 3.3.3.2 Inference in the presence of control over gate initialization

In this subsection, we discuss the possibility of inferring $\alpha$ and $\beta$ in the case where we can control the initial state of the gate $\sigma_0$. Using the fact that $p_t(A|A) = \pi_A + \pi_I e^{-\lambda t}$ and $p_t(I|A) =$

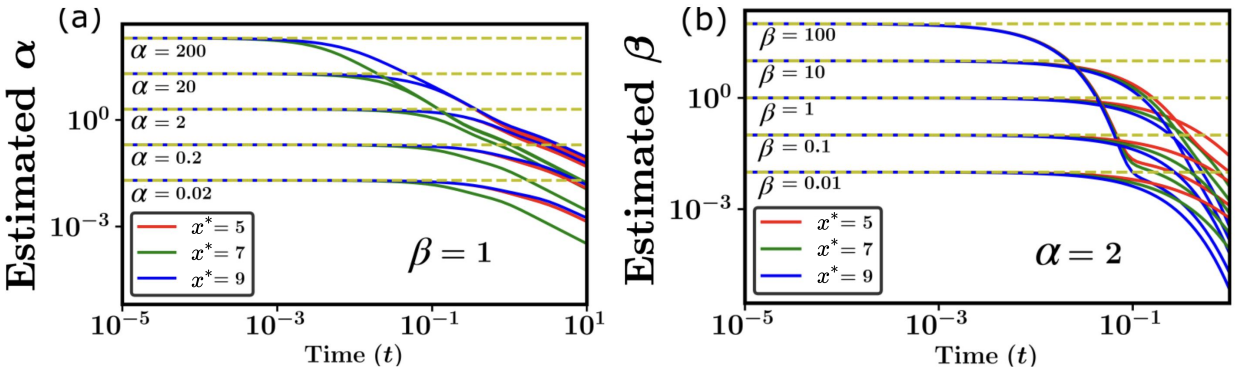


Figure 3.5: Inference of the gating rates $\alpha$ and $\beta$ from short-time asymptotics for the birth-death process (defined in Sec. H.3) with $k_+ = 0.1$, $k_1 = 1$, and $N = 10$. (a) A plot demonstrating that early deviations of the detection time distribution from the first-passage time distribution, as captured by Eq. (3.38), can be used to infer the numerical value of $\alpha$. (b) Inference of $\beta$ through the short-time asymptotic behaviour of $D_t(x^*, I)$ given by Eq. (3.39). It is clear that the short-time asymptotics of the detection time distributions can be leveraged to infer the gating rates in gated first-passage processes.

$\pi_I - \pi_I e^{-\lambda t}$, we have

$$D_t(x_0, A) = F_t(x^*|x_0)(\pi_A + \pi_I e^{-\lambda t}) + \int_0^t F_{t'}(x^*|x_0)\left(\pi_I(1 - e^{-\lambda t'})\right) D_{t-t'}(x^*, I)dt'.$$

In the limit of short-time ($t \to 0$), we can write $e^{-\lambda t} \simeq 1 - \lambda t$, which gives us

$$D_t(x_0,A) \simeq F_t(x^*|x_0) - \pi_I \lambda t F_t(x^*|x_0), \tag{3.37}$$

where we neglect the second term. It is a matter of simple algebra to see that

$$\alpha = \lim_{t\to 0} \frac{F_t(x^*|x_0) - D_t(x_0, A)}{t \cdot F_t(x^*|x_0)}. \tag{3.38}$$

Equation (3.38) asserts that the early deviations of $D_t(x_0, A)$ from $F_t(x^*|x_0)$ can be leveraged to obtain the gating rate $\alpha$ corresponding to deactivation of the gate. On the other hand, Eq. (3.22) is sufficient to infer $\beta$ as

$$\beta = \lim_{t\to 0} D_t(x^*, I). \tag{3.39}$$

In Fig. 3.5, we corroborate the validity of Eqs. (3.38) and (3.39) using the birth-death process described in Sec. H.3.

#### 3.3.3.3 Inference in the case of diffusion

An important quantity in the inference of $\alpha$ and $\beta$ from the detection time distributions is the short-time asymptotics of $D_t(x^*, I)$. This quantity was derived in Eq. (3.22) using the fact that, at short-times, the dominant contribution to detection events comes from trajectories where the gate opens before the underlying process escapes the target-region (i.e., for detection of threshold crossing events, it means that the time-series has not dropped below the threshold, and for gated chemical reactions, it corresponds to the particle not escaping the target site before the opening of the gate). However, in continuous-space Markov processes this underlying assumption does not hold, since the process can leave and return to the target region multiple times during an infinitesimally small time interval. This means that the second term on the right-hand side of Eq. (3.19) can no longer be ignored.

Let us consider the example of a freely diffusing particle in 1-dimension, whose position at time $t$ we denote by $X_{x_0}(t)$ given that it starts from position $x_0$. We define $T_d(x_0, I)$ to be the time taken for the particle to be detected in a location $X_{x_0}(t) \geq x^*$, given that initially, the gate is in state $\sigma_0 = I$. While Eq. (3.24) is valid even in this setting, Eq. (3.26) is not. Thus, in order to infer $\alpha$ and $\beta$, our goal is to compute the short-time asymptotics of the probability density $D_t(x^*, I)$ of the random variable $T_d(x^*, I)$.

We note that the dominant contribution to $D_t(x^*, I)$ at short-times comes from the events where detection happens as soon as the gate opens. Note that, in this time, owing to the continuous nature of the process, $X_{x^*}(t)$ could have dropped below the threshold $x^*$ and crossed it subsequently several times. Thus, instead of looking at the first time when it drops below the threshold, the more meaningful question to ask in this setting is: what is the probability that $X_{x^*}(t) \geq x^*$ when the gate opens? Owing to the symmetry of the free diffusion problem, the answer is clearly $\frac{1}{2}$. This observation allows us to write

$$\lim_{t\to 0} D_t(x^*, I) = \frac{\beta}{2}, \tag{3.40}$$

and thus

$$\lim_{t\to 0} D_t(x^*, E) = \pi_I \lim_{t\to 0} D_t(x^*, I) = \pi_I \frac{\beta}{2}. \tag{3.41}$$

Rearranging, we get the analogue of Eq. (3.26) for continuous processes as

$$\pi_I = \frac{2}{\beta} \lim_{t \to 0} D_t(x^*, E), \tag{3.42}$$

where we remark that the right-hand side of Eq. (3.42) differs from the right-hand side of Eq. (3.26) only by a factor of 2. This relation can be utilized along with Eq. (3.24) to obtain

$$\beta = \lim_{t \to 0} \frac{2\, D_t(x^*, E) F_t(x^*|x_0)}{F_t(x^*|x_0) - D_t(x_0, E)}, \tag{3.43}$$

and following the same steps as in the previous sections, we get

$$\alpha = \lim_{t \to 0} \frac{2\, D_t(x^*, E) F_t(x^*|x_0)}{D_t(x_0, E)}. \tag{3.44}$$

This completes our derivation of the inference relations for $\alpha$ and $\beta$ for the case of continuous Markov processes. It is to be noted that though Eq. (3.40) was derived for the detection of $X_{x^*}(t)$ above $x^*$, we expect it to be valid at short-times for detection in any finite sized interval $[x^*, x^* + \Delta]$ as well. The reason is that at short times the probability that the process $X_{x^*}(t)$ crosses above $x^* + \Delta$ is negligible. Thus, finite-size effects do not play a role at this level. Clearly, the threshold crossing problem is recovered in the $\Delta \to \infty$ limit.

### 3.3.4 Inferring the diffusion coefficient

We now illustrate how one can utilize our framework to infer physically meaningful parameters like the diffusion coefficient $\mathcal{D}$. Importantly, we show that this can be done even when the actual motion of the particle cannot be tracked. Imagine a scenario like that depicted in Fig. 3.1(b), namely we inject an unobservable particle—whose detection is possible only upon reaction—at a known location $x_0$. Assume that the internal state of the particle is initially equilibrated ($\sigma_0 = E$); and further assume that it is freely diffusing inside an effectively one-dimensional box $[0, L]$ with reflecting boundaries and a gated target located at $x_0 < x^* < L$. Utilizing Eq. (3.18) we find that

$$\mathcal{D} = \frac{1}{2} \frac{x^{*2} - x_0^2}{\langle T_d(x_0, E) \rangle - \langle T_d(x^*, E) \rangle}. \tag{3.45}$$

Equation (3.45) asserts that the diffusion coefficient can be inferred from the difference in the measurable detection times $\langle T_d(x_0, E) \rangle$ and $\langle T_d(x^*, E) \rangle$.

To corroborate this finding, we simulate the aforementioned scenario and test it for a wide

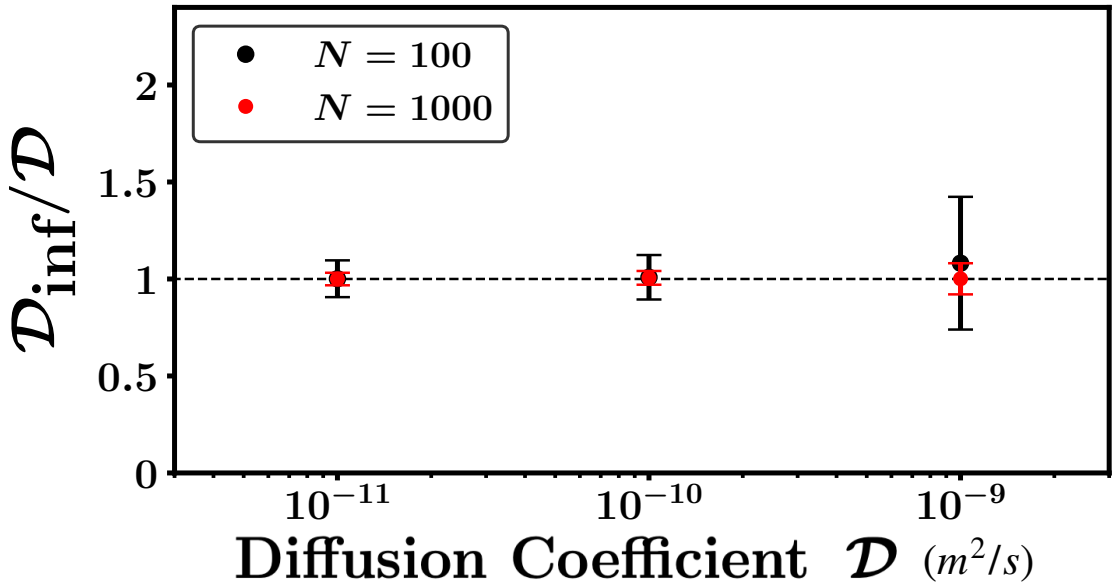


Figure 3.6: Inference of the diffusion coefficient. Equation (3.45) is used to infer the diffusion coefficient of an unobservable particle that is injected at a known location $x_0 = 0$ into a box $[0, 5\mu m]$ with reflecting boundaries. The initial internal state is equilibrated $\sigma_0 = E$, and a gated point target is located at $x^* = 4\mu m$, with gating rates $\alpha = \beta = 10^2 s^{-1}$.

range of possible diffusion coefficients (Fig. 3.6). As implied by Eq. (3.18), the difference in the detection times is independent of the transition rates, the box size $L$, and the target size (the same equation will hold for threshold crossing). It is thus up to the experimentalist to tune these parameters such that the detection times can be measured with sufficient accuracy. Here we set $\alpha = \beta = 10^2 s^{-1}$ and $L = 5\mu m$. For each value of $\mathcal{D}$, the corresponding mean detection times were estimated from averages of $N = 10^2$ and $10^3$ simulations, and the diffusion coefficient was inferred via Eq. (3.45). The errors bars were estimated by repeating this procedure $10^2$ times and noting the standard deviation. In Fig. 3.6 we plot the ratio between the inferred values and the actual ones. We find this estimation procedure robust, even when the number of measurements is relatively small ($N = 10^2$). For the parameters used here, the estimation is especially accurate for smaller diffusion coefficients, where mean detection times are longer.

## 3.4 Discussion

Using the unified framework of gated first-passage processes, we demonstrated how the first-passage time distribution can be inferred from gated measurements, and using these quantities, key features of the process can be extracted. The exact results obtained in this chapter can help

inform statistical inference frameworks designed to deal with situations pertaining to imperfect observation conditions, including sparsely sampled time-series or missing data problems. The asymptotic results presented herein moreover provide a systematic approach to the inference of gating rates which, depending on the accessible timescales of the problem, can be improved upon by considering higher-order corrections to the asymptotics.

# CHAPTER 4

# Applications

In this thesis thus far, our focus has been two-fold – first, we have derived general formulas to compute the statistics of the detection time distribution and relate it to the details of the underlying process; second, we built a model-free framework through which the detection time statistics can be leveraged to obtain the first-passage time distribution of the underlying process, along with the inference of several other relevant parameters.

In this chapter, we switch our focus towards exploring how the frameworks developed in this thesis can be utilized to tackle practically relevant problems that do not appear to fall under the purview of gated first-passage processes at first glance. In particular, we look at the following three applications:

1. **Optimal sampling of a first-passage process:** By extending the formalism developed in Chapter 2, we solve the problem of finding the optimal rate for sampling a time-series when the first-passage properties of the time-series are of interest but making measurements is costly.

2. **Extreme value statistics of partially observed stochastic processes:** We show how the framework of gated first-passage processes can be leveraged to obtain insight into the statistics of extremes of partially observed time-series. Using our work on the inverse problem presented in Chapter 3, we also discuss the inference of the true extreme statistics of the process through knowledge of the statistics of the partially observed process.

3. **Imputation of missing statistics using stochastic bridges:** We extend our discussion on conditioned first-passage processes and show how information about the observed data can be incorporated to make data-informed estimates of missed first-passage events.

We begin by outlining how the theory of gated first-passage processes can be used to find the optimal sampling rate of a first-passage process.

## 4.1 Optimal sampling of a first-passage process

Suppose we are interested in a time-series which we denote by $X(t)$. This time-series could denote the temperature of a city over time, the price fluctuations of a stock, or even the number of infected individuals in a pandemic. As discussed in previous chapters, in all of these disparate settings, an important question to ask is when does $X(t)$ cross a pre-defined threshold $x^*$ for the first time. If we can perfectly observe $X(t)$ at all times, then the answer to this question relies on the computation of the *first-passage time*. Unfortunately, measurements are often costly, and in several practical applications, $X(t)$ can only be intermittently observed – be it due to energy costs of monitoring, imperfect observation conditions, or the inevitable finite resolution of measurement devices. In such scenarios, the instance of first-passage can be missed, and the time when $X(t)$ is *observed* to be above the threshold for the time, called the *first detection time*, is the quantity of interest.

Despite the costs associated with sampling the process of interest, making a reliable estimate of the first-passage time of the underlying process is crucial in several applications, albeit it requires making a large number of measurements. At the heart of this discussion lies an optimization problem: what are the optimal rates for sampling a time-series, so that the difference between first-passage and first detection times is small, while also keeping the number of measurements low? Of course, if we can fully observe the process of interest $X(t)$, then the first-passage and detection times would be identical, and their difference would be $0$. However, performing such continuous measurements is impractical, and in most cases, one needs to reduce the number of measurements being made, often resorting to sparse sampling. These competing features of the problem and the trade-off lead to a non-trivial optimization problem. The goal of this section is to address this optimization problem.

### 4.1.1 Problem Statement

Suppose $X_{x_0}(t)$ is a 1-dimensional stochastic process that undergoes Markovian evolution, which is being monitored by a sensor modeled as a two-state Markov process. This is the typical scenario assumed throughout the thesis. We are especially interested in the limit $\alpha \to \infty$, which corresponds to the case where the sensor switches off immediately after turning on, thus making only point measurements and effectively sampling the time-series $X_{x_0}(t)$ at rate $\beta$.

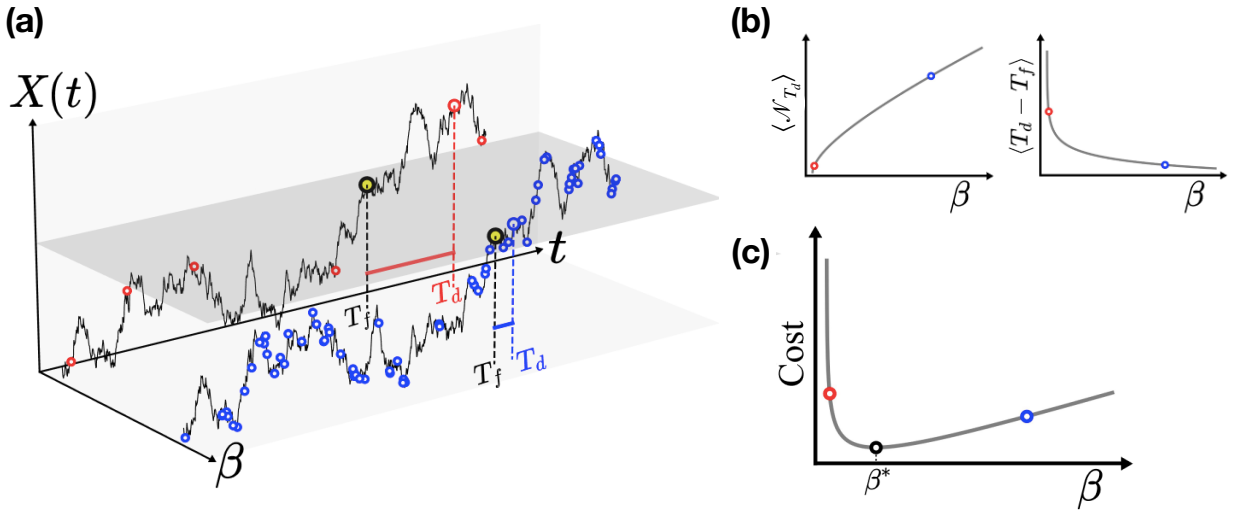


Figure 4.1: Schematic depiction of a fundamental trade-off arising out of intermittent sensing. (a) a time-series being monitored at two different sampling rates $\beta$. Higher sampling rate (blue) leads to a smaller gap between the first-passage and detection times. (b) Mean number of samples needed until detection, $\langle \mathcal{N}_{T_d} \rangle$, and the mean gap between the first-passage and detection times plotted as a function of the sampling rate $\beta$. (c) The cost function $C(\beta)$, plotted as a function of $\beta$, with a minimum occurring at $\beta = \beta^*$.

To formalize our optimization problem, we postulate a cost function $C(\beta)$ as follows,

$$C(\beta) = \langle T_d(x_0, \sigma_0) - T_f(x^*|x_0) \rangle \; + \; \delta \cdot \langle \mathcal{N}_{T_d(x_0,\sigma_0)} \rangle, \tag{4.1}$$

where $\mathcal{N}_{T_d(x_0,\sigma_0)}$ is the number of samples taken until detection. In other words, $\mathcal{N}_{T_d(x_0,\sigma_0)}$ corresponds to the number of times the sensor switches on until the first threshold crossing event is detected. We define $\delta$ to be a parameter that denotes how much each sample "costs". It can be perceived as the penalty (in units of time) that an observer has to pay for each measurement that it makes. As schematically outlined in Fig. 4.1(a), if $\beta$ is low, the number of samples collected is low, but the difference between the first-passage and detection times is high. Conversely, when $\beta$ is high, the first detection time is a more accurate estimate of the first-passage time, but this accuracy comes at the cost of collecting a large number of samples. We aim to find $\beta^*$ for which $C(\beta)$ is minimized.

### 4.1.2 Our Approach

To solve this optimization problem, we consider the quantity $D(t, n|x_0, \sigma_0)$, which denotes the joint probability density of, starting from an initial condition of $x_0$ and $\sigma_0$, a detection event

occurring at time $t$ and until then, exactly $n$ switching events (which include both – switch from on to off and from off to on) having occurred. Defining the Laplace transformed generating function of $D(t, n|x_0, \sigma_0)$ as

$$\widetilde{D}(s, z|x_0, \sigma_0) = \sum_{n=0}^{\infty} z^n \int_0^{\infty} dt e^{-st} D(t, n|x_0, \sigma_0), \tag{4.2}$$

we note that the important terms in the cost function defined in Eq. (4.1) can be extracted from $\widetilde{D}(s, z|x_0, \sigma_0)$. For instance,

$$\langle T_d(x_0, \sigma_0) \rangle = -\lim_{s\to 0} \lim_{z\to 1} \left( \frac{\partial \widetilde{D}(s, z|x_0, \sigma_0)}{\partial s} \right). \tag{4.3}$$

Similarly, $\langle \mathcal{N}_{T_d(x_0,\sigma_0)} \rangle$ can be obtained as

$$\langle \mathcal{N}_{T_d(x_0,I)} \rangle = \frac{1}{2} \left( \lim_{z\to 1} \lim_{s\to 0} \frac{\partial \widetilde{D}(s, z|x_0, \sigma_0)}{\partial z} + 1 \right), \tag{4.4}$$

where we have taken $\sigma_0 = I$, which is the natural initialization of the sensor for $\alpha \to \infty$. If $\sigma_0 = A$, we have

$$\langle \mathcal{N}_{T_d(x_0,A)} \rangle = \left( \frac{1}{2} \lim_{z\to 1} \lim_{s\to 0} \frac{\partial \widetilde{D}(s, z|x_0, \sigma_0)}{\partial z} \right) + 1 \tag{4.5}$$

Finally, we aim to find $\beta^*$, for which $C(\beta)$ is a minimum. That is achieved by solving the following equation

$$\frac{\partial C(\beta)}{\partial \beta} = 0. \tag{4.6}$$

The main step towards solving this optimization problem is noting that $D(t, n|x_0, \sigma_0)$ satisfies the following equation

$$D(t, n|x_0, \sigma_0) = F_t(x|x_0)\, p_t(A, n|\sigma_0) + \sum_{n=0}^{\infty} \int_0^t F_{t'}(x|x_0) p_{t'}(I, n'|\sigma_0)\, D(t, n-n'|x, I) dt', \tag{4.7}$$

which is analogous to Eq. (2.4) in Chapter 2 for the quantity $D_t(x_0, \sigma_0)$. The term $p_t(\sigma, n|\sigma_0)$ denotes the probability that a sensor that is initially in state $\sigma_0$ is in state $\sigma$ at time $t$ and has switched exactly $n$ times until then. It is a similar generalization of the quantity $p_t(\sigma|\sigma_0)$ used in Eq. (2.4), which now also tracks the number of transitions that the sensor has had up to time $t$.

In Appendix H, we show how one can obtain the Laplace transformed generating function of

$p_t(\sigma, n|\sigma_0)$. We summarize the resulting equations below,

$$\begin{aligned}
\widetilde{p}_s(A, z|A) &= \frac{s+\beta}{(s+\alpha)(s+\beta) - z^2\alpha\beta} \\
\widetilde{p}_s(I, z|A) &= \frac{z\alpha}{(s+\alpha)(s+\beta) - z^2\alpha\beta} \\
\widetilde{p}_s(A, z|I) &= \frac{z\beta}{(s+\alpha)(s+\beta) - z^2\alpha\beta} \\
\widetilde{p}_s(I, z|I) &= \frac{s+\alpha}{(s+\alpha)(s+\beta) - z^2\alpha\beta}.
\end{aligned} \tag{4.8}$$

Furthermore, the inverse Laplace transform of the above equations gives

$$\begin{aligned}
\hat{p}_t(I, z|I) &= e^{-(\alpha+\beta)t/2}\left(\cosh\frac{t\Delta}{2} + \frac{\alpha-\beta}{\Delta}\sinh\frac{t\Delta}{2}\right) \\
\hat{p}_t(A, z|A) &= e^{-(\alpha+\beta)t/2}\left(\cosh\frac{t\Delta}{2} - \frac{\alpha-\beta}{\Delta}\sinh\frac{t\Delta}{2}\right) \\
\hat{p}_t(A, z|I) &= \frac{2z\beta}{\Delta}e^{-(\alpha+\beta)t/2}\sinh\frac{t\Delta}{2} \\
\hat{p}_t(I, z|A) &= \frac{2z\alpha}{\Delta}e^{-(\alpha+\beta)t/2}\sinh\frac{t\Delta}{2}
\end{aligned} \tag{4.9}$$

where we have defined $\Delta = \sqrt{(\alpha-\beta)^2 + 4\alpha\beta z^2}$ for brevity. Note that we have still not taken the $\alpha \to \infty$ limit yet. However, one can take the limit right here and the above equations will greatly simplify. For the time being, we will assume in the following that $\alpha > 0$, unless explicitly stated otherwise.

We can now use the above results in Eq. (4.7), and express the Laplace transformed generating function of $D(t, n|x_0, \sigma_0)$ as

$$\widetilde{D}(s, z|x_0, \sigma_0) = \mathcal{L}\big\{F_t(x|x_0)\,\hat{p}_t(A, z|\sigma_0)\big\} + \mathcal{L}\big\{F_t(x|x_0)\hat{p}_t(I, z|\sigma_0)\big\}\,\widetilde{D}(s, z|x, I). \tag{4.10}$$

Similarly, assuming the underlying process to be a continuous-time Markov process in discrete state-space, we can see that $D(t, n|x, I)$ satisfies the following equation

$$D(t, n|x, I) = \delta_{n,1}\beta e^{-\beta t}\int_t^\infty F_{t'}(x-1|x)\,dt' + \int_0^t e^{-\beta t'}F_{t'}(x-1|x)\,D(t-t', n|x-1, I)\,dt', \tag{4.11}$$

and its Laplace transformed generating function can be expressed as,

$$\widetilde{D}(s, z|x, I) = \frac{z\beta\big(1 - \widetilde{F}_{s+\beta}(x-1|x)\big)}{s+\beta} + \widetilde{F}_{s+\beta}(x-1|x)\widetilde{D}(s, z|x-1, I). \tag{4.12}$$

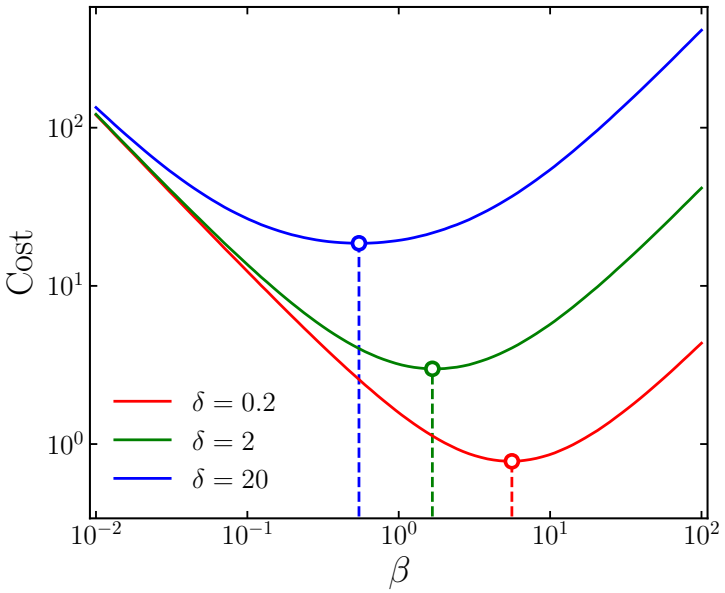


Figure 4.2: A plot of the cost as a function of the sampling rate $\beta$ when the underlying process is modeled as a two-state Markov process with two states low $(L)$ and high $(H)$ for different values of $\delta$. The circles denote the values of $\beta^*$ predicted by Eq. (4.20) and are in excellent agreement with the minimum of the cost function obtained from simulations. The initial condition is chosen to be $I$ (inactive) for the sensor and $L$ (low) for the underlying process.

In a calculation closely mimicking that of Chapter 2, we can arrive at the following generalization of 2.14

$$\widetilde{D}(s,z|x_0,\sigma_0) = \widetilde{w}_1(s,z) + \widetilde{w}_2(s,z)\frac{z\beta\big(1-\widetilde{F}_{s+\beta}(x-1|x)\big) + (s+\beta)\widetilde{F}_{s+\beta}(x-1|x)\widetilde{w}_3(s,z)}{(s+\beta)\big(1-\widetilde{F}_{s+\beta}(x-1|x)\widetilde{w}_4(s,z)\big)}, \tag{4.13}$$

where we have defined

$$\widetilde{w}_1(s,z) = \mathcal{L}\big\{F_t(x|x_0)\ \hat{p}_t(A,z|\sigma_0)\big\} \tag{4.14}$$

$$\widetilde{w}_2(s,z) = \mathcal{L}\big\{F_t(x|x_0)\hat{p}_t(I,z|\sigma_0)\big\} \tag{4.15}$$

$$\widetilde{w}_3(s,z) = \mathcal{L}\big\{F_t(x|x-1)\ \hat{p}_t(A,z|I)\big\} \tag{4.16}$$

$$\widetilde{w}_4(s,z) = \mathcal{L}\big\{F_t(x|x-1)\hat{p}_t(I,z|I)\big\}. \tag{4.17}$$

As a toy example, we model the underlying process as a two-state Markov process with two states, low $(L)$ and high $(H)$. The transition from $L$ to $H$ happens at rate $\kappa$, while the transition from $H$ to $L$ occurs at rate $\gamma$. We are interested in the time when the underlying process is observed to be in the state $H$ for the first time. Choosing the initial condition to be $I$ for the

sensor and $L$ for the underlying process, in the limit $\alpha \to \infty$, we can get

$$\langle \mathcal{N}_{T_d(L,I)} \rangle = 1 + \frac{2(\beta + \gamma)}{\kappa}, \tag{4.18}$$

and

$$\langle T_d(L, I) \rangle = \frac{\beta + \gamma + \kappa}{\beta + \kappa}, \tag{4.19}$$

where we use the fact that $F_t(H|L) = \kappa e^{-\kappa t}$ and $F_t(L|H) = \gamma e^{-\gamma t}$. Then, from Eq. (4.6), it is easy to see that $\beta^*$ the following remarkably simple form,

$$\beta^* = \sqrt{\frac{\gamma + \kappa}{\delta}} \tag{4.20}$$

which is further corroborated by simulations in Fig. 4.2. The circles denote the values of $\beta^*$ predicted by Eq. (4.20) and are in excellent agreement with the minimum of the cost function obtained from simulations. Obtaining the expressions of $\beta^*$ for more realistic underlying processes and uncovering the universal properties of the optimal sampling rate is an exciting direction for future research.

## 4.2 Extreme Value Statistics of Partially Observed Stochastic Processes

From market crashes and floods to internet breakdowns and power outages – extreme events are a major cause for concern across disciplines [121]. Thus, developing a better understanding of the statistics of these extremes is of paramount importance. Not surprisingly, there is an increasing interest in studying these extreme events using statistical methods. The branch of statistics concerning the properties of such events that deviate significantly from the mean/median behavior is called Extreme Value Statistics [122, 123].

### 4.2.1 The Extreme Value Problem

The central problem of interest in the field of Extreme Value Statistics is the following. Suppose you have a collection of data points that are denoted by the set $\{x_1, x_2, x_3, \ldots, x_N\}$, where $N$ is large. What are the statistical properties of $x_{max}$ which is given by

$$x_{max} = \max\big(\{x_1, x_2, x_3, \ldots, x_N\}\big), \tag{4.21}$$

denoting the element with the maximum value in the data set? The theory for the case where $x_1, x_2, \ldots, x_N$ are independent and identically distributed (*iid*) random variables is well developed. On the other hand, the scenario where these elements are strongly correlated is an active area of research [124].

Recently, it has become possible to derive a series of exact results on the extremal statistics of a class of strongly correlated random variables through the study of Markovian stochastic processes [124]. The position of a Brownian particle in 1-dimension as a function of time serves as a paradigmatic example of a set of strongly correlated random variables. It has been shown that the distribution of the maximum position achieved by such a particle can be linked to the first-passage statistics of the particle. However, what happens when the time-series can only be intermittently observed? Just like in the case of first-passage under intermittent sensing, the statistics of the maximum can also be strikingly different. By leveraging the close connection between first-passage statistics and extreme value statistics, in what follows, we demonstrate how the frameworks developed in this thesis can shed insight into the extreme statistics of partially observed stochastic time-series.

### 4.2.2 Connection between Extreme Statistics and First-Passage Statistics

Consider a continuous stochastic process $X_{x_0}(t)$ which undergoes Markovian evolution. We define $S_t(x^*|x_0)$ to be the probability that, starting from a $x_0$, the underlying process does not cross the value $x^*$ until time $t$. Concretely, $S_t(x^*|x_0)$, called the survival probability, denotes the probability that for all $0 \leq t' \leq t$, $X_{x_0}(t') < x^*$. At this point, the connection between survival statistics and the first-passage statistics can be made immediately clear through the following equation

$$S_t(x^*|x_0) = \int_t^\infty F_{t'}(x^*|x_0)\, dt'. \tag{4.22}$$

Equation (4.22) essentially equates the survival probability until time $t$ to the probability that the first-passage to $x^*$ occurs strictly after time $t$. In Laplace space, the above integral takes a simpler form

$$\widetilde{S}_s(x^*|x_0) = \frac{1 - \widetilde{F}_s(x^*|x_0)}{s}. \tag{4.23}$$

Now, one may ask: what is the relation of Eq. (4.22) and Eq. (4.23) to extreme value statistics? To answer this question, we point out that the survival probability $S_t(x^*|x_0)$ is directly related to

the cumulative probability distribution of the maximum of $X_{x_0}(t)$. In fact,

$$S_t(x^*|x_0) = P_t(X_{\max} < x^*|x_0). \tag{4.24}$$

can also be taken to be an alternative definition of the survival probability for a continuous stochastic process $X_{x_0}(t)$ – the probability that $X_{x_0}(t)$ does not cross $x^*$ until time $t$ is equivalent to the probability that the maximum value (also called the extreme value) of $X_{x_0}(t)$ is less than $x^*$ until time $t$.

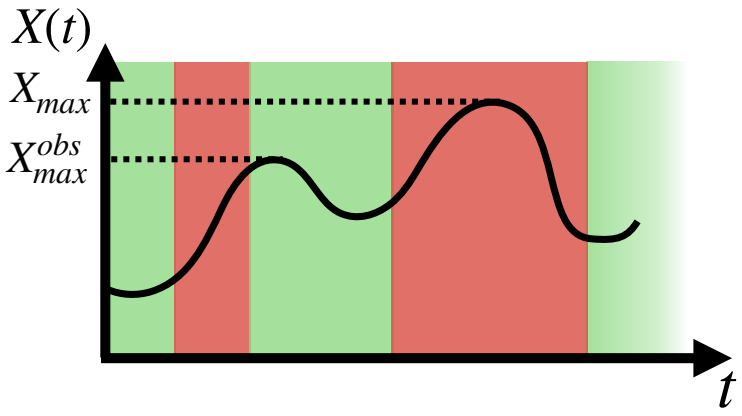


Figure 4.3: A schematic illustration of a partially observed time-series generated by a continuous stochastic process $X(t)$. Evidently, the true maximum $X_{max}$ of $X(t)$ may be missed due to intermittent sensing, and the observed maximum $X^{obs}_{max}$ might be quite different from $X_{max}$.

We now move to the case of a partially observed time-series. Following the setup in the previous chapter, we model the observation process using a two-state Markovian sensor that switches between active and inactive states. In Fig. 4.3, we illustrate a schematic of such a partially observed time-series. In such a scenario, the true maximum $X_{\max}$ of the time-series may be missed due to intermittent sensing, and the observed maximum $X^{\text{obs}}_{\max}$ might be quite different from $X_{\max}$. Though these random variables are constrained to satisfy the inequality $X^{\text{obs}}_{\max} \leq X_{\max}$.

We define $S^{\text{obs}}_t(x_0, \sigma_0)$ to be the *observed* survival probability which denotes the probability that, starting from an initial condition, the sensor is in state $\sigma_0$ and the time-series has the value $x_0$, the time-series is not *observed* to take a value greater than or equal to $x^*$ until time $t$. Note that $S^{\text{obs}}_t(x_0, \sigma_0)$ also depends on $x^*$ but that is suppressed in our notation. Formally, $S^{\text{obs}}_t(x_0, \sigma_0)$ denotes the probability that the stochastic process $X_{x_0}(t') < x^*$ for time times $t'$ between $0$ and $t$ when the sensor is in its active state, i.e., while the process is being observed. Alternatively, one

can also write

$$S_t^{\text{obs}}(x_0, \sigma_0) = P_t(X_{\max}^{\text{obs}} < x^* | x_0, \sigma_0), \tag{4.25}$$

which is a generalization of Eq. (4.24) to the case of intermittent observatons. Using an argument similar to Eq. (4.22), it is evident that the detection time density $D_t(x_0, \sigma_0)$ can be related to the observed survival probability by the following

$$S_t^{\text{obs}}(x_0, \sigma_0) = \int_t^\infty D_{t'}(x_0, \sigma_0)\, dt', \tag{4.26}$$

which in Laplace space gives

$$\widetilde{S}_s^{\text{obs}}(x_0, \sigma_0) = \frac{1 - \widetilde{D}_s(x_0, \sigma_0)}{s}. \tag{4.27}$$

Put together, the above set of equations demonstrates that the computation of the first detection time statistics, which was one of the central objectives of this thesis (especially Chapter 2), can also be used to shed light on the extreme value statistics of the partially observed time-series. In the next subsection, we illustrate the consequences of our results from Chapter 3 on the extreme value problem.

### 4.2.3 Inference of *True* Extreme Statistics from Gated Measurements

We recall Eq. (3.8) from Chapter 3

$$\widetilde{F}_s(x^* | x_0) = \frac{\widetilde{D}_s(x_0, E)}{\widetilde{D}_s(x^*, E)}, \tag{4.28}$$

that asserts that the first-passage time distribution (or at least its Laplace transform) can be reconstructed using solely the knowledge of the first detection time statistics starting from the above two initial conditions. Using Eq. (4.23), we can write

$$\widetilde{S}_s(x^* | x_0) = \frac{\widetilde{D}_s(x^*, E) - \widetilde{D}_s(x_0, E)}{s\ \widetilde{D}_s(x^*, E)}, \tag{4.29}$$

which reveals a novel connection between the survival probability under perfect observation conditions and the first detection time density under intermittent observations. Through Eq. (4.27),

the above equation can be recast as the following

$$\widetilde{S}_s(x^*|x_0) = \frac{\widetilde{S}_s^{\text{obs}}(x_0, E) - \widetilde{S}_s^{\text{obs}}(x^*, E)}{1 - s\widetilde{S}_s^{\text{obs}}(x^*, E)}, \tag{4.30}$$

relating the gated and ungated survival probabilities. It is now immidiately clear from Eq. (4.25) that the following equation holds

$$\widetilde{P}_s(X_{\text{max}} < x^*|x_0) = \frac{\widetilde{P}_s(X_{\text{max}}^{\text{obs}} < x^*|x_0, E) - \widetilde{P}_s(X_{\text{max}}^{\text{obs}} < x^*|x^*, E)}{1 - s\widetilde{P}_s(X_{\text{max}}^{\text{obs}} < x^*|x^*, E)}, \tag{4.31}$$

asserting that the *true* extremal statistics (i.e., extremal statistics under perfect observation conditions) of the stochastic process $X_{x_0}(t)$ can be expressed in terms of the extremal statistics of the partially observed process starting from two different initial conditions. This intriguing insight in Eq. (4.31) is obtained as a simple corollary of Eq. (3.8).

## 4.3 Working with Data: Imputation of Missing Statistics using Stochastic Bridges

### 4.3.1 The Key Challenge of Working with Data

Throughout this thesis, we have discussed the computation of the first detection time density and how we can use it to reconstruct the unconditioned first-passage time density. However, the knowledge of probability distributions or densities implies the ability to perform a large number of independent experiments starting from identical initial conditions and histogramming the data. This is often not feasible, and reality resembles something like the scenario depicted in Fig. 4.4: one is likely to have access to only one realization of a sparsely sampled stochastic process. Depending on the threshold of interest, the time of the first observation of a threshold-crossing event is denoted as the first detection time. The central question, then, is: can we reliably estimate when the true first-passage event could have occurred? In this section, we aim to provide an answer to this question, following arguments similar to the ones in Chapter 2, Sec. 2.3.1.3.

### 4.3.2 The Stochastic Bridge Method

As an appetizer, consider time-series data consisting of only two data-points. At time $t_1$, the underlying process $X(t)$ takes value $x_1$, and at time $t_2$ it takes value $x_2$. This data can be compactly

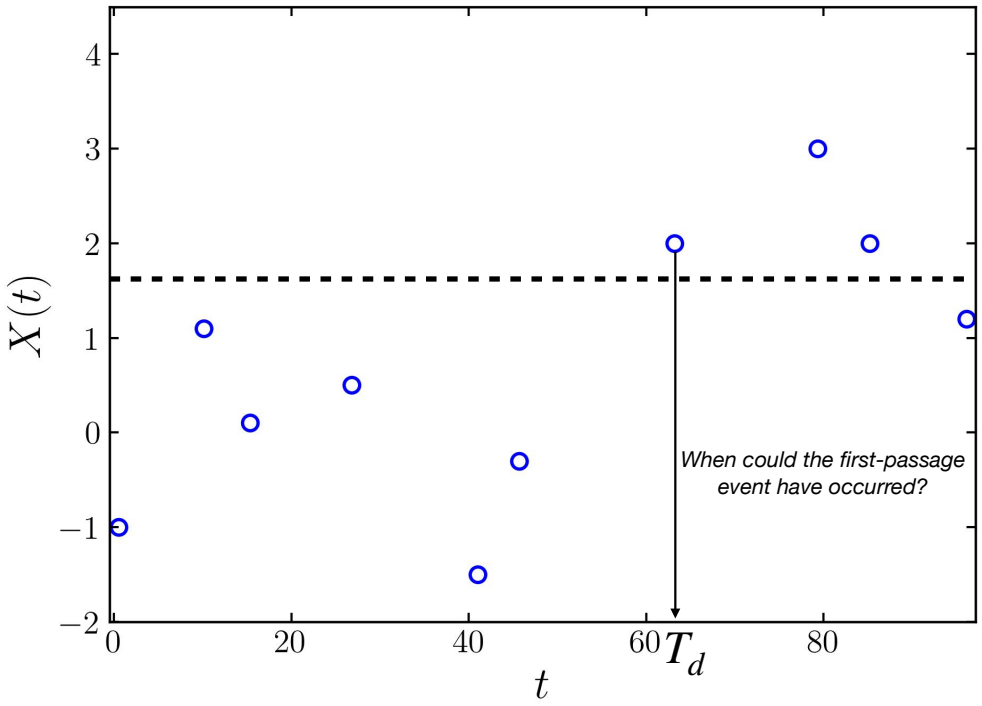


Figure 4.4: One realization of a stochastic process that has been sparsely sampled. The time at which a threshold crossing event is observed for the first time is termed the first detection time. The key question at hand: when could the first-passage event have occurred?

represented as $\vec{x} = \{(x_1, t_1), (x_2, t_2)\}$. Let the predefined threshold be $x^*$. We want to assign probabilities to the first threshold crossing event occurring at some time $t_1 \leq t \leq t_2$.

Some comments are in order now. First, we note that if $x_1 \geq x^*$ then the probability density of the first threshold crossing time density must be the delta function $\delta(t-t_1)$ peaked at $t_1$. However, let us assume that this is not the case and say that $x_1 < x^*$. Then, if $x_2 \geq x^*$, assuming $X(t)$ to be a continuous process, we can safely say that the first threshold crossing event must have occurred at some time between $t_1$ and $t_2$, and the probability density beyond the timestamp $t_2$ would be identically $0$ for all $t > t_2$.

Supposing $x_1 < x^*$, we want to compute $F_t(x^*|\vec{x})$, denoting the probability that the first-passage to $x^*$ occurs at time $t$ between $t_1$ and $t_2$, conditioned on the additional information that the process starts at $x_1$ at time $t_1$ and is at $x_2$ at time $t_2$ (this additional information is encoded in $\vec{x}$). The approach we adopt is the method of *stochastic bridges*. In simple words, we consider a Markovian stochastic process which is conditioned to start at $x_1$ at time $t_1$ and is at $x_2$ at time $t_2$, thereby creating a "bridge" between the two data points. Now, the missing statistics are estimated by computing the statistics of this stochastic bridge. It is clear that the choice of the Markovian

stochastic process is cruicial as it will strongly dictate the statistics of missing events. Making this choice requires some knowledge about the underlying generating mechanisms of the dataset. However, the formulas that we describe below will hold for *any* continuous Markovian process.

Following Sec. 2.3.1.3, we can express $F_t(x^*|\vec{\mathbb{x}})$ as

$$F_t(x^*|\vec{\mathbb{x}}) = \frac{F_{t-t_1}(x^*|x_1)C(x_2, t_2 - t|x^*)}{C(x_2, t_2 - t_1|x_1)} \tag{4.32}$$

where $C(x, t|x_0)$ is the propagator denoting the probability that starting from $x_0$, the process of interest takes a value $x$ at time $t$ and $F_t(x|x_0)$ is the first-passage time density. The same notation has been used throughout the thesis to denote the propagator and first-passage densities.

Let us take a moment to unravel the different components of Eq. (4.32). Trajectories which start from $x_1$ at time $t_1$ and end at $x_2$ at time $t_2$, while the first crossing of the threshold $x^*$ occurs at time $t$ can be broken into two parts: (i) A first-passage path from $x_1$ to $x^*$ which takes time $t-t_1$. The term $F_{t-t_1}(x^*|x_1)$ in Eq. (4.32) accounts for the weight of this part of the trajectory. (ii) A path which starts from $x^*$ and ends at $x_2$ in time $t_2 - t$. The term $C(x_2, t_2 - t|x^*)$ accounts for the weight of this second part of the trajectory. The term in the denominator $C(x_2, t_2 - t_1|x_1)$ acts as a normalization factor. Now assume that an additional data-point is added to the time-series dataset $\vec{\mathbb{x}}$ – at time $t_3$, the process takes value $x_3$. How can we incorporate this new information into our calculation? First, we note that if $x_2 \geq x^*$, then as discussed before, $F_t(x^*|\vec{\mathbb{x}}) = 0$ for all $t_2 < t \leq t_3$. On the other hand, the interesting case is when $x_2 < x^*$. In this case, one may naively assume that Eq. (4.32) should directly be applicable for all $t \in (t_2, t_3]$. This is not the case as an additional consideration is required – one must ensure that a first-passage event has not already occurred in the previous interval $(t_1, t_2]$. To account for that, we define the survival probability $S_1$ in the time interval $(t_1, t_2]$ as the probability that the first-passage event does not occur in this interval. This can also be computed by numerically integrating the probability obtained from Eq. (4.32) for $t \in (t_1, t_2]$ and subtracting it from 1, i.e., $S_1 = 1 - \int_{t_1}^{t_2} dt F_t(x^*|\vec{\mathbb{x}})$. Next, for $t \in (t_2, t_3]$, we have,

$$F_t(x^*|\vec{\mathbb{x}}) = \frac{F_{t-t_2}(x^*|x_2)C(x_3, t_3 - t|x^*)}{C(x_3, t_3 - t_2|x_2)} \cdot S_1. \tag{4.33}$$

This result can now be generalized to a much bigger dataset $\vec{\mathbb{x}} = \{(x_1, t_1), (x_2, t_2), \ldots, (x_N, t_N)\}$.

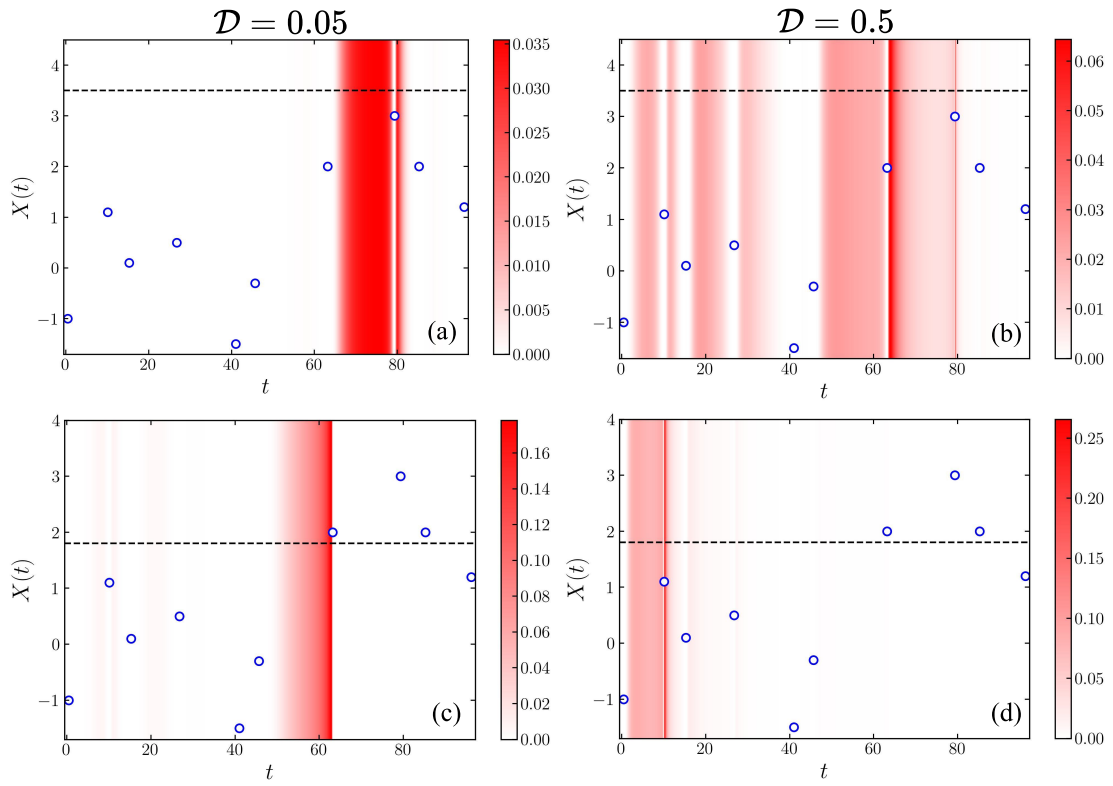


Figure 4.5: First-passage density conditioned on observed data computed using stochastic bridges. The stochastic process of interest is chosen to be Brownian motion. Probability densities are shown as a red color gradient. Panels (a) and (b) correspond to the case when the observed time-series does not cross the threshold. Relatively small diffusion constant $\mathcal{D}$ leads to probability densities, concentrated around the time intervals when the observed time-series is closest to the threshold. Panels (c) and (d) depict the estimated first-passage probability densities for the same observed time-series with a lower threshold.

Let us denote the $i$th interval to be the time interval $(t_i, t_{i+1}]$. Then, for $t \in (t_i, t_{i+1}]$, we can write

$$F_t(x^*|\vec{x}) = \frac{F_{t-t_i}(x^*|x_i)C(x_{i+1}, t_{i+1} - t|x^*)}{C(x_{i+1}, t_{i+1} - t_i|x_i)} \cdot \prod_{j=0}^{i-1} S_j, \tag{4.34}$$

where we define

$$S_0 = 1 \tag{4.35}$$

and

$$S_j = 1 - \int_{t_j}^{t_{j+1}} \frac{F_{t-t_j}(x^*|x_j)C(x_{j+1}, t_{j+1} - t|x^*)}{C(x_{j+1}, t_{j+1} - t_j|x_j)}\, dt`. \tag{4.36}$$

The term $\prod_{j=0}^{i-1} S_j$ ensures that a first-passage has not occurred in the previous intervals.

Figure 4.5 depicts the iterative use of Eq. (4.34) to create a heatmap of probabilities of missed

first-passage events using simple Brownian motion (without drift) as the example of the underlying process. Probability densities are shown as a red color gradient heatmap. For the same dataset, we show how different choices of the threshold and model parameters can lead to different estimates for the probability of missed first-passage events.

## 4.4 Discussion

The main objective of this chapter of the thesis was to illustrate how the framework of gated first-passage processes developed in the first three chapters of the thesis can be extended and leveraged to gain insight into practical applications. In particular, we discussed the computation of optimal sampling rates in situations where measurement costs are involved, explored the statistics of extremes in partially observed time-series, and outlined how some of our results can be used to deal with real-world sparsely sampled data. These applications underscore the practical relevance and utility of the framework of gated first-passage processes in more applicable domains. These applications will be described in this chapter.

# CHAPTER 5

# Summary and Outlook

## 5.1 Summary

As we come to the end of this thesis, we put forth a brief summary of the work contained in it. Our main aim in this thesis was to address the problem of dealing with first-passage processes under imperfect observation conditions. The notion of first-passage time is crucial across various fields, determining events such as the initiation of chemical reactions or the execution of orders in financial markets. However, in many practical situations, continuous observation of the process is not feasible, leading to scenarios where key events may be missed. How can we reliably discuss the first-passage statistics of such partially observed processes? From our imperfect observations, what can we learn about the true underlying first-passage process at hand? These issues were at the heart of this thesis and formed the key motivation behind several of the discussions presented here.

Throughout, we posited that the framework of gated first-passage processes provides an excellent paradigm for studying scenarios of imperfect observations. The main contributions presented in this thesis can be summarized in the following three parts.

- **Computing the statistics of the *observed* first-passage time or the first detection time.** We presented in Chapter 2 a framework that allows us to obtain the statistics of the first detection time from the first-passage time statistics. These results can be found in Eq. (2.14) (for Markov processes with discrete states) and Eq. (2.61) (for continuous state-space) and the discussion surrounding these equations. Using these results, one can delve deeper and gain further insight into the statistics of gated first-passage processes. The results discussed in this chapter have been presented in Refs. [30] and [31].

- **Solving the inverse problem.** A major challenge addressed in this thesis is the inference problem: how to deduce the properties of the underlying process when only the detection times can be measured. Our approach to this problem was discussed in Chapter 3, where

we developed a model-free formalism that allowed for the inference of first-passage times ( Equation (3.8) being one of the central results) and other physically meaningful parameters, such as diffusion coefficients, directly from the measurable first detection time statistics. We note that our result on the estimation of gating rates by examining the short-time behavior of the first detection time distribution using Eqs. (3.28) and (3.32) is the first known result regarding the inference of gating rates of gated chemical reactions – a field whose history spans over 4 decades. The ideas presented in this chapter have been published in Ref. [32].

- **Applying these frameworks to practically relevant problems beyond gated first-passage processes.** The frameworks developed in Chapters 2 and 3 can be extended to applications beyond the realm of first-passage processes. In particular, we illustrated in Chapter 4 how our results can be extended to compute the optimal sampling rate for a time-series where the first-passage is of interest but each sample comes with a cost. We then demonstrated a close relationship between extreme statistics and first-passage problems and discussed how all of our results can also be viewed in the light of extreme value statistics. Finally, we discussed the estimation of the statistics of missing first-passage events in real life scenarios, where we do not have access to first detection time distributions but rather only have a single realization of a sparsely sampled time-series at hand. These applications underscore the practical relevance and utility of the framework in real-world situations.

## 5.2 Future Directions

Looking forward, the modeling framework of gated first-passage processes presented here opens several promising directions for future research. Extending these methods to other types of stochastic processes and exploring different scenarios of partial observability, as depicted schematically in Fig.. 5.1 could further improve the current state of understanding of first-passage processes under imperfect observation conditions. We have been able to extend the theory to a certain class of problems where the underlying process is a discontinuous stochastic process or a non-Markov process (renewal process in discrete state-space). However, dealing with a non-Markovian sensor has been very challenging. One of the most interesting directions for future

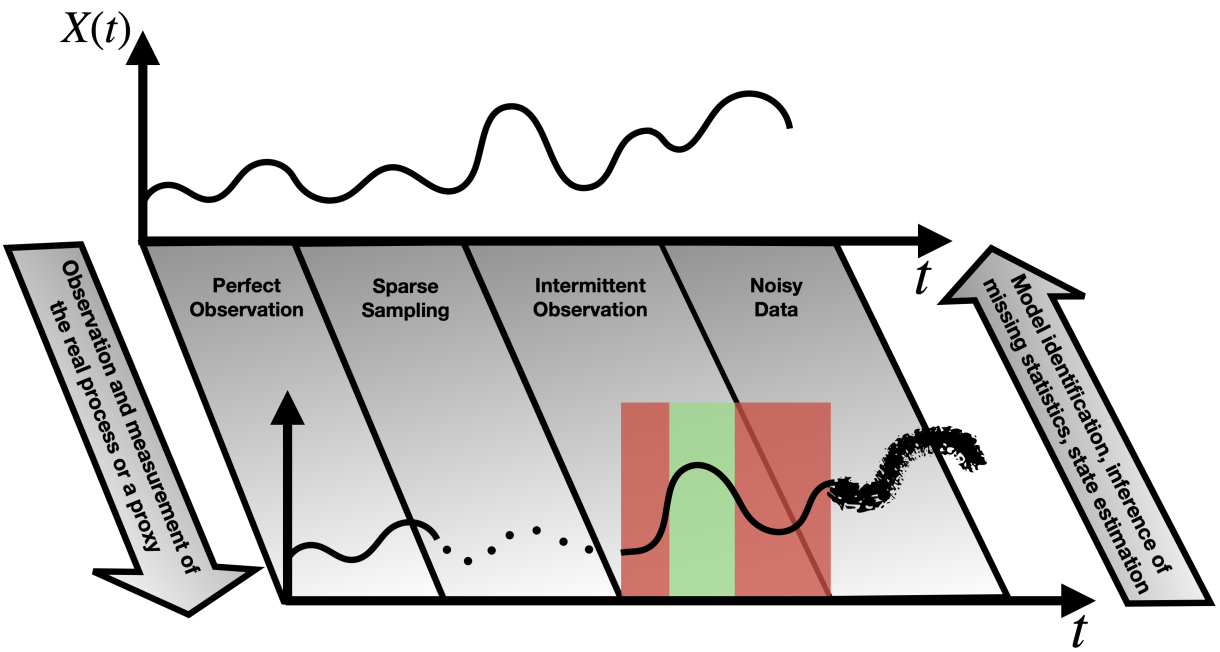


Figure 5.1: A schematic illustration of some statistical challenges of working with imperfect observation conditions. This thesis focused on imperfect observations modeled by an intermittent stochastic sensor, but there are several more opportunities and exciting research directions in this domain.

research is extending the presented framework to incorporate a sensor which is not necessarily Markovian. Even if the extension to a semi-Markov (renewal process) sensor is possible, that opens up a lot of interesting directions to explore – crucially, it will allow us to talk about optimal sampling strategies. Additionally, the broadly applicable nature of the theory of gated first-passage processes suggests numerous unexplored avenues beyond event detection in time-series. In particular, all the results derived in this thesis can also be interpreted in the context of imperfect chemical reactions (as explained in Chapter 1).

Apart from first-passage problems, the broader theme of *Statistical Physics of Partially-Observed Complex Systems* is an extremely rich area where there is a lot left unexplored.

## Statistical Physics of Partially-Observed Complex Systems

The time evolution of various complex systems can be described by a Markov process, consisting of a set of states, where the system evolves through transitions between *adjacent* states according to prescribed transition rates. However, many real-world systems, e.g., biological systems, exhibit long-range correlations and highly non-Markov dependencies. These effects often arise from our

ability to only partially observe the system of interest. This partial observability can manifest itself in various ways – from viewing a coarse-grained description of the state-space or some states being completely unobservable to only being able to intermittently monitor or discretely sample the time-evolution of the system dynamics. These are schematically outlined in the figure below.

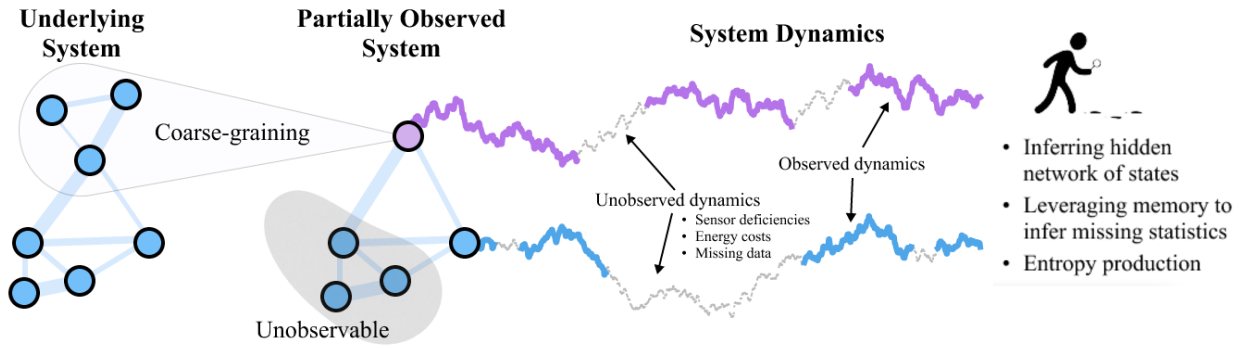


Irrespective of the specific cause behind the imperfect observations, we must aim to harness the observations and data at our disposal and extract meaningful insights about the true underlying process. Within this research program, one could immediately begin to investigate the following directions.

- **Estimating irreversibility from partial observations:** An important element of the statistical physics and information theory toolbox is the so-called *entropy production* of a system. Several complex systems, including living organisms, continuously consume energy to maintain order and function, and their entropy production is a marker of this out-of-equilibrium behavior. However, differentiating in general between equilibrium and non-equilibrium steady states at coarse-grained scales is quite difficult, and coarse-graining of the state-space can lead to a significant underestimation of the entropy production. Leveraging recent advances in thermodynamic inference and non-equilibrium statistical physics, one could potentially look to build principled ways of obtaining improved bounds on the true entropy production of the system.

- **Fundamental limits on inference from incomplete data:** Making sense of partial observations is a central challenge in data analysis and statistical inference. An important question to ask is: How much more can we learn about a system if we gain more information

about it? Crucial to this discussion is the Cramér-Rao bound, which unveils the inherent limitations on parameter estimation accuracy when dealing with incomplete or limited data by providing a fundamental lower bound on the variance of parameter estimates. However, a large part of this discussion assumes that the data being collected are *iid* samples, which is often not the case in real experiments. Data drawn from a dynamical process can display strong correlations. This research area is ripe for developing novel statistical tools to investigate the trade-offs between accuracy in learning parameters and the amount of available data in the presence of strong correlations.

## 5.3 Conclusions

Put together, the aforementioned research directions constitute an actionable roadmap for investigating and pushing the limits of inference from partial observations. This thesis specifically tackled first-passage problems, but there is a plethora of other classes of problems where partial observability is a key challenge, and we need to come up with ways to deal with it. As mentioned above, most conventional studies in statistical analysis of data are centered around *iid* samples as they are generally more tractable and easier to analyze. But one thing I hope to communicate to the reader is the following: Not only is the presence of strong correlations and memory effects a ubiquitous feature of data generated from stochastic processes, but in scenarios where we can only partially observe the system and its time evolution, these features are in fact a valuable resource. These features, often overlooked in the literature, can be leveraged to compensate for gaps in the data and build a more complete understanding of the underlying process. Diving deeper into this direction of research is an exciting prospect for the future.

# Bibliography


[1] Sidney Redner. *A Guide to First-Passage Processes*. Cambridge University Press, 2001.

[2] Denis S Grebenkov, David Holcman, and Ralf Metzler. Preface: new trends in first-passage methods and applications in the life sciences and engineering. *Journal of Physics A: Mathematical and Theoretical*, 53(19):190301, 2020.

[3] Ralf Metzler, Gleb Oshanin, and Sidney Redner. *First-passage Phenomena and Their Applications*. World Scientific, 2014.

[4] George H Weiss. First passage time problems in chemical physics. *Adv. Chem. Phys*, 13:1–18, 1967.

[5] Rémy Chicheportiche and Jean-Philippe Bouchaud. Some applications of first-passage ideas to finance. In *First-passage Phenomena And Their Applications*, pages 447–476. World Scientific, 2014.

[6] Srividya Iyer-Biswas and Anton Zilman. First-Passage Processes in Cellular Biology. In *Advances in Chemical Physics*, pages 261–306. 2016.

[7] Yaojun Zhang and Olga K. Dudko. First-Passage Processes in the Genome. *Annual Review of Biophysics*, 45:117–134, 2016.

[8] Antonio Auffinger, Michael Damron, and Jack Hanson. *50 years of first-passage percolation*, volume 68. American Mathematical Soc., 2017.

[9] Attila Szabo, Klaus Schulten, and Zan Schulten. First passage time approach to diffusion controlled reactions. *The Journal of chemical physics*, 72(8):4350–4357, 1980.

[10] G. A. Whitmore. First-Passage-Time Models for Duration Data: Regression Structures and Competing Risks. *Journal of the Royal Statistical Society. Series D (The Statistician)*, 35:207–219, 1986.

[11] J. W. Shipley and M. C. Bernard. The First Passage Time Problem for Simple Structural Systems. *Journal of Applied Mechanics*, 39, 1972.

[12] H. Vanvinckenroye, T. Andrianne, and V. Denoël. First passage time as an analysis tool in experimental wind engineering. *Journal of Wind Engineering and Industrial Aerodynamics*, 177:366–375, 2018.

[13] Remy Chicheportiche and Jean-Philippe Bouchaud. *Some Applications of First-Passage Ideas to Finance*, chapter Chapter 1, pages 447–476. World Scientific, 2014.

[14] Di Zhang and Roderick VN Melnik. First passage time for multivariate jump-diffusion processes in finance and other areas of applications. *Applied Stochastic Models in Business and Industry*, 25(5):565–582, 2009.

[15] T. Chou and M. R. DOrsogna. *First Passage Problems in Biology*, chapter Chapter 1, pages 306–345. World Scientific, 2014.

[16] Luigi M Ricciardi. *Diffusion processes and related topics in biology*, volume 14. Springer Science & Business Media, 2013.

[17] Joseph Klafter and Igor M Sokolov. *First steps in random walks: from tools to applications*. OUP Oxford, 2011.

[18] Vladimir Ivanovič Mel'nikov. The kramers problem: Fifty years of development. *Physics Reports*, 209:1–71, 1991.

[19] Rajeev Motwani and Prabhakar Raghavan. *Randomized algorithms*. Cambridge university press, 1995.

[20] Mohammad S. Obaidat and Sudip Misra. *Principles of Wireless Sensor Networks*. Cambridge University Press, 2014.

[21] Waltenegus Dargie and Christian Poellabauer. *Fundamentals of wireless sensor networks: theory and practice*. John Wiley & Sons, 2010.

[22] H. Inaltekin, C. R. Tavoularis, and S. B. Wicker. Event detection time for mobile sensor networks using first passage processes. In *IEEE GLOBECOM 2007 - IEEE Global Telecommunications Conference*, pages 1174–1179, 2007.

[23] C. Hsin and M. Liu. Randomly duty-cycled wireless sensor networks: Dynamics of coverage. *IEEE Transactions on Wireless Communications*, 5(11):3182–3192, 2006.

[24] D. Song, C. Kim, and J. Yi. On the time to search for an intermittent signal source under a limited sensing range. *IEEE Transactions on Robotics*, 27(2):313–323, 2011.

[25] Patrick Chisan Hew. An intermittent sensor versus a target that emits glimpses as a homogeneous poisson process. *Journal of the Operational Research Society*, 71(3):433–446, 2020.

[26] Josiah Hester and Jacob Sorber. The future of sensing is batteryless, intermittent, and awesome. In *Proceedings of the 15th ACM Conference on Embedded Network Sensor Systems*, SenSys '17, New York, NY, USA, 2017. Association for Computing Machinery.

[27] Paul C. Bressloff. Stochastic switching in biology: from genotype to phenotype. *Journal of Physics A: Mathematical and Theoretical*, 50:133001, February 2017.

[28] Jian Li, Johnathan Labbadia, and Richard I. Morimoto. Rethinking HSF1 in Stress, Development, and Organismal Health. *Trends in Cell Biology*, 27, 2017.

[29] Peter K. Sorger. Heat shock factor and the heat shock response. *Cell*, 65:363–366, 1991.

[30] Aanjaneya Kumar, Aniket Zodage, and M. S. Santhanam. First detection of threshold crossing events under intermittent sensing. *Physical Review E*, 104:L052103, 2021.

[31] Yuval Scher, Aanjaneya Kumar, MS Santhanam, and Shlomi Reuveni. Continuous gated first-passage processes. *arXiv preprint arXiv:2211.09164*, 2022.

[32] Aanjaneya Kumar, Yuval Scher, Shlomi Reuveni, and MS Santhanam. Inference from gated first-passage times. *Physical Review Research*, 5(3):L032043, 2023.

[33] Mi F Perutz and FS Mathews. An x-ray study of azide methaemoglobin. *Journal of molecular biology*, 21:199–202, 1966.

[34] J Andrew McCammon and Scott H Northrup. Gated binding of ligands to proteins. *Nature*, 293:316–317, 1981.

[35] Attila Szabo, David Shoup, Scott H. Northrup, and J. Andrew McCammon. Stochastically gated diffusion-influenced reactions. *The Journal of Chemical Physics*, 77:4484–4493, 1982.

[36] Scott H Northrup, Fahimeh Zarrin, and J Andrew McCammon. Rate theory for gated diffusion-influenced ligand binding to proteins. *The Journal of Physical Chemistry*, 86:2314–2321, 1982.

[37] George H Weiss. Overview of theoretical models for reaction rates. *Journal of Statistical Physics*, 42:3–36, 1986.

[38] Huan-Xiang Zhou and Attila Szabo. Theory and simulation of stochastically-gated diffusion-influenced reactions. *The Journal of Physical Chemistry*, 100:2597–2604, 1996.

[39] Alexander M Berezhkovskii, Dah-Yen Yang, Sheng Hsien Lin, Yu A Makhnovskii, and Sheh-Yi Sheu. Smoluchowski-type theory of stochastically gated diffusion-influenced reactions. *The Journal of chemical physics*, 106:6985–6998, 1997.

[40] Yurii A. Makhnovskii, Alexander M. Berezhkovskii, Sheh-Yi Sheu, Dah-Yen Yang, Jimmy Kuo, and Sheng Hsien Lin. Stochastic gating influence on the kinetics of diffusion-limited reactions. *The Journal of Chemical Physics*, 108:971–983, 1998.

[41] O Bénichou, M Moreau, and G Oshanin. Kinetics of stochastically gated diffusion-limited reactions and geometry of random walk trajectories. *Physical Review E*, 61:3388, 2000.

[42] T Bandyopadhyay, K Seki, and M Tachiya. Theoretical analysis of the influence of stochastic gating on the transient effect in fluorescence quenching by electron transfer. *The Journal of Chemical Physics*, 112:2849–2862, 2000.

[43] Paul C Bressloff and Sean D Lawley. Stochastically gated diffusion-limited reactions for a small target in a bounded domain. *Physical Review E*, 92:062117, 2015.

[44] Irina V Gopich and Attila Szabo. Reversible stochastically gated diffusion-influenced reactions. *The Journal of Physical Chemistry B*, 120:8080–8089, 2016.

[45] CE Budde, MO Cáceres, and MA Ré. Transient behaviour in the absorption probability distribution in the presence of a non-markovian dynamic trap. *EPL (Europhysics Letters)*, 32:205, 1995.

[46] Aljaž Godec and Ralf Metzler. First passage time statistics for two-channel diffusion. *Journal of Physics A: Mathematical and Theoretical*, 50:084001, 2017.

[47] Gabriel Mercado-Vásquez and Denis Boyer. First hitting times to intermittent targets. *Physical Review Letters*, 123(25):250603, 2019.

[48] Gabriel Mercado-Vásquez and Denis Boyer. First hitting times between a run-and-tumble particle and a stochastically gated target. *Physical Review E*, 103:042139, 2021.

[49] Yuval Scher and Shlomi Reuveni. Unified Approach to Gated Reactions on Networks. *Physical Review Letters*, 127:018301, 2021.

[50] Vimal Kishore, M. S. Santhanam, and R. E. Amritkar. Extreme Events on Complex Networks. *Physical Review Letters*, 106:188701, 2011.

[51] Nishant Malik and Ugur Ozturk. Rare events in complex systems: Understanding and prediction. *Chaos: An Interdisciplinary Journal of Nonlinear Science*, 30:090401, 2020.

[52] Aanjaneya Kumar, Suman Kulkarni, and M. S. Santhanam. Extreme events in stochastic transport on networks. *Chaos: An Interdisciplinary Journal of Nonlinear Science*, 30:043111, 2020.

[53] Denis S. Grebenkov. First passage times for multiple particles with reversible target-binding kinetics. *The Journal of Chemical Physics*, 147(13):134112, 2017.

[54] S. D. Lawley and J. B. Madrid. First passage time distribution of multiple impatient particles with reversible binding. *The Journal of Chemical Physics*, 150:214113, 2019.

[55] K. Dao Duc and D. Holcman. Threshold activation for stochastic chemical reactions in microdomains. *Physical Review E*, 81:041107, 2010.

[56] Denis S. Grebenkov and Aanjaneya Kumar. Reversible target-binding kinetics of multiple impatient particles. *The Journal of Chemical Physics*, 156:084107, 2022.

[57] Denis S Grebenkov and Aanjaneya Kumar. First-passage times of multiple diffusing particles with reversible target-binding kinetics. *Journal of Physics A: Mathematical and Theoretical*, 55:325002, 2022.

[58] Sandro Azaele, Samir Suweis, Jacopo Grilli, Igor Volkov, Jayanth R. Banavar, and Amos Maritan. Statistical mechanics of ecological systems: Neutral theory and beyond. *Reviews of Modern Physics*, 88:035003, 2016.

[59] Artem S. Novozhilov, Georgy P. Karev, and Eugene V. Koonin. Biological applications of the theory of birth-and-death processes. *Briefings in Bioinformatics*, 7:70–85, 2006.

[60] Forrest W. Crawford and Marc A. Suchard. Transition probabilities for general birth–death processes with applications in ecology, genetics, and evolution. *Journal of Mathematical Biology*, 65:553–580, 2012.

[61] John Freidenfelds. Capacity Expansion when Demand Is a Birth-Death Random Process. *Operations Research*, 28:712–721, 1980.

[62] Antonio Di Crescenzo and Paola Paraggio. Logistic growth described by birth-death and diffusion processes. *Mathematics*, 7, 2019.

[63] Lam Si Tung Ho, Jason Xu, Forrest W. Crawford, Vladimir N. Minin, and Marc A. Suchard. Birth/birth-death processes and their computable transition probabilities with biological applications. *Journal of Mathematical Biology*, 76:911–944, 2018.

[64] Tom Israeli and Michael Assaf. Population switching under a time-varying environment. *Phys. Rev. E*, 101:022109, Feb 2020.

[65] Ami Taitelbaum, Robert West, Michael Assaf, and Mauro Mobilia. Population dynamics in a changing environment: Random versus periodic switching. *Phys. Rev. Lett.*, 125:048105, Jul 2020.

[66] D. P. Sanders and H. Larralde. How rare are diffusive rare events? *EPL (Europhysics Letters)*, 82:40005, 2008.

[67] F. Di Lauro, J.-C. Croix, M. Dashti, L. Berthouze, and I. Z. Kiss. Network inference from population-level observation of epidemics. *Scientific Reports*, 10:18779, 2020.

[68] István Z. Kiss, Joel Miller, and Péter L. Simon. *Mathematics of Epidemics on Networks: From Exact to Approximate Models*. Interdisciplinary Applied Mathematics. Springer International Publishing, 2017.

[69] N. Nagy, I. Z. Kiss, and P. L. Simon. Approximate Master Equations for Dynamical Processes on Graphs. *Mathematical Modelling of Natural Phenomena*, 9:43–57, 2014.

[70] P. R. Parthasarathy and R. Sudhesh. Exact transient solution of a state-dependent birth-death process. *Journal of Applied Mathematics and Stochastic Analysis*, 2006:e97073, 2006. Publisher: Hindawi.

[71] Ryu Sasaki. Exactly solvable birth and death processes. *Journal of Mathematical Physics*, 50(10):103509, 2009. Publisher: American Institute of Physics.

[72] Aljaž Godec and Ralf Metzler. Universal Proximity Effect in Target Search Kinetics in the Few-Encounter Limit. *Physical Review X*, 6:041037, 2016.

[73] David Hartich and Aljaž Godec. Duality between relaxation and first passage in reversible Markov dynamics: rugged energy landscapes disentangled. *New Journal of Physics*, 20(11):112002, 2018.

[74] David Hartich and Aljaž Godec. Interlacing relaxation and first-passage phenomena in reversible discrete and continuous space Markovian dynamics. *Journal of Statistical Mechanics: Theory and Experiment*, 2019:024002, 2019.

[75] Gabriel Mercado-Vásquez and Denis Boyer. First hitting times to intermittent targets. *Phys. Rev. Lett.*, 123:250603, 2019.

[76] Martin R. Evans and Satya N. Majumdar. Diffusion with Stochastic Resetting. *Physical Review Letters*, 106:160601, 2011.

[77] Shlomi Reuveni. Optimal Stochastic Restart Renders Fluctuations in First Passage Times Universal. *Physical Review Letters*, 116:170601, 2016.

[78] Arnab Pal and Shlomi Reuveni. First Passage under Restart. *Physical Review Letters*, 118:030603, 2017.

[79] Martin R. Evans, Satya N. Majumdar, and Grégory Schehr. Stochastic resetting and applications. *Journal of Physics A: Mathematical and Theoretical*, 53:193001, 2020.

[80] Arnab Pal, Lukasz Kusmierz, and Shlomi Reuveni. Search with home returns provides advantage under high uncertainty. *Physical Review Research*, 2:043174, 2020.

[81] Arnab Pal and V. V. Prasad. First passage under stochastic resetting in an interval. *Physical Review E*, 99:032123, 2019.

[82] A. Di Crescenzo, V. Giorno, A. G. Nobile, and L. M. Ricciardi. A note on birth–death processes with catastrophes. *Statistics & Probability Letters*, 78:2248–2257, 2008.

[83] A. Di Crescenzo, V. Giorno, A.G. Nobile, and L.M. Ricciardi. On the M/M/1 Queue with Catastrophes and Its Continuous Approximation. *Queueing Systems*, 43:329–347, 2003.

[84] B. Krishna Kumar and D. Arivudainambi. Transient solution of an M/M/1 queue with catastrophes. *Computers & Mathematics with Applications*, 40:1233–1240, 2000.

[85] Martin R. Evans and Satya N. Majumdar. Effects of refractory period on stochastic resetting. *Journal of Physics A: Mathematical and Theoretical*, 52(1):01LT01, 2018.

[86] Zhen Wang, Chris T Bauch, Samit Bhattacharyya, Alberto d'Onofrio, Piero Manfredi, Matjaž Perc, Nicola Perra, Marcel Salathé, and Dawei Zhao. Statistical physics of vaccination. *Physics Reports*, 664:1–113, 2016.

[87] David Hartich and Aljaž Godec. Emergent memory and kinetic hysteresis in strongly driven networks, 2021.

[88] T Ha, Th Enderle, DS Chemla, PR Selvin, and S Weiss. Quantum jumps of single molecules at room temperature. *Chemical Physics Letters*, 271(1-3):1–5, 1997.

[89] H Peter Lu and X Sunney Xie. Single-molecule spectral fluctuations at room temperature. *Nature*, 385(6612):143–146, 1997.

[90] Robert M Dickson, Andrew B Cubitt, Roger Y Tsien, and William E Moerner. On/off blinking and switching behaviour of single molecules of green fluorescent protein. *Nature*, 388(6640):355–358, 1997.

[91] Erwin JG Peterman, Sophie Brasselet, and WE Moerner. The fluorescence dynamics of single molecules of green fluorescent protein. *The Journal of Physical Chemistry A*, 103(49):10553–10560, 1999.

[92] David A Vanden Bout, Wai-Tak Yip, Dehong Hu, Dian-Kui Fu, Timothy M Swager, and Paul F Barbara. Discrete intensity jumps and intramolecular electronic energy transfer in the spectroscopy of single conjugated polymer molecules. *Science*, 277(5329):1074–1077, 1997.

[93] Manoj Nirmal, Bashir O Dabbousi, Moungi G Bawendi, JJ Macklin, JK Trautman, TD Harris, and Louis E Brus. Fluorescence intermittency in single cadmium selenide nanocrystals. *Nature*, 383(6603):802–804, 1996.

[94] M Kuno, DP Fromm, HF Hamann, Alan Gallagher, and David J Nesbitt. "on"/"off" fluorescence intermittency of single semiconductor quantum dots. *The Journal of Chemical Physics*, 115:1028–1040, 2001.

[95] J Schuster, F Cichos, and C Von Borczyskowski. Blinking of single molecules in various environments. *Optics and Spectroscopy*, 98:712–717, 2005.

[96] Kevin Claytor, Saumyakanti Khatua, Jason M Guerrero, Alexei Tcherniak, James M Tour, and Stephan Link. Accurately determining single molecule trajectories of molecular motion on surfaces. *The Journal of chemical physics*, 130:04B624, 2009.

[97] Saumyakanti Khatua, Jason M Guerrero, Kevin Claytor, Guillaume Vives, Anatoly B Kolomeisky, James M Tour, and Stephan Link. Micrometer-scale translation and monitoring of individual nanocars on glass. *ACS nano*, 3:351–356, 2009.

[98] Anders S Hansen, Maxime Woringer, Jonathan B Grimm, Luke D Lavis, Robert Tjian, and Xavier Darzacq. Robust model-based analysis of single-particle tracking experiments with spot-on. *Elife*, 7:e33125, 2018.

[99] Thorsten Kues and Ulrich Kubitscheck. Single molecule motion perpendicular to the focal plane of a microscope: application to splicing factor dynamics within the cell nucleus. *Single Molecules*, 3:218–224, 2002.

[100] Jürgen Reingruber and David Holcman. Gated narrow escape time for molecular signaling. *Phys. Rev. Lett.*, 103:148102, Sep 2009.

[101] Jürgen Reingruber and David Holcman. Narrow escape for a stochastically gated brownian ligand. *Journal of Physics: Condensed Matter*, 22:065103, 2010.

[102] Ben NG Giepmans, Stephen R Adams, Mark H Ellisman, and Roger Y Tsien. The fluorescent toolbox for assessing protein location and function. *Science*, 312:217–224, 2006.

[103] Srabanti Chaudhury, Divya Singh, and Anatoly B Kolomeisky. Theoretical investigations of the dynamics of chemical reactions on nanocatalysts with multiple active sites. *The Journal of Physical Chemistry Letters*, 11:2330–2335, 2020.

[104] Bhawakshi Punia, Srabanti Chaudhury, and A. B. Kolomeisky. Understanding the Reaction Dynamics on Heterogeneous Catalysts Using a Simple Stochastic Approach. *The Journal of Physical Chemistry Letters*, 12:11802–11810, 2021.

[105] Elliott W Montroll and George H Weiss. Random walks on lattices. ii. *Journal of Mathematical Physics*, 6:167–181, 1965.

[106] Naoki Masuda, Mason A Porter, and Renaud Lambiotte. Random walks and diffusion on networks. *Physics Reports*, 716:1–58, 2017.

[107] Ralf Metzler and Joseph Klafter. The random walk's guide to anomalous diffusion: a fractional dynamics approach. *Physics Reports*, 339:1–77, 2000.

[108] Peter K Kang, Marco Dentz, Tanguy Le Borgne, and Ruben Juanes. Spatial markov model of anomalous transport through random lattice networks. *Physical Review Letters*, 107:180602, 2011.

[109] Felix Höfling and Thomas Franosch. Anomalous transport in the crowded world of biological cells. *Reports on Progress in Physics*, 76:046602, 2013.

[110] Denis S Grebenkov and Liubov Tupikina. Heterogeneous continuous-time random walks. *Physical Review E*, 97:012148, 2018.

[111] Brian Berkowitz and Harvey Scher. Anomalous transport in random fracture networks. *Physical Review Letters*, 79:4038, 1997.

[112] Brian Berkowitz and Harvey Scher. Theory of anomalous chemical transport in random fracture networks. *Physical Review E*, 57(5):5858, 1998.

[113] Thomas Guérin, Maxim Dolgushev, Olivier Bénichou, and Raphaël Voituriez. Universal kinetics of imperfect reactions in confinement. *Communications Chemistry*, 4:1–7, 2021.

[114] Roman Belousov, Muhammad Nawaz Qaisrani, Ali Hassanali, and Edgar Roldan. First-passage fingerprints of water diffusion near glutamine surfaces. *Soft Matter*, 16:9202–9216, 2020.

[115] Roman Belousov, Ali Hassanali, and Édgar Roldán. Statistical physics of inhomogeneous transport: Unification of diffusion laws and inference from first-passage statistics. *Physical Review E*, 106:014103, 2022.

[116] Biswajit Das, Sreekanth K Manikandan, and Ayan Banerjee. Inferring entropy production in anharmonic brownian gyrators. *Physical Review Research*, 4:043080, 2022.

[117] Sreekanth K Manikandan, Subhrokoli Ghosh, Avijit Kundu, Biswajit Das, Vipin Agrawal, Dhrubaditya Mitra, Ayan Banerjee, and Supriya Krishnamurthy. Quantitative analysis of non-equilibrium systems from short-time experimental data. *Communications Physics*, 4:258, 2021.

[118] Jann Van der Meer, Benjamin Ertel, and Udo Seifert. Thermodynamic inference in partially accessible markov networks: a unifying perspective from transition-based waiting time distributions. *Physical Review X*, 12:031025, 2022.

[119] Alice L. Thorneywork, Jannes Gladrow, Yujia Qing, Marc Rico-Pasto, Felix Ritort, Hagan Bayley, Anatoly B. Kolomeisky, and Ulrich F. Keyser. Direct detection of molecular intermediates from first-passage times. *Science Advances*, 6:eaaz4642, 2020.

[120] Xin Li and Anatoly B Kolomeisky. Mechanisms and topology determination of complex chemical and biological network systems from first-passage theoretical approach. *The Journal of Chemical Physics*, 139:10B606_1, 2013.

[121] Sergio Albeverio, Volker Jentsch, and Holger Kantz. *Extreme events in nature and society*. Springer Science & Business Media, 2006.

[122] Laurens Haan and Ana Ferreira. *Extreme value theory: an introduction*, volume 3. Springer, 2006.

[123] Stuart Coles, Joanna Bawa, Lesley Trenner, and Pat Dorazio. *An introduction to statistical modeling of extreme values*, volume 208. Springer, 2001.

[124] Satya N Majumdar, Arnab Pal, and Grégory Schehr. Extreme value statistics of correlated random variables: a pedagogical review. *Physics Reports*, 840:1–32, 2020.

# APPENDIX A

# Appendix A

## A.1 Computation of Laplace Transform of the First Detection Time Density

We start from Eq. (2.41). Laplace transforming it we get

$$\widetilde{D}_s(x_0,\sigma_0) = \left\langle e^{-sT_d(x_0,\sigma_0)} \right\rangle = \left\langle e^{-s\left[T_f(\rho,x_0)+I_f T_d(\rho,I)\right]} \right\rangle, \tag{A.1}$$

which in turn gives

$$\begin{aligned}\widetilde{D}_s(x_0,\sigma_0) &= \left\langle p_{T_f(\rho|x_0)}(A \mid \sigma_0) e^{-sT_f(\rho|x_0)} \right\rangle \\ &+ \left\langle p_{T_f(\rho|x_0)}(I \mid \sigma_0) e^{-s\left[T_f(\rho|x_0)+T_d(\rho,I)\right]} \right\rangle \\ &= \left\langle pT_f(\rho \mid x_0)(A \mid \sigma_0) e^{-sT_f(\rho|x_0)} \right\rangle \\ &+ \left\langle p_{T_f(\rho|x_0)}(I \mid \sigma_0) e^{-sT_f(\rho|x_0)} \right\rangle \left\langle e^{-sT_d(\rho,I)} \right\rangle .\end{aligned} \tag{A.2}$$

Setting $\sigma_0 = A$ and using Eq. (2.3), we obtain

$$\begin{aligned}\widetilde{D}_s(x_0, A) &= \left\langle \pi_A e^{-sT_f(\rho|x_0)} + \pi_I e^{-(s+\lambda)T_f(\rho|x_0)} \right\rangle \\ &+ \left\langle \pi_I e^{-sT_f(\rho|x_0)} - \pi_I e^{-(s+\lambda)T_f(\rho|x_0)} \right\rangle \left\langle e^{-sT_d(\rho,I)} \right\rangle \end{aligned} \tag{A.3}$$

$$\begin{aligned}&= \pi_A \widetilde{F}_s(\rho \mid x_0) + \pi_I \widetilde{F}_s(\rho \mid x_0) \widetilde{D}_s(\rho, I) \\ &+ \pi_I \widetilde{F}_{s+\lambda}(\rho \mid x_0) - \pi_I \widetilde{D}_s(\rho, I) \widetilde{F}_{s+\lambda}(\rho \mid x_0)\end{aligned}$$

$$\begin{aligned}&= \pi_A \widetilde{F}_s(\rho \mid x_0) + \pi_I \widetilde{F}_{s+\lambda}(\rho \mid x_0) \\ &+ \left[\pi_I \widetilde{F}_s(\rho \mid x_0) - \pi_I \widetilde{F}_{s+\lambda}(\rho \mid x_0)\right] \widetilde{D}_s(\rho, I).\end{aligned}$$

After repeating the same calculation for $\sigma_0 = I$ and $\sigma_0 = E$, we summarize the results in Eq. (2.55).

Similarly, Laplace transforming Eq. (2.42)

$$\begin{aligned}\widetilde{D}_s(\rho, I) &= \int_a^b \left\langle C(y, W_\beta \mid \rho) e^{-sW_\beta} \right\rangle dy \\ &+ \int_{-\infty}^{\infty} \left\langle C(y, W_\beta \mid \rho) e^{-sW_\beta} \right\rangle \left\langle e^{-sT_d(y,A)} \right\rangle \left[\Theta_-(y) + \Theta_+(y)\right] dy\end{aligned} \tag{A.4}$$

$$\begin{aligned}&= \int_a^b \beta \widetilde{C}(y, s+\beta \mid \rho) dy \\ &+ \int_{-\infty}^{\infty} \beta \widetilde{C}(y, s+\beta \mid \rho) \widetilde{D}_s(y, A) \left[\Theta_-(y) + \Theta_+(y)\right] dy.\end{aligned}$$

Let us denote the first integral term as

$$\widetilde{\phi}_\rho(s) \equiv \beta \int_a^b \widetilde{C}(y, s+\beta \mid \rho) dy \equiv \int_a^b \widetilde{\Phi}_\rho(s+\beta) dy. \tag{A.5}$$

Consider the second term in Eq. (A.4). By plugging $\widetilde{D}_s(y, A)$ according to Eq. (A.3) we obtain

$$\begin{aligned}&\int_{-\infty}^{\infty} \widetilde{\Phi}_\rho(s+\beta) \widetilde{D}_s(y, A) \left[\Theta_-(y) + \Theta_+(y)\right] dy \\ &\qquad = \widetilde{\chi}_\rho(s) + \widetilde{\psi}_\rho^- \widetilde{D}_s(a, I) + \widetilde{\psi}_\rho^+ \widetilde{D}_s(b, I),\end{aligned} \tag{A.6}$$

where

$$\widetilde{\chi}_\rho(s) \equiv \int_{-\infty}^{\infty} \widetilde{\Phi}_\rho(s+\beta)\times \\ \Big[\pi_A \widetilde{F}_s(\iota_\pm \mid y) + \pi_I \widetilde{F}_{s+\lambda}(\iota_\pm \mid y)\Big]\Big[\Theta_-(y) + \Theta_+(y)\Big]dy, \tag{A.7}$$

and

$$\widetilde{\psi}^\pm_\rho(s) \equiv \int_{-\infty}^{\infty} \widetilde{\Phi}_\rho(s+\beta)\times \\ \pi_I\Big[\widetilde{F}_s(\iota_\pm \mid y) - \widetilde{F}_{s+\lambda}(\iota_\pm \mid y)\Big]\Theta_\pm(y)dy, \tag{A.8}$$

where $\iota_- = a$ and $\iota_+ = b$. Overall we have

$$\widetilde{D}_s(\rho, I) = \widetilde{\Phi}_\rho(s+\beta) + \widetilde{\chi}_\rho(s) \\ + \widetilde{\psi}^-_\rho \widetilde{D}_s(a, I) + \widetilde{\psi}^+_\rho \widetilde{D}_s(b, I). \tag{A.9}$$

Note that Eq. (A.9) represents a linear system of two equations with the two unknowns $\widetilde{D}_s(a, I)$ and $\widetilde{D}_s(b, I)$. Solving we get:

$$\widetilde{D}_s(a, I) = \frac{(\widetilde{\phi}_a + \widetilde{\chi}_a)(1 - \widetilde{\psi}^+_b) + \widetilde{\psi}^+_a(\widetilde{\phi}_b + \widetilde{\chi}_b)}{1 - \widetilde{\psi}^-_a - \widetilde{\psi}^+_b + \widetilde{\psi}^-_a\widetilde{\psi}^+_b - \widetilde{\psi}^-_b\widetilde{\psi}^+_a}, \tag{A.10}$$

and

$$\widetilde{D}_s(b, I) = \frac{(\widetilde{\phi}_b + \widetilde{\chi}_b)(1 - \widetilde{\psi}^-_a) + \widetilde{\psi}^-_b(\widetilde{\phi}_a + \widetilde{\chi}_a)}{1 - \widetilde{\psi}^-_a - \widetilde{\psi}^+_b + \widetilde{\psi}^-_a\widetilde{\psi}^+_b - \widetilde{\psi}^-_b\widetilde{\psi}^+_a}. \tag{A.11}$$

For the symmetric case in which the spatial dynamics and the boundary conditions to the left and the right of the target center are the same (e.g., diffusion on the infinite line) Eqs. (A.10) and (A.11) are equal and simplify considerably ($\phi_a = \phi_b := \phi$, $\chi_a = \chi_b := \chi$ and $\psi^\pm_a = \psi^\pm_b := \psi^\pm$)

$$\widetilde{D}_s(a, I) = \widetilde{D}_s(b, I) = \frac{\widetilde{\phi} + \widetilde{\chi}}{1 - \widetilde{\psi}^- - \widetilde{\psi}^+}. \tag{A.12}$$

# APPENDIX B

## Appendix B

## B.1 Long Time Asymptotics and the Inheritance of Power-Law Decay

Assume the symmetric case in which the spatial dynamics and the boundary conditions to the left and the right of the target center are the same. Further assume that the underlying ungated process has an asymptotic power-law behavior of the form of $\widetilde{F}_s(\rho \mid y) \simeq 1 - (\tau_f s)^\theta$ (for $s \ll 1$), where $0 < \theta < 1$ and $\tau_f > 0$. Note that $\tau_f$ is a function of $|y - \rho|$. Taking the limit $s \to 0$ and plugging this form into Eq. (2.61) we obtain

$$\widetilde{D}_s(\rho, I) \simeq \frac{K_{eq}A - Bs^\theta}{K_{eq}A' + K_{eq}Bs^\theta}, \tag{B.1}$$

where $K_{eq} = \alpha/\beta$ and

$$A = \int_{-\infty}^{a} \widetilde{\Phi}_a(\beta)\widetilde{F}_\lambda(a \mid y)dy + \int_{b}^{\infty} \widetilde{\Phi}_a(\beta)\widetilde{F}_\lambda(b \mid y)dy + \frac{\pi_A^{-1}\int_a^b \widetilde{\Phi}_a(\beta)dy + \int_{-\infty}^{a} \widetilde{\Phi}_a(\beta)dy + \int_b^{\infty} \widetilde{\Phi}_a(\beta)dy}{K_{eq}}, \tag{B.2}$$

$$B = \int_{-\infty}^{a} \widetilde{\Phi}_a(\beta)\tau_f^\theta(y)dy + \int_{b}^{\infty} \widetilde{\Phi}_a(\beta)\tau_f^\theta(y)dy \tag{B.3}$$

and

$$A' = \pi_I^{-1} - \int_{-\infty}^{a} \widetilde{\Phi}_a(\beta)dy - \int_{b}^{\infty} \widetilde{\Phi}_a(\beta)dy + \int_{-\infty}^{a} \widetilde{\Phi}_a(\beta)\widetilde{F}_\lambda(a \mid y)dy + \int_{b}^{\infty} \widetilde{\Phi}_a(\beta)\widetilde{F}_\lambda(b \mid y)dy. \tag{B.4}$$

The numerator of the second row in Eq. (B.2) can be rewritten as

$$\begin{aligned}
&\pi_A^{-1}\int_a^b \widetilde{\Phi}_a(\beta)dy + \int_{-\infty}^a \widetilde{\Phi}_a(\beta)dy + \int_b^\infty \widetilde{\Phi}_a(\beta)dy \\
&= \int_{-\infty}^\infty \widetilde{\Phi}_a(\beta)dy + (\pi_A^{-1}-1)\int_a^b \widetilde{\Phi}_a(\beta)dy \\
&= \int_{-\infty}^\infty \widetilde{\Phi}_a(\beta)dy + K_{eq}\int_a^b \widetilde{\Phi}_a(\beta)dy \\
&= 1 + K_{eq}\int_a^b \widetilde{\Phi}_a(\beta)dy,
\end{aligned} \tag{B.5}$$

where in the last transition we recall that $\widetilde{\Phi}_a(\beta) = \beta\widetilde{C}(y,\beta \mid a)$ and note that $\int_{-\infty}^{\infty}\widetilde{C}(y,\beta \mid a)dy = \int_{-\infty}^{\infty}\int_0^\infty C(y,t \mid a)e^{-\beta t}dtdy = \int_0^\infty\int_{-\infty}^{\infty} C(y,t \mid a)e^{-\beta t}dydt = \int_0^\infty e^{-\beta t}dydt = \beta^{-1}$. Thus, $A$ in Eq. (B.2) can be rewritten as

$$\begin{aligned}
A = K_{eq}^{-1} + \int_a^b \widetilde{\Phi}_a(\beta)dy + \\
\int_{-\infty}^a \widetilde{\Phi}_a(\beta)\widetilde{F}_\lambda(a \mid y)dy + \int_b^\infty \widetilde{\Phi}_a(\beta)\widetilde{F}_\lambda(b \mid y)dy.
\end{aligned} \tag{B.6}$$

By noting that $\pi_I^{-1} - 1 = K_{eq}^{-1}$ it is easy to see that

$$A = A'. \tag{B.7}$$

By algebraic manipulations, and given Eq. (B.7), Eq. (B.1) can be rewritten as

$$\widetilde{D}_s(\rho,I) \simeq \frac{K_{eq}A\left(1-\frac{Bs^\theta}{K_{eq}A}\right)}{K_{eq}A'\left(1+\frac{Bs^\theta}{A'}\right)} = \frac{1-\frac{Bs^\theta}{K_{eq}A}}{1+\frac{Bs^\theta}{A}}, \tag{B.8}$$

which is equivalent to

$$\widetilde{D}_s(\rho,I) \simeq \left(1-\frac{Bs^\theta}{K_{eq}A}\right)\frac{1}{1+\frac{Bs^\theta}{A}}. \tag{B.9}$$

Expanding the fraction on the right, we obtain

$$\widetilde{D}_s(\rho,I) \simeq \left(1-\frac{Bs^\theta}{K_{eq}A}\right)\left(1-\frac{Bs^\theta}{A}\right). \tag{B.10}$$

Now by carefully multiplying these terms and neglecting higher order products we get

$$\widetilde{D}_s(\rho,I) \simeq 1 - \frac{B(1+K_{eq})}{K_{eq}A}s^\theta = 1 - \pi_I^{-1}\frac{B}{A}s^\theta. \tag{B.11}$$

Lastly, by an indirect application of the Tauberian theorem (see pp. 43-45 in [17]) we obtain

$$D_t(\rho, I) \simeq \frac{\theta}{\Gamma(1-\theta)} \frac{\left(\pi_I^{-1} \frac{B}{A}\right)}{t^{1+\theta}}. \tag{B.12}$$

# APPENDIX C

## Appendix C

## C.1 Transient Power-Law Decay under High Crypticity

### Ungated first-passage distributions with power-law tails

Recall Eq. (B.1) (we keep working under the same assumptions of Appendix B)

$$\widetilde{D}_s(\rho, I) \simeq \frac{K_{eq}A - Bs^\theta}{K_{eq}A + K_{eq}Bs^\theta}, \tag{C.1}$$

where A and B are defined as in the previous section and we recall that $A = A'$ (Eq. (B.7)). By taking the limit $K_{eq} \gg 1$, we obtain

$$\widetilde{D}_s(\rho, I) \simeq \frac{K_{eq}A}{K_{eq}A + K_{eq}Bs^\theta} = \frac{1}{1 + \frac{B}{A}s^\theta}. \tag{C.2}$$

To obtain a transient pre-asymptotic behaviour, we require the existence of $s$ values such that $\beta > s \gg (\frac{A}{B})^{1/\theta}$. In this case, $\frac{B}{A}s^\theta \gg 1$, and we have

$$\widetilde{D}_s(\rho, I) \simeq \frac{1}{\frac{B}{A}s^\theta}. \tag{C.3}$$

Applying the Tauberian theorem gives

$$D_t(\rho, I) \simeq \frac{1}{\Gamma(\theta)}\frac{A}{B}t^{\theta-1}, \tag{C.4}$$

which is a transient regime with a different power law than the asymptotic power law. Furthermore, we can exactly determine this power, and the pre-exponential factor. Thus, to guarantee the existence of the pre-asymptotic behaviour in Eq. (C.4), we require $\frac{B}{A}\beta^\theta \gg 1$. We note that if this requirement is not fulfilled, the transition from Eq. (C.2) to Eq. (C.3) is invalid. Expanding Eq. (C.2) (in the limit $s \to 0$) we then obtain

$$\widetilde{D}_s(\rho, I) \simeq 1 - \frac{B}{A}s^\theta, \tag{C.5}$$

which, as expected, is the $K_{eq} \gg 1$ limit of Eq. (B.11). This means that there is no transient regime before the asymptotic regime kicks in.

To understand the meaning of the additional requirement $\frac{B}{A}\beta^\theta \gg 1$, we focus on propagators whose Laplace transform has a scaling form

$$\widetilde{C}(y, s \mid a) \simeq s^{-\theta} H(|y-a| s^\theta), \tag{C.6}$$

where $H$ is the scaling function. Note that this form generalizes the one displayed by one-dimensional free-diffusion, $\widetilde{C}(x, s|x_0) = \frac{1}{\sqrt{4Ds}} e^{-\sqrt{\frac{s}{D}}|x-x_0|}$. It is then easy to show that under this assumption $B\beta^\theta \sim O(1)$, i.e., this product does not scale with $\beta$. Indeed, the assumed scaling sets a relation between length and time scales in our problem: length $\sim$ time$^\theta$. This means that

$$\begin{aligned} B &= \int_{-\infty}^{a} \widetilde{\Phi}_a(\beta)\tau_f^\theta(y)dy + \int_b^{\infty} \widetilde{\Phi}_a(\beta)\tau_f^\theta(y)dy \\ &\sim \int_{-\infty}^{a} \widetilde{\Phi}_a(\beta)|y-a|dy + \int_b^{\infty} \widetilde{\Phi}_a(\beta)|y-b|dy \sim \beta^{-\theta}, \end{aligned} \tag{C.7}$$

where we have noted that $\beta^{-1}$ sets the time scale, and hence the typical length scale that is set by $\widetilde{\Phi}_\rho(\beta) = \beta\widetilde{C}(y, \beta \mid \rho)$ (recall that this function is normalized to unity over space) scales like $\beta^{-\theta}$. Hence, $B\beta^\theta$ is order one, which means that to satisfy $\frac{B}{A}\beta^\theta \gg 1$, one only needs $A \ll 1$.

Equation (B.6) gives $A$ as a sum of four terms. The first term is small since we assumed $K_{eq} \gg 1$. To make the second term small, we require $\int_a^b \widetilde{\Phi}_a(\beta) = \beta \int_a^b \widetilde{C}(y, \beta \mid a)dy \ll 1$, which can also be written as $\int_a^b \widetilde{C}(y, \beta \mid a)dy \ll \beta^{-1}$. We anticipate that this condition can be fulfilled by taking $\beta$ to be small. In this limit, we can approximate

$$\beta \int_a^b \widetilde{C}(y, \beta \mid a)dy \simeq (b-a)\beta\widetilde{C}(a, \beta \mid a), \tag{C.8}$$

since the probability of being at different points inside the interval is practically the same at long times, which corresponds here to the small $\beta$ limit of the Laplace transform $\widetilde{C}(y, \beta \mid a)$. To find how the expression in Eq. (C.8) scales with $\beta$, we utilize a well established relation between

$\widetilde{C}(y, s \mid a)$, $\widetilde{C}(a, s \mid a)$ and $\widetilde{F}_s(y \mid a)$:

$$\begin{aligned}\widetilde{F}_s(y \mid a) =& \frac{\widetilde{C}(y, s \mid a)}{\widetilde{C}(a, s \mid a)} \\ \approx& \frac{\widetilde{C}(a, s \mid a) + |y-a| \frac{d\widetilde{C}(y,s|a)}{dy}\Big|_{y=a}}{\widetilde{C}(a, s \mid a)}.\end{aligned} \tag{C.9}$$

We thus see that for $\widetilde{F}_s(\rho \mid y) \simeq 1 - (\tau_f s)^\theta$ , where $0 < \theta < 1$ and $\tau_f > 0$, we have

$$\widetilde{C}(a, s \mid a) \simeq \left( \frac{|y-a| \frac{d\widetilde{C}(y,s|a)}{dy}}{\tau_f^\theta} \right)_{y=a} s^{-\theta} \equiv (\tau_r s)^{-\theta}. \tag{C.10}$$

Recalling the scaling form in Eq. (C.6), we see that the derivative with respect to $y$, evaluated at $y = a$, is independent of $s$. Thus, $\widetilde{C}(a, s \mid a)$ in Eq. (C.10) scales like $s^{-\theta}$, with a prefactor $\tau_r \equiv \left( |y-a| \frac{d\widetilde{C}(y,s|a)}{dy} \tau_f^{-\theta}(|y-a|) \right)^{-1/\theta} \Big|_{y=a}$, where we have explicitly recalled that $\tau_f$ is a function of $|y-a|$. Plugging Eq. (C.10) back into Eq. (C.8) we obtain

$$\beta \int_a^b \widetilde{C}(y, \beta \mid a) dy \simeq \frac{b-a}{\tau_r^\theta} \beta^{1-\theta}, \tag{C.11}$$

which is indeed small for small enough $\beta$ since $0 < \theta < 1$. More precisely, the additional requirement $\beta \int_a^b \widetilde{C}(y, \beta \mid a) dy \ll 1$ translates to

$$\frac{b-a}{\tau_r^\theta} \ll \beta^{\theta-1}, \tag{C.12}$$

which asserts that the second term in Eq. (B.6) is small.

We are left with the last two terms in Eq. (B.6). To analyze their scaling with $\beta$, we once again observe that the typical length scale that is set by $\widetilde{\Phi}_\rho(\beta) = \beta \widetilde{C}(y, \beta \mid \rho)$ scales like $\sim \beta^{-\theta}$. Hence, for the third term

$$\int_{-\infty}^a \widetilde{\Phi}_a(\beta) \widetilde{F}_\lambda(a \mid y) dy \sim \widetilde{F}_\lambda(a \mid \bar{y}), \tag{C.13}$$

with $\bar{y}$ set such that $|\bar{y} - a| \sim \beta^{-\theta}$. We now note that $\widetilde{F}_\lambda(a \mid \bar{y})$ is a Laplace transform, which in the limit $\lambda \tau_f(|\bar{y} - a|) \ll 1$ can be approximated by $\widetilde{F}_\lambda(a \mid \bar{y}) \simeq 1 - (\tau_f \lambda)^\theta$. In the other limit, i.e., when

$$\lambda \tau_f(|\bar{y} - a|) \gg 1, \tag{C.14}$$

$\widetilde{F}_\lambda(a \mid \bar{y})$ rapidly tends to zero. To see that we are in the limit specified by Eq. (C.14), we simply observe that

$$\lambda\tau_f(|\bar{y}-a|) \sim \lambda|\bar{y}-a|^{1/\theta} \sim \lambda/\beta = K_{eq}+1 \gg 1, \tag{C.15}$$

since we started by assuming $K_{eq} \gg 1$. As the analysis of the fourth term yields the same result, we conclude that the additional condition in Eq. (C.12) is sufficient to guarantee the pre-asymptotic behaviour in Eq. (C.4).

## Implications to gated CTRW on networks

We return to Eq. (G.5), where we recall that $\gamma$ is the rate of escape from the target site, $K_D = \beta/\gamma$. Equation. (G.5) can be rewritten as

$$\widetilde{D}_s(\mathbf{0}_I) = \frac{K_D + \pi_A\left[\widetilde{D}_s(\vec{X}_1) - \widetilde{F}_{s+\lambda}(\vec{X}_1)\right]}{\frac{s}{\gamma} + K_D + 1 - \pi_A K_{eq}\widetilde{F}_s(\vec{X}_1) - \pi_A\widetilde{F}_{s+\lambda}(\vec{X}_1)}$$

Taking the limit $K_{eq} \gg 1$ (such that $\pi_A \ll 1$ and $K_{eq}\pi_A \approx 1$), we obtain

$$\widetilde{F}_s(\mathbf{0}_I) \simeq \frac{K_D}{\frac{s}{\gamma} + K_D + 1 - \widetilde{F}_s(\vec{X}_1)} \tag{C.16}$$

Next we take the limit $s \to 0$, while assuming that in this limit $\widetilde{F}_s(\vec{X}_1) \simeq 1 - (\tau_f s)^\theta$. If $K_D \ll 1$, which is equivalent to $\gamma^{-1} \ll \beta^{-1}$, we obtain

$$\widetilde{F}_s(\mathbf{0}_I) \simeq \frac{K_D}{(\tau_f s)^\theta}, \tag{C.17}$$

By using the Tauberian theorem the inverse Laplace transform gives

$$D_t(\rho, I) \simeq \frac{1}{\Gamma(\theta)}\frac{K_D}{\tau_f^\theta}t^{\theta-1}, \tag{C.18}$$

which is a transient regime with a different power law than the asymptotic power law. Furthermore, we can exactly determine this power, and the pre-exponential factor.

If $K_D \not\ll 1$, Eq. (C.17) is not valid, and we instead have

$$\widetilde{D}_s(\mathbf{0}_I) \simeq \frac{1}{1 + \frac{(\tau_f s)^\theta}{K_D}}, \tag{C.19}$$

which, in the limit $s \to 0$, can be expanded as

$$\widetilde{D}_s(\mathbf{0}_I) \simeq 1 - \frac{(\tau_f s)^\theta}{K_D}. \tag{C.20}$$

Thus, when $K_D \not\ll 1$, we do not have a transient regime before the asymptotic behavior kicks in.

# APPENDIX D

# Appendix D

## D.1 Diffusion in an Interval with Two Reflecting Boundaries

### The conserved propagator

The propagator obeys the diffusion equation. The initial condition is $C(x, t = 0|x_0) = \delta(x - x_0)$, and we require two Neumann boundary conditions $\frac{\partial C(x,t|x_0)}{\partial x}\big|_{x=0} = 0$ and $\frac{\partial C(x,t|x_0)}{\partial x}\big|_{x=L} = 0$.

Laplace transforming the diffusion equation we get

$$s\widetilde{C}(x, s|x_0) = \mathcal{D}\frac{d^2\widetilde{C}(x, s|x_0)}{dx^2}, \tag{D.1}$$

which is a second-order, linear, homogeneous differential equation. It has a general solution

$$\widetilde{C}(x, s|x_0) = \begin{cases} \widetilde{C}_< = A_1(s)\mathrm{e}^{\alpha_+ x} + B_1(s)\mathrm{e}^{\alpha_- x}, \ x < x_0, \\ \widetilde{C}_> = A_2(s)\mathrm{e}^{\alpha_+ x} + B_2(s)\mathrm{e}^{\alpha_- x}, \ x > x_0, \end{cases} \tag{D.2}$$

where $\alpha_\pm = \pm\sqrt{\frac{s}{\mathcal{D}}}$.

Similarly, Laplace transforming the boundary conditions we obtain

$$\frac{d\widetilde{C}(x, s|x_0)}{dx}\big|_{x=0} = 0, \tag{D.3}$$

and

$$\frac{d\widetilde{C}(x, s|x_0)}{dx}\big|_{x=L} = 0. \tag{D.4}$$

Finally, the initial condition is translated to two matching conditions at the initial position of the particle, one for the continuity of the Laplace transform of the probability density

$$\widetilde{C}_+(x, s|x_0) = \widetilde{C}_-(x, s|x_0), \tag{D.5}$$

and one for the Laplace transform of the fluxes

$$-1 = \mathcal{D}\Big[\frac{d\widetilde{C}_+(x, s|x_0)}{dx}\big|_{x=0} - \frac{d\widetilde{C}_-(x, s|x_0)}{dx}\big|_{x=0}\Big], \tag{D.6}$$

which is obtained by integrating both sides of the Laplace transformed diffusion equation (Eq. (D.1)) over an infinitesimally small interval surrounding the initial position. Note that the 1 on the left-hand side comes from the Laplace transform of the delta function initial condition.

Imposing these conditions produces a system of four equations with four unknowns, from which we obtain

$$\begin{cases} A_1(s) = \frac{\operatorname{csch}\left(L\sqrt{\frac{s}{\mathcal{D}}}\right)\cosh\left(\sqrt{\frac{s}{\mathcal{D}}}(L-x_0)\right)}{2\sqrt{\mathcal{D}s}}, \\ B_1(s) = A_1(s), \\ A_2(s) = \frac{\left[\coth\left(L\sqrt{\frac{s}{\mathcal{D}}}\right)-1\right]\cosh\left(x_0\sqrt{\frac{s}{\mathcal{D}}}\right)}{2\sqrt{\mathcal{D}s}}, \\ B_2(s) = \frac{\left[\coth\left(L\sqrt{\frac{s}{\mathcal{D}}}\right)+1\right]\cosh\left(x_0\sqrt{\frac{s}{\mathcal{D}}}\right)}{2\sqrt{\mathcal{D}s}}. \end{cases} \tag{D.7}$$

## First passage time to an absorbing boundary at $a$

We now assume that $x_0 \in [0, a]$, where $0 < a \leq b < L$, and repeat the exact same procedure but with different boundary conditions, $\frac{\partial C(x,t|x_0)}{\partial x}\big|_{x=0} = 0$ and $C(a|x_0) = 0$. The Laplace transformed boundary conditions are

$$\widetilde{C}_>(a, s) = 0, \tag{D.8}$$

and

$$\frac{d\widetilde{C}_<(x, s)}{dx}\Big|_{x=0} = 0. \tag{D.9}$$

Solving, we get

$$\begin{cases} A_1(s) = \frac{\operatorname{sech}\left(a\sqrt{\frac{s}{\mathcal{D}}}\right)\sinh\left((a-x_0)\sqrt{\frac{s}{\mathcal{D}}}\right)}{2\sqrt{\mathcal{D}s}}, \\ B_1(s) = A_1(s), \\ A_2(s) = \frac{\left[\tanh\left(a\sqrt{\frac{s}{\mathcal{D}}}\right)-1\right]\cosh\left(x_0\sqrt{\frac{s}{\mathcal{D}}}\right)}{2\sqrt{\mathcal{D}s}}, \\ B_2(s) = \frac{\left[\tanh\left(a\sqrt{\frac{s}{\mathcal{D}}}\right)+1\right]\cosh\left(x_0\sqrt{\frac{s}{\mathcal{D}}}\right)}{2\sqrt{\mathcal{D}s}}. \end{cases} \tag{D.10}$$

The Laplace transform first-passage probability is given by

$$\begin{aligned} \widetilde{T}_f(x = a, s|x_0) &= -\mathcal{D}\frac{d\widetilde{C}_>(x, s)}{dx}\bigg|_{x=a} \\ &= \operatorname{sech}\left(a\sqrt{\frac{s}{\mathcal{D}}}\right)\cosh\left(x_0\sqrt{\frac{s}{\mathcal{D}}}\right) \end{aligned} \tag{D.11}$$

The Laplace transform is a moment generating function, the mean first-passage time is given by

$$\begin{aligned} \langle T_f(a|x_0)\rangle &= -\frac{d\widetilde{T}_f(a,s)}{ds}|_{s=0} \\ &= \frac{a^2 - x_0^2}{2\mathcal{D}}. \end{aligned} \tag{D.12}$$

# APPENDIX E

## Appendix E

## E.1 Diffusion with Drift with a Reflecting Boundary at the Origin

### The conserved propagator

We compute the propagator for the diffusion equation with drift, Eq. (2.72), with the initial condition $C(x, t = 0|x_0) = \delta(x - x_0)$ and boundary conditions $\frac{\partial C(x,t|x_0)}{\partial x}\big|_{x=0} = 0$ and $C(x \to \infty, t|x_0) = 0$. The Drift velocity is $v > 0$ and its direction is towards the reflecting boundary at zero.

Laplace transforming the diffusion equation we have

$$s\widetilde{C}(x, s|x_0) - \delta(x - x_0) = \mathcal{D}\frac{d^2\widetilde{C}(x, s|x_0)}{dx^2} + v\frac{d\widetilde{C}(x, s|x_0)}{dx}. \tag{E.1}$$

This is a second-order, linear, non-homogeneous differential equation. It has general spatial coordinate-dependent solution

$$\widetilde{C}(x, s|x_0) = \begin{cases} \widetilde{C}_< = A_1(s)\mathrm{e}^{\alpha_+ x} + B_1(s)\mathrm{e}^{\alpha_- x}, \, x < x_0, \\ \widetilde{C}_> = A_2(s)\mathrm{e}^{\alpha_+ x} + B_2(s)\mathrm{e}^{\alpha_- x}, \, x > x_0, \end{cases} \tag{E.2}$$

where $\alpha_\pm = \frac{1}{2\mathcal{D}}\left[-v \pm \sqrt{v^2 + 4\mathcal{D}s}\right]$.

At $x_0$ we impose two matching conditions, one for the propagator

$$\widetilde{C}_>(x_0, s) = \widetilde{C}_<(x_0, s), \tag{E.3}$$

and one for the fluxes (by integrating both sides of the transformed diffusion equation around an infinitesimally small interval)

$$-1 = \mathcal{D}\Big[\frac{d\widetilde{C}_>}{dx}\big|_{x=x_0} - \frac{d\widetilde{C}_<}{dx}\big|_{x=x_0}\Big] \tag{E.4}$$

where the 1 in the left-hand side comes from the Laplace transform of the delta function initial condition.

Finally, the transformed boundary conditions are

$$\widetilde{C}_{>}(x \to \infty, s) = 0, \tag{E.5}$$

and

$$v\widetilde{C}_{<}(0, s) + \mathcal{D}\frac{d\widetilde{C}_{<}(x, s)}{dx}\Big|_{x=0} = 0. \tag{E.6}$$

Solving, we get

$$\begin{cases} A_1(s) = \frac{e^{-x_0\alpha_+}}{\mathcal{D}(\alpha_+ - \alpha_-)}, \\ B_1(s) = \frac{(v+\mathcal{D}\alpha_+)e^{-x_0\alpha_+}}{\mathcal{D}(v+\mathcal{D}\alpha_-)(\alpha_- - \alpha_+)}, \\ A_2(s) = 0, \\ B_2(s) = B_1(s) - \frac{e^{-x_0\alpha_-}}{\mathcal{D}(\alpha_+ - \alpha_-)}. \end{cases} \tag{E.7}$$

## First-Passage Time to an absorbing boundary at $a$

We now repeat the exact same process but with different boundary conditions, $\frac{\partial C(x,t|x_0)}{\partial x}\Big|_{x=0} = 0$ and $C(a|x_0) = 0$. The Laplace transformed boundary conditions are

$$\widetilde{C}_{>}(a, s) = 0, \tag{E.8}$$

and

$$\frac{d\widetilde{C}_{<}(x, s)}{dx}\Big|_{x=0} = 0. \tag{E.9}$$

Solving, we get

$$\begin{cases} A_1(s) = \frac{\alpha_- e^{-x_0(\alpha_- + \alpha_+)}\left(e^{x_0\alpha_- + L\alpha_+} - e^{L\alpha_- + x_0\alpha_+}\right)}{\mathcal{D}(\alpha_- - \alpha_+)\left(\alpha_+ e^{L\alpha_-} - \alpha_- e^{L\alpha_+}\right)}, \\ B_1(s) = \frac{e^{L\alpha_-}\left(\alpha_+ e^{-x_0\alpha_+} - \alpha_- e^{-x_0\alpha_-}\right)}{\mathcal{D}(\alpha_- - \alpha_+)\left(\alpha_+ e^{L\alpha_-} - \alpha_- e^{L\alpha_+}\right)}, \\ A_2(s) = \frac{\alpha_+ e^{-x_0(\alpha_- + \alpha_+)}\left(e^{L\alpha_- + x_0\alpha_+} - e^{x_0\alpha_- + L\alpha_+}\right)}{\mathcal{D}(\alpha_- - \alpha_+)\left(\alpha_+ e^{L\alpha_-} - \alpha_- e^{L\alpha_+}\right)}, \\ B_2(s) = \frac{e^{L\alpha_+}\left(\alpha_+ e^{-x_0\alpha_+} - \alpha_- e^{-x_0\alpha_-}\right)}{\mathcal{D}(\alpha_- - \alpha_+)\left(\alpha_+ e^{L\alpha_-} - \alpha_- e^{L\alpha_+}\right)}. \end{cases} \tag{E.10}$$

The Laplace transform first-passage probability is given by

$$\begin{aligned}\widetilde{F}_s(x=a,\widetilde{F}) =& -\mathcal{D}\frac{d\widetilde{C}_>(x,s)}{dx}\bigg|_{x=a} \\ &= \frac{e^{(a-x_0)(\alpha_-+\alpha_+)}\left(\alpha_- e^{x_0\alpha_+}-\alpha_+ e^{x_0\alpha_-}\right)}{\alpha_- e^{a\alpha_+}-\alpha_+ e^{a\alpha_-}}.\end{aligned} \tag{E.11}$$

The Laplace transform is a moment generating function, the mean first-passage time is given by

$$\begin{aligned}\langle T_f(a|x_0)\rangle =& -\frac{d\widetilde{F}_s(a|x_0)}{ds}|_{s=0} \\ &= \frac{\mathcal{D}\left(-e^{-\frac{av}{\mathcal{D}}}+e^{\frac{(x_0-2a)v}{\mathcal{D}}}\right)+e^{\frac{(x_0-a)v}{\mathcal{D}}}(a-x_0)v}{v^2}.\end{aligned} \tag{E.12}$$

# APPENDIX F

# Appendix F

## F.1 Gating in higher dimensions

In Chapter 2, we developed a general framework to treat one-dimensional gated processes. In this appendix, we discuss a generalization to higher dimensional underlying processes for cases where target and underlying dynamics are rotationally symmetric – instead of a gated interval $[a, b]$ one can consider a gated annulus, or spherical shell, with some inner radius $r_a$ and outer radius $r_b$. Furthermore, one can study a gated disk, or sphere, by taking the limit $r_a \to 0$ (The corresponding sphere in one-dimension would be the interval $[0, b]$, where there is a reflecting wall at the origin). In this case, the equations for the mean and distribution of the detection time simplify considerably, since exiting the target through $r_a$ is impossible, and so all contributions associated with such trajectories vanish.

Moreover, the case of d-dimensional free diffusion and a spherically symmetric target, can be further simplified by utilizing the well-established mapping between the distance from the origin of d-dimensional free diffusion (Bessel process) and one-dimensional diffusion in a logarithmic potential. The gated first detection time for the latter can then be is easily attained with the formalism of Chapter 2, and the solution can be mapped back onto the d-dimensional case.

Next, we take time to explain the mapping by writing the corresponding Fokker-Planck equations and comparing them. Starting with the equation for a freely diffusing particle in d-dimensions, we note that the propagator does not depend on the angular part of the Laplacian. Hence, we are left only with the radial part $\frac{1}{r^{d-1}}\frac{\partial}{\partial r}\left(r^{d-1}\frac{\partial}{\partial r}\right)$, where the distance from the origin is denoted by $r \equiv |\vec{r}|$. The d-dimensional diffusion equation can thus be written as

$$\frac{\partial C(\vec{r}, t \mid \vec{r}_0)}{\partial t} = D\frac{d-1}{r}\frac{\partial C(\vec{r}, t \mid \vec{r}_0)}{\partial r} + D\frac{\partial^2 C(\vec{r}, t \mid \vec{r}_0)}{\partial r^2}. \tag{F.1}$$

Equation (F.1) is written for the propagator. Here we are interested in $C(r, t \mid r_0) = \Omega_d r^{d-1} C(\vec{r}, t \mid \vec{r}_0)$, where $\Omega_d$ is the surface area of a d-dimensional *unit* sphere. By plugging this relation into

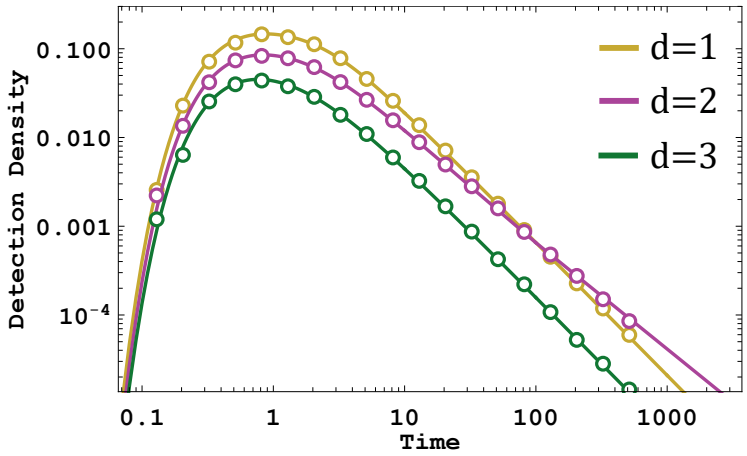


Figure F.1: The detection time density where the target is a gated d-dimensional unit sphere centered at the origin. The particle is freely diffusing, and we have set $\alpha = \beta = 1$, $D = 1$, $r_0 = 3$ and $\sigma_0 =$ eq. We consider diffusion in $d \in \{1, 2, 3\}$ dimensions. For each $d$, the lines are numerical Laplace inversions of Eq. (2.55) to which we have plugged in Eq. (F.3). Circles come from Monte-Carlo simulations with $10^5$ particles and a simulation time step $\Delta t = 10^{-4}$.

Eq. (F.1) we obtain the Fokker-Planck equation for $C(r, t \mid r_0)$:

$$\frac{\partial C(r,t \mid r_0)}{\partial t} = \frac{\partial}{\partial r}\left[\left(D\frac{1-d}{r}\right)C(r,t \mid r_0)\right] + D\frac{\partial^2 C(r,t \mid r_0)}{\partial r^2}. \tag{F.2}$$

We will now show that Eq. (F.2) is similar in form to the Fokker-Planck equation for a particle diffusing on the semi-infinite line in a logarithmic potential $U(x) = U_0 \log|x|$, where $U_0$ has units of energy and $x$ is dimensionless. At $x = 0$ the wall is completely reflective. Given that the particle has started at $x_0$, the conserved spatial propagator follows the Smoluchowski diffusion equation

$$\frac{\partial C(x,t \mid x_0)}{\partial t} = \frac{\partial}{\partial x}\left[\left(\frac{U_0}{\zeta x}\right)C(x,t \mid x_0)\right] + D\frac{\partial^2 C(x,t \mid x_0)}{\partial x^2},$$

with initial condition $C(x, 0 \mid x_0) = \delta(x - x_0)$ and boundary conditions

$$\left[D\frac{\partial C(x,t|x_0)}{\partial x} + \frac{U_0}{\zeta x}C(x,t|x_0)\right]_{x=0} = 0$$

and

$$C(x \to \infty, t|x_0) = 0,$$

where $\zeta$ is the friction coefficient such that $D = k_B T/\zeta$.

In the following, we will use the formalism of Chapter 2 to obtain the detection probability

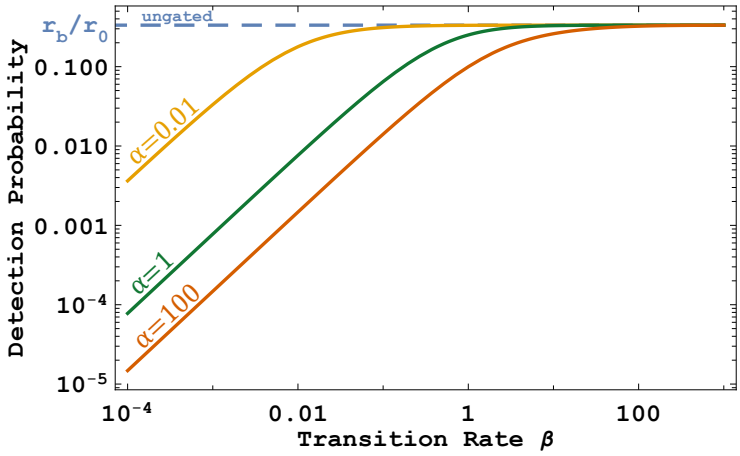


Figure F.2: Detection probability by a three-dimensional unit sphere. We plot the detection probability, namely the probability to be detected eventually, vs. the transition rate $\beta$. Each curve represents a different value of the transition rate $\alpha$. The dashed horizontal line is the ungated benchmark, where the detection probability is $r_b/r_0$. Here, we used $D = 1$, $\sigma_0 = \text{eq}$ and $r_0 = 3$.

for the gated version of the one-dimensional logarithmic potential problem, and then use the aforementioned mapping to obtain the detection time distribution of diffusion in d-dimensions by a gated sphere centered at the origin.

Assuming an interval target $[0, b]$, the detection time of a diffusing particle on the semi-infinite line in logarithmic potential, where $x_0 = b$ and $\sigma_0 = I$, is given by Eq. (2.57). In fact, since exiting the target through $a = 0$ is impossible (there is a reflecting wall at $x = 0$), Eq. (2.57) simplifies substantially

$$\widetilde{D}_s(b, I) = \frac{\widetilde{\phi}_b + \widetilde{\chi}_b}{1 - \widetilde{\psi}_b^+}, \tag{F.3}$$

where $\phi_b$, $\chi_b$ and $\psi_b^+$ were defined in Eqs. (2.58), (2.59) and (2.60) respectively. These functions require in turn the conserved spatial propagator and the first-passage time to a point $b$. Plugging these results into Eq. (F.3) gives the gated detection time given the initial condition $(b, I)$. To obtain the detection time for a general initial condition, we plug this result into Eq. (2.55). Finally, by identifying $x$ with $r$ and $d$ with $1 - \frac{U_0}{D\zeta}$ we obtain the detection time distribution for diffusion in d-dimensions by a gated sphere of radius $r_b$ centered at the origin. In Fig. F.1, we plot the detection time of a freely diffusing particle by a d-dimensional unit sphere, for $d = 1, 2, 3$, with $\sigma_0 = E$ and $r_0 = 3$.

The one and two-dimensional ungated first-passage processes are recurrent, the probability to eventually arrive at the sphere is one. Thais can be seen by looking at the small $s$ expansion

of the Laplace transform of the first-passage distribution, and noting that the first term in this expansion is 1. By definition, this term corresponds to $\int_0^\infty f(t \mid \vec{x})dt$, where $f$ is the first-passage distribution. However, the three-dimensional process is transient, the probability to eventually arrive at the sphere is $r_b/r_0$ (the ratio between the spherical target radius and the initial distance from the origin), which can be strictly smaller than one.

Recall that the asymptotic form of the one-dimensional first-passage distribution fits exactly the form assumed in Sec. 2.4.2.3 for the inheritance of the power-law. The proof can be easily generalized to include the three-dimensional case, and with more care to account for the logarithmic corrections of the two-dimensional case as well. The detection probability by the d-dimensional sphere can also be obtained for the Laplace transform of the detection time. As expected, in one and two dimensions we find that the particle will eventually be detected with probability one (regardless of the gating rates). However, intriguingly, while in the ungated three-dimensional case the detection probability is only dependent on the ratio $r_b/r_0$, in the corresponding gated case the detection probability is also a function of the transition rates and the diffusion coefficient. In particular, taking $\beta \to 0$, or $\alpha \to \infty$, we find that the detection probability vanishes. This finding is illustrated in Fig. (F.2).

# APPENDIX G

# Appendix G

## G.1 Models used for Simulations in Chapter 3

### The birth-death process

In this section, we describe the birth-death process (BDP) used in this chapter to produce produce Figs. 3.2 and 3.4.

We considered a BDP on a state space $\mathcal{S} \in \{0, 1, 2, \cdots, N\}$, with transition rates

$$W_+(j) = k_+(N - j), \tag{G.1}$$

$$W_-(j) = k_- j, \tag{G.2}$$

which govern the rate of transitioning from state $j$ to states $j + 1$ and $j - 1$ respectively, with $j \in \{0, 1, 2, \cdots, N\}$. Clearly, states 0 and $N$ act as reflecting boundaries, as $W_-(0) = W_+(N) = 0$.

Let us define $F_t(x^*|x_0)$ to be the probability distribution of the time the BDP reaches state $x^*$ for the first time, starting from state $x_0$. $F_t(x^*|x_0)$ is called the first-passage time density, and it is known that $F_t(x^*|x_0)$ obeys a Phase-type distribution whose Laplace transform is easy to compute.

More explicitly, taking the example of $x_0 = 0$, we note that $F_t(x^*|0)$ can be simply expressed as

$$F_t(x^*|0) = k_+(N - m + 1)\left[\exp(\mathbb{W}^{(x^*)}t)\right]_{x^*,1}. \tag{G.3}$$

where $\mathbb{W}^{(x^*)}$ is the $x^* \times x^*$ matrix obtained by retaining only the first $x^*$ columns and $x^*$ rows of the $N + 1 \times N + 1$ transition matrix $\mathbb{W}$ containing all zeros, except where

$$\mathbb{W}_{i+1,i} = k_+(N + 1 - i) \quad \text{and} \quad \mathbb{W}_{i,i+1} = k_- i,$$

for $i \in \{1, 2, \ldots, N\}$, and $\mathbb{W}_{i,i}$ are chosen so that the columns of $\mathbb{W}$ add up to zero.

Alternatively, one can also use the renewal method to determine the Laplace transformed

first-passage distribution as

$$\widetilde{F}_s(x^*|x_0) = \frac{\widetilde{C}(x^*, s|x_0)}{\widetilde{C}(x^*, s|x^*)}, \tag{G.4}$$

where $\widetilde{C}(i, s|j)$ is the Laplace transform of the propagator $C(i, t|j)$, which denotes the probability of finding the BDP in state $i \in \mathcal{S}$ at time $t$, given that the system started from state $j \in \mathcal{S}$ initially.

The parameters chosen for the production of Fig. 3.2 are $N = 10$, $x^* = 9$, $k_+ = 0.5$, $k_- = 1$, $\alpha = 2$, and $\beta = 0.5$. For Fig. 3.4, the parameters are $N = 10$, and $k_+ = k_- = 1$, for various values of $x^*$ and gating rates $\alpha$ and $\beta$.

In Fig. G.1, we further show that the first-passage time distribution of the BDP using in Fig. 3.2 inferred from a *numerical Laplace inversion* of the ratio of the detection time densities on the right hand side of Eq. (3.8) (yellow circles) agrees with the true first-passage time distribution.

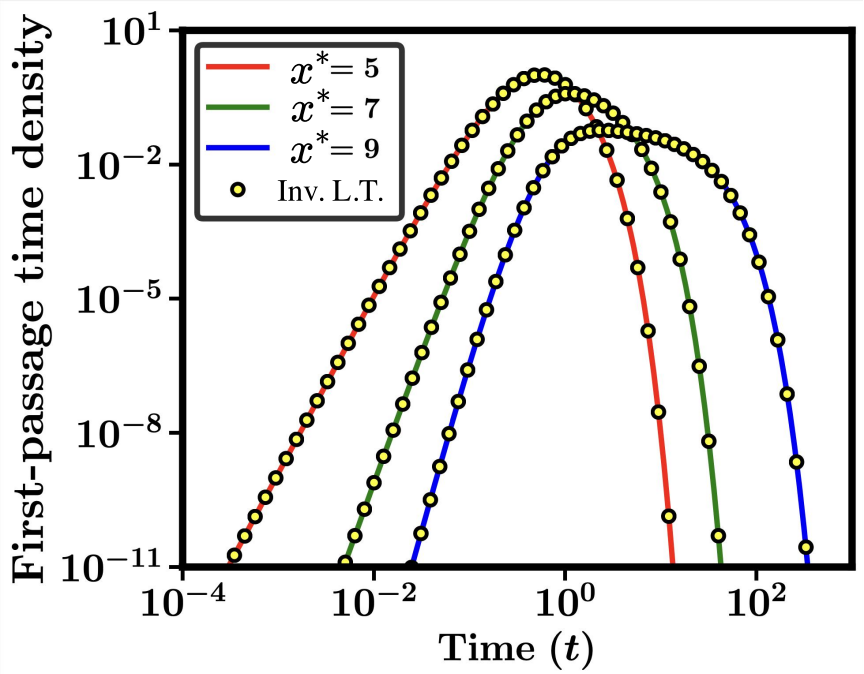


Figure G.1: First-passage time distribution for the birth-death process used in the text for three different values of the threshold. Solid lines denote the true first-passage time distribution and symbols (yellow circles) denote the inferred distribution from a numerical Laplace inversion of the ratio of the detection time densities on the right hand side of Eq. (3.8). The parameter values chosen for the birth-death process are $N = 10$ and $k_+ = k_- = 1$.

## Diffusing particle in a closed interval with one reflective boundary and one absorbing boundary

We start by computing the propagator $C(x,t \mid x_0)$, namely, the conditional probability density function to find the particle at position $x$ at time $t$, given that the initial position is $x_0$, and given a reflective boundary at 0 and an absorbing boundary at $x^*$. The initial condition is $C(x,t=0|x_0) = \delta(x-x_0)$ by definition, and the boundary conditions we require are a Neumann boundary condition $\frac{\partial C(x,t|x_0)}{\partial x}\big|_{x=0} = 0$ and a Dirichlet boundary condition $C(x=x^*,t|x_0) = 0$.

Laplace transforming the diffusion equation, we obtain

$$s\widetilde{C}(x,s|x_0) = \mathcal{D}\frac{d^2\widetilde{C}(x,s|x_0)}{dx^2}, \tag{G.5}$$

which is a second-order, linear, homogeneous differential equation. It has a general solution

$$\widetilde{C}(x,s|x_0) = \begin{cases} \widetilde{C}_-(x,s|x_0) = c_1(s)e^{x\sqrt{\frac{s}{\mathcal{D}}}} + c_2(s)e^{-x\sqrt{\frac{s}{\mathcal{D}}}}, & x < x_0 \\ \widetilde{C}_+(x,s|x_0) = c_3(s)e^{x\sqrt{\frac{s}{\mathcal{D}}}} + c_4(s)e^{-x\sqrt{\frac{s}{\mathcal{D}}}}. & x > x_0 \end{cases} \tag{G.6}$$

Similarly, Laplace transforming the boundary conditions we obtain

$$\frac{d\widetilde{C}(x,s|x_0)}{dx}\Big|_{x=0} = 0, \tag{G.7}$$

and

$$\widetilde{C}(x^*,s|x_0) = 0. \tag{G.8}$$

Finally, the initial condition is translated to two matching conditions at the initial position of the particle, one for the continuity of the Laplace transform of the probability density

$$\widetilde{C}_+(x_0,s|x_0) = \widetilde{C}_-(x_0,s|x_0), \tag{G.9}$$

and one for the Laplace transform of the fluxes

$$-1 = \mathcal{D}\Big[\frac{d\widetilde{C}_+(x,s|x_0)}{dx}\Big|_{x=x_0} - \frac{d\widetilde{C}_-(x,s|x_0)}{dx}\Big|_{x=x_0}\Big], \tag{G.10}$$

which is obtained by integrating both sides of the Laplace transformed diffusion equation (Eq. (G.5)) over an infinitesimally small interval surrounding the initial position. Note that the 1 on the left-hand side comes from the Laplace transform of the delta function initial condition.

Imposing the above conditions produces a system of four equations with four unknowns, from which we can obtain $c_i(s)$ $(1 \leq i \leq 4)$

$$c_1(s) = \frac{\text{sech}\left(x^*\sqrt{\frac{s}{\mathcal{D}}}\right)\sinh\left(\sqrt{\frac{s}{\mathcal{D}}}\,(x^* - x_0)\right)}{2\sqrt{\mathcal{D}s}}, \tag{G.11}$$

$$c_2(s) = \frac{\text{sech}\left(x^*\sqrt{\frac{s}{\mathcal{D}}}\right)\sinh\left(\sqrt{\frac{s}{\mathcal{D}}}\,(x^* - x_0)\right)}{2\sqrt{\mathcal{D}s}}, \tag{G.12}$$

$$c_3(s) = \frac{\left(\tanh\left(x^*\sqrt{\frac{s}{\mathcal{D}}}\right) - 1\right)\cosh\left(x_0\sqrt{\frac{s}{\mathcal{D}}}\right)}{2\sqrt{\mathcal{D}s}}, \tag{G.13}$$

$$c_4(s) = \frac{e^{x^*\sqrt{\frac{s}{\mathcal{D}}}}\,\text{sech}\left(x^*\sqrt{\frac{s}{\mathcal{D}}}\right)\cosh\left(x_0\sqrt{\frac{s}{\mathcal{D}}}\right)}{2\sqrt{\mathcal{D}s}}. \tag{G.14}$$

The Laplace transform of the first-passage probability density function is given by

$$\widetilde{F}_s(x^*|x_0) = -\,\mathcal{D}\frac{d\widetilde{C}_+(x,s|x_0)}{dx}\bigg|_{x=x^*} = \text{sech}\left[x^*\sqrt{\frac{s}{\mathcal{D}}}\right]\cosh\left[x_0\sqrt{\frac{s}{\mathcal{D}}}\right] \tag{G.15}$$

The Laplace transform is a moment generating function, and so the mean first-passage time is given by

$$\langle T_f(x^*|x_0)\rangle = -\frac{d\widetilde{F}_s(x^*|x_0)}{ds}\bigg|_{s=0} = \frac{x^{*2} - x_0^2}{2\mathcal{D}}. \tag{G.16}$$

The parameter values chosen for the production of Fig. 2 in the main text are $L = 2$, $D = \frac{1}{2}$, $x_0 = 0.2$, $x^* = 1.6$, and gating rates $\alpha = \beta = 0.5$.

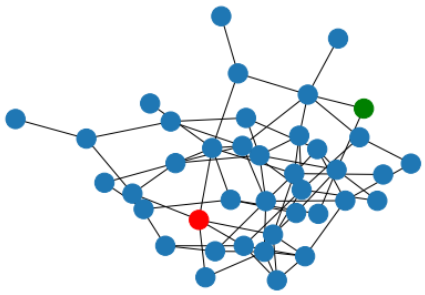

Figure G.2: The network used for simulations of gated target search by a CTRW, with the red and green nodes denoting the initial position of the CTRW and the target respectively. For the CTRW on this network, the waiting time distribution was taken to be uniform on the interval $[0, 0.2]$, whereas the gating rates were chosen to be $\alpha = \beta = 1$.

## Continuous-time random walk (non-Markovian) on a network

A continuous-time random walk (CTRW) on a network is a mathematical framework for modeling the random movement of particles or agents on a network over time. CTRWs on networks have found numerous applications in various fields, including physics, biology, sociology, and computer science. In this model, a random walker, jumps successively from a node of the network to one of its neighbouring nodes after waiting for a random time, drawn from its waiting time distribution.

For the production of Fig. 2 in the main text, we simulated a CTRW on the network depicted in Fig. G.2 – an Erdös-Rényi random network with $40$ nodes, where each pair of nodes is connected with probability of $0.1$. For the CTRW on this network, the waiting time distribution was taken to be uniform on the interval $[0, 0.2]$, whereas the gating rates were chosen to be $\alpha = \beta = 1$.

# APPENDIX H

# Appendix H

## H.1 Including Statistics of Switches in Sensor Dynamics

To derive the equation that governs the dynamics of $p_t(\sigma, n|\sigma_0)$, we consider the possible events that can occur in a time $\Delta t$ and see that the following are satisfied

$$\begin{aligned}
p_{t+\Delta t}(A, n+1|A) &= (1-\alpha\Delta t)\, p_t(A, n+1|A) + \beta\Delta t\, p_t(I, n|A) \\
p_{t+\Delta t}(I, n+1|A) &= (1-\beta\Delta t)\, p_t(I, n+1|A) + \alpha\Delta t\, p_t(A, n|A) \\
p_{t+\Delta t}(A, n+1|I) &= (1-\alpha\Delta t)\, p_t(A, n+1|I) + \beta\Delta t\, p_t(I, n|I) \\
p_{t+\Delta t}(I, n+1|I) &= (1-\beta\Delta t)\, p_t(I, n+1|I) + \alpha\Delta t\, p_t(A, n|I).
\end{aligned} \tag{H.1}$$

In the $\Delta t \to 0$ limit, we have

$$\begin{aligned}
\frac{dp_t(A, n+1|A)}{dt} &= -\alpha\, p_t(A, n+1|A) + \beta\, p_t(I, n|A) \\
\frac{dp_t(I, n+1|A)}{dt} &= -\beta\, p_t(I, n+1|A) + \alpha\, p_t(A, n|A) \\
\frac{dp_t(A, n+1|I)}{dt} &= -\alpha\, p_t(A, n+1|I) + \beta\, p_t(I, n|I) \\
\frac{dp_t(I, n+1|I)}{dt} &= -\beta\, p_t(I, n+1|I) + \alpha\, p_t(A, n|I).
\end{aligned} \tag{H.2}$$

The above equations should be solved with the following boundary conditions valid for all $t$.

$$\begin{aligned}
p_t(A, 0|A) &= e^{-\alpha t} \\
p_t(I, 0|A) &= 0 \\
p_t(A, 0|I) &= 0 \\
p_t(I, 0|I) &= e^{-\beta t}
\end{aligned} \tag{H.3}$$

We now define the generating function and Laplace transform of $p_t(\sigma, n|\sigma_0)$ as

$$\widetilde{p}_s(\sigma, z|\sigma_0) = \sum_{n=0}^{\infty} z^n \int_0^{\infty} dt\; e^{-st}\; p_t(\sigma, n|\sigma_0). \tag{H.4}$$

The Laplace transforms of the equations in Eq. (H.2) can be expressed as

$$\begin{aligned}
s\hat{p}_s(A, n+1|A) &= -\alpha\, \hat{p}_s(A, n+1|A) + \beta\, \hat{p}_s(I, n|A) \\
s\hat{p}_s(I, n+1|A) &= -\beta\, \hat{p}_s(I, n+1|A) + \alpha\, \hat{p}_s(A, n|A) \\
s\hat{p}_s(A, n+1|I) &= -\alpha\, \hat{p}_s(A, n+1|I) + \beta\, \hat{p}_s(I, n|I) \\
s\hat{p}_s(I, n+1|I) &= -\beta\, \hat{p}_s(I, n+1|I) + \alpha\, \hat{p}_s(A, n|I)
\end{aligned} \tag{H.5}$$

and the subsequent generating functions are

$$\begin{aligned}
\frac{s}{z}\big(\widetilde{p}_s(A, z|A) - p_s(A, 0|A)\big) &= -\frac{\alpha}{z}\,\big(\widetilde{p}_s(A, z|A) - p_s(A, 0|A)\big) + \beta\, \widetilde{p}_s(I, z|A) \\
\frac{s}{z}\widetilde{p}_s(I, z|A) &= -\frac{\beta}{z}\,\widetilde{p}_s(I, z|A) + \alpha\, \widetilde{p}_s(A, z|A) \\
\frac{s}{z}\widetilde{p}_s(A, z|I) &= -\frac{\alpha}{z}\,\widetilde{p}_s(A, z|I) + \beta\, \widetilde{p}_s(I, z|I) \\
\frac{s}{z}\big(\widetilde{p}_s(I, z|I) - \widetilde{p}_s(I, 0|I)\big) &= -\frac{\beta}{z}\,\big(\widetilde{p}_s(I, z|I) - \widetilde{p}_s(I, 0|I)\big) + \alpha\, \widetilde{p}_s(A, z|I).
\end{aligned} \tag{H.6}$$

Using the boundary conditions (and their corresponding Laplace transforms), we have

$$\begin{aligned}
s\left(\widetilde{p}_s(A, z|A) - \frac{1}{s+\alpha}\right) &= -\alpha\,\left(\widetilde{p}_s(A, z|A) - \frac{1}{s+\alpha}\right) + z\beta\, \widetilde{p}_s(I, z|A) \\
s\widetilde{p}_s(I, z|A) &= -\beta\, \widetilde{p}_s(I, z|A) + z\alpha\, \widetilde{p}_s(A, z|A) \\
s\widetilde{p}_s(A, z|I) &= -\alpha\, \widetilde{p}_s(A, z|I) + z\beta\, \widetilde{p}_s(I, z|I) \\
s\left(\widetilde{p}_s(I, z|I) - \frac{1}{s+\beta}\right) &= -\beta\,\left(\widetilde{p}_s(I, z|I) - \frac{1}{s+\beta}\right) + z\alpha\, \widetilde{p}_s(A, z|I).
\end{aligned} \tag{H.7}$$

Using the middle two equations in Eq. (H.7), we can write the following relations.

$$\begin{aligned}
\widetilde{p}_s(I, z|A) &= \frac{z\alpha}{s+\beta}\, \widetilde{p}_s(A, z|A) \\
\widetilde{p}_s(A, z|I) &= \frac{z\beta}{s+\alpha}\, \widetilde{p}_s(I, z|I).
\end{aligned} \tag{H.8}$$

Substituting Eq. (H.8) in the remaining two equations of (H.7), we get

$$\begin{aligned}\widetilde{p}_s(A,z|A) &= \frac{1}{s+\alpha} + \frac{z^2\alpha\beta}{(s+\beta)(s+\alpha)}\,\widetilde{p}_s(A,z|A)\\ \widetilde{p}_s(I,z|I) &= \frac{1}{s+\beta} + \frac{z^2\alpha\beta}{(s+\alpha)(s+\beta)}\,\widetilde{p}_s(I,z|I).\end{aligned} \tag{H.9}$$

Putting it all together, we obtain the generating function and Laplace transform of the sensor dynamics

$$\begin{aligned}\widetilde{p}_s(A,z|A) &= \frac{s+\beta}{(s+\alpha)(s+\beta)-z^2\alpha\beta}\\ \widetilde{p}_s(I,z|A) &= \frac{z\alpha}{(s+\alpha)(s+\beta)-z^2\alpha\beta}\\ \widetilde{p}_s(A,z|I) &= \frac{z\beta}{(s+\alpha)(s+\beta)-z^2\alpha\beta}\\ \widetilde{p}_s(I,z|I) &= \frac{s+\alpha}{(s+\alpha)(s+\beta)-z^2\alpha\beta}.\end{aligned} \tag{H.10}$$